UNIVERSIDAD DE INVESTIGACIÓN DE TECNOLOGÍA EXPERIMENTAL YACHAY

Escuela de Ciencias Químicas e Ingeniería

TÍTULO: Synthesis, Characterization, and Cell Viability Studies of Coordination Compounds with Transition Metals and Polydentate Ligands based on Ethylenediamine.

Trabajo de integración curricular presentado como requisito para la obtención del título de Químico

Autor:

Menoscal Saltos Diego David

Tutor:

PhD. Saucedo Vázquez Juan Pablo

Urcuquí, marzo 2020

Urcuquí, 26 de marzo de 2020

SECRETARÍA GENERAL
(Vicerrectorado Académico/Cancillería)
ESCUELA DE CIENCIAS QUÍMICAS E INGENIERÍA
CARRERA DE QUÍMICA
ACTA DE DEFENSA No. UITEY-CHE-2020-00013-AD

A los 26 días del mes de marzo de 2020, a las 10:00 horas, de manera virtual mediante videoconferencia, y ante el Tribunal Calificador, integrado por los docentes:

Presidente Tribunal de Defensa	Dr. FERREIRA DE MENEZES AREIAS , FILIPE MIGUEL , Ph.D.
Miembro No Tutor	Dra. HIDALGO BONILLA, SANDRA PATRICIA , Ph.D.
Tutor	Dr. SAUCEDO VAZQUEZ, JUAN PABLO , Ph.D.

El(la) señor(ita) estudiante **MENOSCAL SALTOS, DIEGO DAVID**, con cédula de identidad No. **1250948658**, de la **ESCUELA DE CIENCIAS QUÍMICAS E INGENIERÍA**, de la Carrera de **QUÍMICA**, aprobada por el Consejo de Educación Superior (CES), mediante Resolución **RPC-SO-39-No.456-2014**, realiza a través de videoconferencia, la sustentación de su trabajo de titulación denominado: **Synthesis, Characterization, and Cell Viability Studies of Coordination Compounds with Transition Metals and Polydentate Ligands based on Ethylenediamine.**, previa a la obtención del título de **QUÍMICO/A**.

El citado trabajo de titulación, fue debidamente aprobado por el(los) docente(s):

Tutor	Dr. SAUCEDO VAZQUEZ, JUAN PABLO , Ph.D.

Y recibió las observaciones de los otros miembros del Tribunal Calificador, las mismas que han sido incorporadas por el(la) estudiante.

Previamente cumplidos los requisitos legales y reglamentarios, el trabajo de titulación fue sustentado por el(la) estudiante y examinado por los miembros del Tribunal Calificador. Escuchada la sustentación del trabajo de titulación a través de videoconferencia, que integró la exposición de el(la) estudiante sobre el contenido de la misma y las preguntas formuladas por los miembros del Tribunal, se califica la sustentación del trabajo de titulación con las siguientes calificaciones:

Tipo	Docente	Calificación
Presidente Tribunal De Defensa	Dr. FERREIRA DE MENEZES AREIAS , FILIPE MIGUEL , Ph.D.	10,0
Tutor	Dr. SAUCEDO VAZQUEZ, JUAN PABLO , Ph.D.	10,0
Miembro Tribunal De Defensa	Dra. HIDALGO BONILLA, SANDRA PATRICIA , Ph.D.	10,0

Lo que da un promedio de: **10 (Diez punto Cero)**, sobre 10 (diez), equivalente a: **APROBADO**

Para constancia de lo actuado, firman los miembros del Tribunal Calificador, el/la estudiante y el/la secretario ad-hoc.

Certifico que *en cumplimiento del Decreto Ejecutivo 1017 de 16 de marzo de 2020, la defensa de trabajo de titulación (o examen de grado modalidad teórico práctica) se realizó vía virtual, por lo que las firmas de los miembros del Tribunal de Defensa de Grado, constan en forma digital.*

MENOSCAL SALTOS, DIEGO DAVID
Estudiante

FILIPE MIGUEL FERREIRA MENEZES AREIAS
Firmado digitalmente por FILIPE MIGUEL FERREIRA MENEZES AREIAS
Fecha: 2020.06.10 20:24:41 -05'00'

Dr. FERREIRA DE MENEZES AREIAS , FILIPE MIGUEL , Ph.D.
Presidente Tribunal de Defensa

JUAN PABLO SAUCEDO VAZQUEZ

Dr. SAUCEDO VAZQUEZ, JUAN PABLO , Ph.D.
Tutor

SANDRA PATRICIA HIDALGO BONILLA

Dra. HIDALGO BONILLA, SANDRA PATRICIA , Ph.D.
Miembro No Tutor

ESCOBAR LANDAZURI, ANA MARIA
Secretario Ad-hoc

ANA MARIA ESCOBAR LANDAZURI

AUTORÍA

Yo, **DIEGO DAVID MENOSCAL SALTOS**, con cédula de identidad 1250948658, declaro que las ideas, juicios, valoraciones, interpretaciones, consultas bibliográficas, definiciones y conceptualizaciones expuestas en el presente trabajo; así cómo, los procedimientos y herramientas utilizadas en la investigación, son de absoluta responsabilidad de el/la autora (a) del trabajo de integración curricular. Así mismo, me acojo a los reglamentos internos de la Universidad de Investigación de Tecnología Experimental Yachay.

Urcuquí, marzo 2020.

Diego David Menoscal Saltos
CI:1250948658

AUTORIZACIÓN DE PUBLICACIÓN

Yo, **DIEGO DAVID MENOSCAL SALTOS,** con cédula de identidad 1250948658, cedo a la Universidad de Investigación de Tecnología Experimental Yachay, los derechos de publicación de la presente obra, sin que deba haber un reconocimiento económico por este concepto. Declaro además que el texto del presente trabajo de titulación no podrá ser cedido a ninguna empresa editorial para su publicación u otros fines, sin contar previamente con la autorización escrita de la Universidad.

Asimismo, autorizo a la Universidad que realice la digitalización y publicación de este trabajo de integración curricular en el repositorio virtual, de conformidad a lo dispuesto en el Art. 144 de la Ley Orgánica de Educación Superior

Urcuquí, marzo 2020.

Diego David Menoscal Saltos
CI:1250948658

DEDICATORIA

A mi madre Ingrid Saltos, por estar presente en cada momento importante de mi vida y guiarme por este largo camino.

A mi padre Wilter Menoscal, por todo el apoyo brindado durante mi carrera universitaria.

A mis hermanos Wilter, Juan y Ximena, por confiar siempre en su hermano mayor.

Diego David Menoscal Saltos

AGRADECIMIENTO

A Juan Pablo Saucedo, por ser gran tutor y amigo. Por apoyarme desde el momento en que le propuse el proyecto y brindarme su ayuda durante todo el proceso.

A PhD. Juan Carlos García Ramos, PhD. Yanis Toledano Magaña, Toño, White y a Vicky, por sus valiosas lecciones y consejos durante mi estadía de investigación en el laboratorio de nanomedicina del CNyN, UNAM.

A mi hermano de otra madre, Alexander.

A mis amigos/as Adrián, Emilia, José, María José, Nadia y Nicolás por todos estos años juntos, entre noches interminables de estudio, peleas y reconciliaciones. No podría pedir mejores amigos en mi carrera universitaria.

A la Escuela de Ciencias Químicas e Ingeniería por el apoyo económico brindado para poder realizar este proyecto de investigación en México y Ecuador.

A Lola, Manuel, Solmar y todos los profesores con quienes tuve el honor de compartir un laboratorio, un salón de clases o una investigación.

Finalmente, gracias a todas aquellas personas que representaron una parte importante de este proceso y que por diversos motivos ya no están.

Diego David Menoscal Saltos

RESUMEN

El cáncer es considerado una de las principales causas de muerte en el planeta. Hoy en día, los principales tratamientos consisten en cirugías, radioterapias y el uso de agentes citotóxicos. En este sentido, el *Cisplatino* se ha convertido en el compuesto predominante relacionado a las quimioterapias. Sin embargo, dicho compuesto presenta varios efectos secundarios, entre ellos el desarrollo de resistencia por parte de las células cancerígenas y elevados niveles de acumulación del compuesto, lo cual genera altos grados de toxicidad en contra de células sanas. Estos factores representan limitaciones en cuanto a su uso clínico. Por esto, el desarrollo de compuestos nuevos que presenten actividad anticancerígena y reduzcan el número de efectos secundarios presentados por el Cisplatino es una prioridad.

El presente proyecto de tesis muestra la síntesis y caracterización de un ligando donador orgánico basado en etilendiamina y ácido tartárico. Los compuestos de coordinacion con metales divalentes (Co(II), Ni(II), y Cu(II)) y un metal trivalente (Ru(III)) también son presentados. La difracción de rayos X en polvo (DRX-P) del ligante reveló una estructura con fórmula molecular $C_{13}H_{26}N_2O_{13}$ y nombre monohidrato de (R)-2-metilpiperazinadiium bis[tartrato (2S,3S) de hidrógeno]. Las Espectroscopías de Reflectancia Difusa (ERD), Ultravioleta-Visible (UV-Vis), Infrarrojo (IR) y de Fotoemisión de Rayos-X (XPS) confirmaron la presencia de enlaces metal-oxígeno del ligante y permitieron proponer posibles estructuras para los compuestos de coordinación.

Los estudios de viabilidad celular fueron desarrollados en triplicado utilizando cultivos celulares de linfocitos y los compuestos en disolución, a cuatro diferentes concentraciones. Los estudios sugieren que el ligante y el compuesto de coordinación cobalto (II) no presentaron valores elevados de citotoxicidad. En el caso de los compuestos de cobre (II), níquel (II) y rutenio (III), valores de citotoxicidad elevados fueron presentados a medida que la concentración de los compuestos incrementaba, siendo el compuesto de rutenio el de mayor citotoxicidad, mientras que el compuesto de níquel, el de menor valor. Los valores de dosis letal media (DL_{50}) fueron obtenidos para los compuestos de cobre, níquel y rutenio dado que su efecto citotóxico en los cultivos celulares alcanzó el 50%.

Palabras Clave: Ligando; Compuesto de Cobalto (II); Compuesto de Cobre (II); Compuesto de Níquel (II); Compuesto de Rutenio (III); Síntesis; Caracterización; Linfocitos.

ABSTRACT

Cancer is one of the principal causes of death around the world. Nowadays, treatments against cancer consist of radiotherapy, surgeries, and the use of cytotoxic agents. In this sense, Cisplatin has arisen as one of the predominant compounds related to chemotherapies. However, it presents various side effects, such as the development of cancer cells resistance, and elevated levels of accumulation of the compound, which leads to high cytotoxicity against healthy cells. These are factors that represent limits to its clinical uses. For instance, the development of novel compounds that present activities against cancer, and reduce the number of side effects presented by Cisplatin is a priority.

The present thesis project shows the synthesis and characterization of an oxygen donor ligand based on ethylenediamine and tartaric acid. Its coordination compounds with divalent essential metals (Co(II), Ni(II), and Cu(II)) and a trivalent transition metal Ru(III) are presented as well. X-Ray Powder Diffraction (XRPD) of the ligand revealed the structure with molecular formula $C_{13}H_{26}N_2O_{13}$ and name (R)-2-methylpiperazinediium bis[hydrogen (2S,3S)-tartrate] monohydrate. Diffuse Reflectance Spectroscopy (DRS), Ultraviolet-Visible Spectroscopy (UV-Vis), Infrared Spectroscopy (IR) and X-ray photoemission spectroscopy (XPS) confirmed the presence of the bonds corresponding to metals with the oxygen atoms of the ligand and allowed to propose the structures of the coordination compounds.

The cell viability studies were performed in triplicate using lymphocytes cell cultures and each compound at four different concentrations. Also, the studies suggest that the ligand compound and the cobalt (II) coordination complex did not present high cytotoxicity values against lymphocytes. In the case of copper (II), nickel (II) and ruthenium (III) compounds, high cytotoxicity values were presented as the concentration of the compounds increased, being the ruthenium compound the most cytotoxic and the nickel compound, the least. The half lethal dose (LD_{50}) values were obtained for the complexes of copper, nickel, and ruthenium as their effect in the lymphocytes culture reached the 50% of cytotoxicity.

Keywords: Ligand; Cobalt (II) compound; Copper (II) compound; Ni (II) compound; Ru(III) compound; Synthesis; Characterization; Lymphocytes.

List of abbreviations

LD_{50}: Half Lethal Dose

UV-Vis: Ultraviolet – Visible Spectroscopy

NIR: Near Infrared Spectroscopy

DRS: Diffuse Reflectance Spectroscopy

FT-IR: Fourier Transform Infrared Spectroscopy

XRPD: X – Ray Powder Diffraction

XPS: X – Ray Photoelectron Spectroscopy

RPMI: Roswell Park Memorial Institute cell medium

EDTA: Ethylenediaminetetraacetic Acid

FBS: Fetal Bovine Serum

COD: Crystallographic Open Database

NO: Nitrogen-Oxygen

ML: Metal-Ligand

MN: Metal -Nitrogen

MO: Metal-Oxygen

Index

List of figures

List of tables

1. CHAPTER ONE: INTRODUCTION – JUSTIFICATION

1.1. General considerations about Coordination Complexes

Coordination complexes are considered as the product of a reaction between a central metallic atom (or ion) and neutral molecules (can be presented as anions as well) called ligands[1]. The metallic atoms are called Lewis acids due to their tendency to accept electron pairs coming from the ligands (Lewis bases)[1]. The atom directly bonded to the metallic center is called a donor atom. Then, a coordinate covalent bond is referred to as the donation of an electron pair from the donor atoms to electron acceptor species, and this bond differs from a normal covalent one in the sense that two electrons are proportioned instead of one from each atom[1].

The beginning of the study and analysis of coordination complexes dates from 1798 with Tassaert studies[2]. Nowadays, there exist advances in the organic and inorganic chemistry behind the synthesis, characterization, and uses of this kind of metallic compounds. Regarding the structure of such complexes, Alfred Werner proposed a theory in which two types of valences were identified. The first one was called an ionizable valence (*Hauptvalenz*), and the second one as non-ionizable valence (*Nebenvalenz*)[2]. The theory then consisted of that every element tends to satisfy both types of valences. Following the previous proposal, the coordination number (*Nebenvalenz*) and oxidation state (*Haupvalenz*) of the Werner compound can be assigned [2].

Concerning the classification of the coordination compounds, as a large number of structures exist, a precise systematization is challenging to propose[3]. Moreover, several characteristics are taken into account to classify them; as examples, the charge of the ion complexes, the types of ligands, the structure by taking into consideration the metallic central atoms, and the coordination number[3]. Based on the previous factors, the classification of coordination compounds consisted of Werner complexes, complexes with metal-metal bonds, clusters, chelates, metal carbonyls, macrocyclic ligand complexes, and metal-organic complexes[3].

1.2. Coordination chemistry applied to medicine

Inorganic chemistry has been used in medicine for many centuries, but only as empiric knowledge. However, the design and understanding of the mechanism of action of the compounds are on increasing significance. Actually, the use of coordination complexes as medicinal agents

possess a commercially elevated level[4]. Furthermore, an estimate of the commercial importance of coordination compounds approaches US$5 billion annually for the entire field [4].

Furthermore, some main observations need to be taken into account if an explanation about the relationship between the pharmaceutical activities, the metallic atoms, and the ligands wants to be proposed[4]. For example, the role of metal ions in carrying out vital functions of living organisms, the ligands by themselves developing as chelating agents, and the forming complexes that can be detected by spectroscopic techniques[3]. Also, the chelating properties of the ligands are important in medicine as they can perform antidote behavior in poisoning with metal ions or cyanides; their use is also related to the lack of essential nutrients for viruses, bacteria or microbes, necessary for their correct performance; providing toxic metals against pathogenic agents; or the introduction of essential metals in organisms that present lower levels than required[3].

Two main fields can be illustrated regarding the immersion of inorganic chemistry in medicine. The first one, related to ligands as medicines, in which the metal ions are the principal targets of the ligands[4], and the second ones are related to metallic complexes. In the last case, the metallic ion generally plays a crucial role in determining the mechanism of action of the drug[2]. Regarding the first case, there are illnesses related to the freedom of metallic ions inside the body that can be diminished by the use of chelating agents. One example is Wilson's disease, in which Cu(II) free ions are responsible for the illness[4].

Since the beginning of studies about the relationship between coordination chemistry and medicine, there is the desire to understand how these molecules can affect biochemical functions, which establishes a connection between bioinorganic chemistry and pharmacology[5]. As mentioned before, inorganic compounds possess a long history regarding biological and medical fields. There were several metals used to treat illnesses in ancient ages; gold and copper as examples[6]. Inorganic elements conform the most of the periodic table, which means they proportion broad diversity of characteristics to the possible compounds containing them[6]. The general properties related to the compounds that are taken into account in medicine are the following:

- Charge of the metal: in aqueous solutions, these metal ions are positively charged (cations); and depending on the medium, the charge of the metal-ligand complexes (ML) can change by action of the ligands present. Then, the complex can be neutral, anionic, or cationic[1].

- Interactions with ligands: Ligands can be of organic or inorganic nature. The formation of coordination compounds is due to the proportioning of electron pairs from the electron donor atoms presented in the ligand to the metallic cations. The different characteristics of the ligands can influence changes in the overall coordination compounds; these new properties will differ from those of the individual ligand or metal[1]. Also, the different interactions will be ruled by thermodynamic and kinetic aspects, which will take part in ligand exchange reactions[1].
- Structure and bonding: Metal – Ligand (ML) complexes can present several coordination geometries, resulting in different shapes from the ones related to organic molecules. Properties such as the angles, coordination sites, and bond length will differ depending on the metal and the oxidation state in which it is presented[1].
- Lewis acid character: Hydrolysis reactions are primordial in physiological conditions. Depending on the chemical environment and the electron affinity of the metal ions, they will tend to polarize groups already coordinated to them, opening the possibility for new ligands to be part of the complex[1].
- Redox activity: In biology, several processes are relevant due to metals and the number of redox reactions in which they are involved. The number of electrons in the d-shell plays a vital role in this case[1].

Several chemical and biological aspects take into account metallic ions; for example, some structures can reach higher levels of stabilization due to ML interactions, becoming into macroscopic entities such as protein and nucleic acid folds[6]. The reversibility of ML bonding is also an aspect from which nature takes advantage; metal ions such as Ca^{2+} and Zn^{2+} are used to express and propagate biochemical signals when getting bind or unbind to proteins. Furthermore, the reversibility of the ML bond represents the transporting pathway for molecules like O_2 from hemoglobin[6].

Regarding electrical conductivity and charge balance, there are some alkali and alkaline earth cations such as Na^+, Ca^{2+}, and K^+ used to regulate physiological systems. Moreover, the metallic center will accomplish a determined function depending on the Lewis acid or redox-active character. As an example previously mentioned, if the metallic center possesses a strong Lewis acid character, the ligands coordinated to it will become potent nucleophiles, i.e., a Zn (II) atom,

which owns a coordinated water molecule, will make it more nucleophilic and enhance the possibility for an amide bond hydrolysis of a protein substrate. Regarding redox activity, the transition metals can reach a wide variety of oxidation states, and the capability to undergo redox reactions as enzyme cofactors[5].

1.3. Ancestors metallic compounds

1.3.1. Gold compounds

Gold compounds are characteristics by their use in the treatment of rheumatoid arthritis, a disease that presents continuous erosion of joints, which results in deformities, pain, and immobility[7]. The progression of the illness is caused by the action of reactive oxygen species (ROS), generated when Phagocytic cells release enzymes such as collagenase[7].

There are three primary gold (I) compounds used against rheumatoid arthritis; the two earlier ones are called Myocrisin™ and Solganol™ (Figure 1). Both compounds are oligomers and were used as intramolecular injections. Regarding the significant problems observed, high nephrotoxicity levels were observed due to the accumulation of gold in kidney tissues. Additional side effects found were mouth ulcers, skin reactions, blood disorders, and occasional liver toxicity[7].

Observing the characteristics and side effects presented by the previous drugs, in 1985, a new compound was introduced, called Ridaura™. This compound is a monomer and possesses several improvements compared with its antecessors. The levels of serum are reduced and maintained for more extended periods. Moreover, there exists less retention of gold in the tissues, which diminishes toxicity[7].

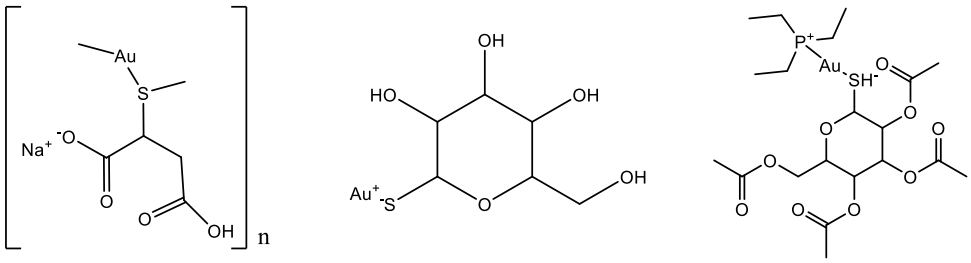

Figure 1. Structures of Myocrisin™, Solganol™, and Ridaura™ gold (I) compounds

1.3.2. Vanadium complexes

In the case of Vanadium complexes, the principal effects presented are in diabetes treatment. Vanadium salts perform similar processes as insulin does; they stimulate the oxidation of glucose and the synthesis of glycogen. They also can inhibit gluconeogenesis in rat hepatocytes[8]. Regarding the principal Vanadium compounds, the sodium metavanadate (SMV) and sodium orthovanadate (SOV) (Figure 2) have succeeded in human diabetic models.

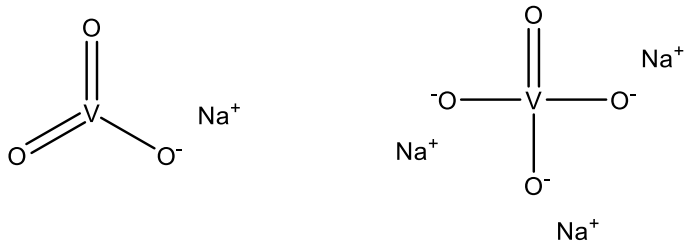

Figure 2. Structures of Sodium metavanadate (SVM) and sodium orthovanadate (SOV).

1.3.3. Platinum complexes

Platinum complexes possess anticancer properties that made them recognized but also started the pathway to the synthesis of several coordination compounds with different metals, trying to approach better results compared to platinum complexes. The most important compounds are the cisplatin and the second-generation platinum complexes, such as oxaliplatin and carboplatin (Figure 3). In this type of complexes, the structure-activity relationship has revealed that only the compounds with *cis* geometry are able to block cell growth[9]. Many derivatives of the cisplatin present inhibitory activity related to cell growth, those compounds possess at least one N-H functional group, a key factor to make the compound highly selective to the biological target[9].

Similar coordination compounds having another metallic center do not present the same activity achieved by the platinum compounds; this difference is assessed to the ligand-exchange kinetics, which is slow compared to other coordination compounds, giving them higher kinetic stability[9]. Ligand-exchange reactions are in the range of microseconds to seconds for several coordination compounds with metallic centers different from Platinum, which possess intervals of minutes to days[9].

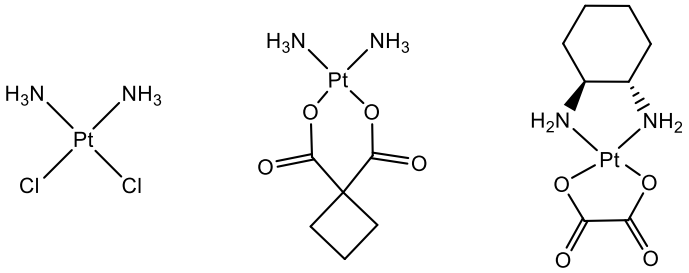

Figure 3. Cisplatin, Carboplatin, and Oxaliplatin anticancer agents.

1.4. Coordination compounds used as anticancer agents

Cancer is caused by faulty DNA, which means that it is a genetic disease[10]. Healthy cells are subjected to become dangerous when mutations occur in genes. Specifically, there are possibilities that a defective gene can pass the mentioned gene to a daughter cell[10]. Then, the following generation of daughter cells will tend to adopt the mutation until structural changes appear, becoming them malignantly[10]. The division of the cells with mutations tends to increase, scatter over the body, and become uncontrolled. This behavior of the cells is called *metastases* and can be dangerous (even lethal) if it is not treated on time[10].

Moreover, metastases represent the most important reason for failure in therapies against cancer[10]. As previously mentioned, the tumors tend to scatter all over the body, which represents a problem in treatments like radiotherapy or surgeries. To deal with metastases, drug therapies appear as better and more reasonable solutions. Nowadays, the discovery of new compounds and their screening as anticancer agents is a topic trend in science. Since the anticancer activity of cisplatin was discovered, the field of metal-based drugs gained relevance, and several metallic coordination compounds are synthesized and tested in different normal and cancer cell lines. As a long term goal, science requires the synthesis of metal-based drugs with exact knowledge of the activity and toxicity presented to deal with the problem of cellular resistance to cisplatin and its limited action against common types of cancer, such as breast and gastrointestinal ones[10].

In metal-based drugs, specific molecular targets can be achieved by molecules with a precise three – dimensional configuration. Different chemical modifications in the structure of the ligands provide a high number of possibilities to deal with cancer[11]. Several redox reactions and ligand substitutions happen in physiological conditions, which facilitate the molecules to interact with the targets. Research in this area focuses on biologically active complexes formed by essential ions, such as copper, zinc, cobalt, and iron[11].

1.4.1. Ruthenium compounds

Ruthenium arises as to the most promising metal of the ones already investigated. Regarding the antitumor activity, it is generally accepted that the ruthenium compounds behave the same way as platinum ones[12]. This kind of compound binds to DNA, forming adducts that do not allow more DNA or RNA to be produced, resulting in induced programmed cell death. Ruthenium presents a wide variety of oxidation states, from -2 in $[Ru(CO)_4]^{2-}$ to +8 in RuO_4, which is related to its kinetic stability[12].

Furthermore, the facilities at the time of synthesis of the coordination compounds, and the reversible behavior of their redox couples makes them attractive as potential anticancer agents[10]. Ruthenium (III) compounds tend to remain in their oxidation state until they reach the tumor; at this stage, the changes in pH and a lower content of oxygen in the medium favor the conversion of Ru(III) to Ru(II), a more reactive species[10]. The process mentioned before is called "activation by reduction". Also, the reduction potential plays a vital role for the compounds to be active *in vivo*; it is necessary to remark that the potential can change according to the ligands used[10].

Four ruthenium coordination compounds have reached clinical trials; the compounds are called NAMI-A, KP1019, KP1339, and TLD1443[12] (Figure 4). In the case of NAMI-A, it showed high inhibitory potential against tumor metastases; however, when Phase II clinical trials were performed, it revealed the side effects of the drug were severe, resulting in no further investigations[13]. Regarding KP1019, its investigation failed as well; on this occasion, due to lower water solubility, which makes it difficult for a compound to access into the cell. KP1019 also presented severe side effects[14]. The compound KP13139 resulted as an approach to improve the water solubility of the compound KP1019; the compound is still used and tested in clinical trials[15]. The photodynamic therapy has also been taken into consideration by researchers; for that reason, a Ru (II) photosensitizer compound has been synthesized. It is named TLD1443 and has an important efficacy against bladder cancer; the compound has been tested in clinical trials-phase II[16].

The great variety of ruthenium complexes leads us to think that there are multiple targets and mechanisms for their antitumor characteristics. As examples, several ruthenium complexes interfere with replication and transcription of DNA; other types act as inhibitors of enzymes related to DNA[17]. In addition, ruthenium complexes can induce the formation of DNA photocrosslinking

compounds that do not allow the RNA polymerization enzymes to bind DNA, resulting in the apoptosis of the tumoral cells[18].

Several studies confirm that the mitochondria are one of the critical targets of the ruthenium complexes, leading to a decrease in the membrane potential, followed by mitochondrial dysfunction and apoptosis[19]. Besides, other targets inside the cell have been identified; for example, the endoplasmic reticulum is involved in tumor cells drug resistance, apoptosis, and autophagy, which converts it into a target of research. Until now, it is believed that Ruthenium complexes act by causing oxidative stress or endoplasmic reticulum stress, which results in tumor cell apoptosis by activation of caspase family members[20]. Moreover, there are other types of targets related to autophagy processes, the lysosomes. As targets of ruthenium compounds, they can induce production of themselves and release hydrolase, which results in an increasing level of apoptosis of tumor cells[21]. Furthermore, there are studies related to ruthenium complexes confirming that they can modify the permeability of the cell membrane, which results in an outflow of the content of the cells, leading them to apoptosis[22].

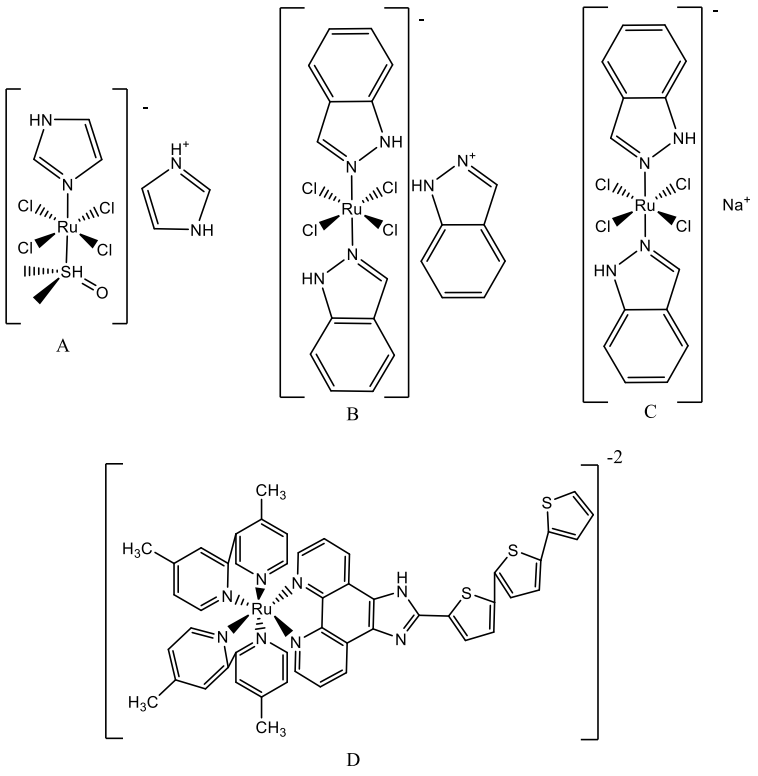

Figure 4. Clinical tested Ruthenium coordination compounds.

1.4.2. Cobalt compounds

Cobalt possesses an important role in biological processes and represents one of the essential trace elements found in animals. Vitamin B12 (Cobalamin) (Figure 5A) is the main form in which it is presented[23]. In cobalamin, the cobalt ion presents a +1-oxidation state, and it can be oxidized to +2 and +3 states. Cobalt(I) is coordinated axially to 5,6-dimethylbenzimidazole and either 5'deoxyadenosy groups, methyl, hydroxide, or cyanide groups. Equatorially, it is coordinated to a corrin ring by its four nitrogen atoms, adopting an octahedral geometry[24]. Cobalamin is presented in different forms, and it is involved in several mechanisms, such as DNA synthesis and regulation, the maintenance of nerve and brain function, and the formation of red blood cells. Also, there is evidence relating Cobalamin to the metabolism of fatty and amino acids[25].

The relevance of cobalt in biological processes is undeniable. It has reached a point in which humans have developed mechanisms to overcome the cobalt overload. Then, cobalt results less toxic for humans than non-essential metals, such as platinum. This fact promotes the research to obtain new compounds with antitumoral properties as alternatives to platinum-based compounds already existing[26].

The first biological studies performed using cobalt compounds revealed the potential of these complexes to be used as antibacterial, antifungal, and antiprotozoal agents[27–31]. Schiff bases were chosen as the ligands used to synthesize approaches of antitumoral compounds. Cobalt (II) and cobalt (III) metals with Schiff bases coordinated to them revealed a reasonable potential anticancer activity. In the case of the cobalt (II) compounds, two types of ligands were used; the compound using 4-(4-aminophenyl) morpholine as ligand show weak in-vitro activity against hepatocellular carcinoma cells (HepgG2)[32]. However, the compound using 2,6-bis(2,6-diethylphenyliminomethyl) (Figure 5C) pyridine revealed better in-vitro cytotoxicity results against colorectal adenocarcinoma (HCT-15) and cervix adenocarcinoma (HeLa) cells, in both cases with IC_{50} values in a range of 45-100 µM[33]. The IC_{50} (half maximal inhibitory concentration) represents a measurement related to the concentration of a compound required to inhibit a specific property of an organism in its 50%[34].

Regarding cobalt (III) compounds, a complex formed by a tridentate Schiff base ligand presented a moderate activity against human breast cancer cells (MCF-7) with IC_{50}<100 µM, the ligand was obtained in a reaction using ethylenediamine and salicylaldehyde[35]. Another type of

cobalt (III) compound, but using two [2-(2-hydroxybenzylideneamino) phenol] (Figure 5B) as ligands, achieved the inhibition of HeLa cells. However, this inhibition was to a lower extent than the one produced by the Cisplatin[36].

Returning to the cobalt (II) complexes, a water-soluble coordination compound with 2-oxo-1,2-dihydroquinoline-3-carbaldehyde (isonicotinic) hydrazine as ligands revealed micromolar toxicities that can be comparable or even better than of Cisplatin. The cell viability assays were performed in several cancer cell lines (HeLa, Hep-2, and A431). Also, this compound was tested in healthy mouse embryonic fibroblast cells (NIH 3T3) and exhibited up to 100-fold lower toxicity compared to Cisplatin[37]. However, more studies related to structure-activity of the complexes need to be made due to certain discrepancies in the biological activity of Schiff bases coordinated to Cobalt (II) and Cobalt (III) atoms, but also to be sure of the pharmaceutical potential of this type of compounds. It is important to be remarked that there are cobalt(III) compounds with surfactant-like properties that have shown to induce DNA damage and apoptosis in human breast cancer cells[38–40].

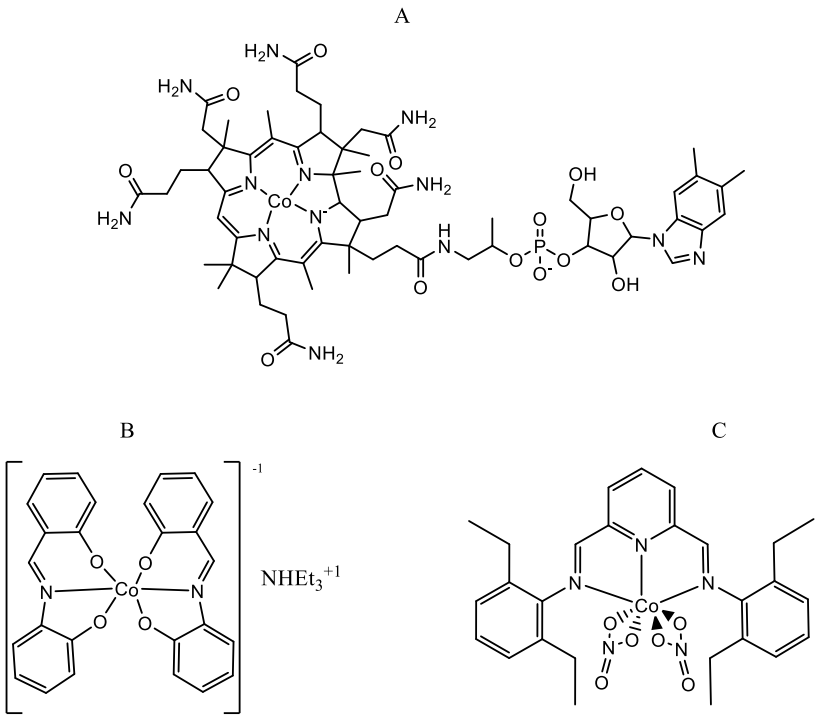

Figure 5. Structure of Cobalamin (A), Cobalt (III) [2-(2-hydroxybenzylideneamino) phenol] (B), and Cobalt (II) 2,6-bis(2,6-diethylphenyliminomethyl) pyridine (C).

1.4.3. Copper compounds

Copper is a relevant atom related to the function of proteins and enzymes involved in respiration and DNA synthesis. It is considered as a crucial trace element that performs an essential role in redox processes, growth, and development[41]. Regarding the significant biological functions of copper, there exists a production of potentially dangerous free radicals when the copper-containing biological molecules react with molecular oxygen[42]. Furthermore, copper compounds have a vital role in cell physiology; they act as catalytic cofactors in iron absorption, elastin cross-linking, free radical scavenging, and in the redox chemistry of mitochondrial respiration[43]. Also, several illnesses such as epilepsy, diabetes, intestinal ulcers, arthritis, and cancer are related to altered levels of copper inside the body[44]. The toxicity presented by copper comes from its capacity to produce reactive oxygen species (ROS) when reacting with molecular oxygen, the ability to displace other metals, and cleavage both DNA and RNA; also, it is involved in the production of lipids peroxidation[42]. Several cancer types are related to high levels of copper, including breast, colon, lung, brain, and prostate types[45].

As an essential trace element, such as cobalt, copper may be less toxic than non-essential metals like platinum. Several studies regarding copper complexes and their antitumoral potential have been realized in recent years, but little information about the molecular basis of the mechanism of action of the compounds has been obtained. However, it has been identified that their mode of action differs from the Cisplatin mode (based on covalent binding to DNA)[41]. For this reason, the information available suggests that other targets related to inhibiting tumoral activity can be achieved and treated by using these kinds of compounds.

Concerning the mechanisms of action, it has been showed that copper-free ions participate in DNA strand breaking and oxidation of bases, which results in the production of ROS. For example, Cu (II) can be reduced to Cu (I) by the presence of superoxide ($^{*}O_2^{-}$) or reducing agents like glutathione or ascorbic acid[46]. The presence of Cu(I) ions promotes the formation of hydroxyl radicals (OH^{*}) from hydrogen peroxide (H_2O_2) which can interact with any biological molecule by getting hydrogen atoms from an unsaturated fatty acid, forming a lipidic radical, but also from an amino-bearing carbon, resulting in a radical of a carbon-centered protein. Both processes result in oxidative cell damage[47].

In the case of anticancer complexes, the study of copper-based compounds has been made due to the assumption that endogenous metals will present lower toxicity. Compounds such as Marboran ™ and Triapine ™ correspond to complexes using Thiosemicarbazones (TSCs) as ligands. This kind of compounds has revealed anticancer properties since 1960s[48]. The inhibitory action of DNA enzyme ribonucleotide diphosphate reductase and the selectivity presented for hormone-responsive cancer have made TSCs a relevant subject of studies. However, the lower water solubility and high cytotoxicity *in vivo* of this type of compounds represent a problem to overcome[49]. The potent antitumor action of Cu(II) complexes using imidazole-type ligands against the B16 murine melanoma cell line has marked an exciting research field to copper-based antitumoral compounds with imidazole ligands[50].

Another type of compounds presenting biological activities are the Cu(II) complexes using benzimidazole and its derivatives as ligands. The types of activities performed by these compounds are antifungal, antibacterial, antiviral, and anticancer[51]. Bidentate and tridentate complexes of Cu(II) based on pyrazole ligands are also investigated due to their higher affinity with DNA and elevated cytotoxicity compared to the uncoordinated pyrazole ligand and its derivative complexes, but changing the central metallic atom. In fact, *in vitro* cell viability assays showed that the copper (II) compound was more effective against a reasonable variety of cancer cell lines, including leukemia HL-60, human mammary gland cancer BGC-823[52].

Triazole-type ligands coordinated to copper (II) atoms are another example of anticancer agents related to compounds with nitrogen atoms in their structure, but their efficacy is lower compared to the ligands previously mentioned[53]. Besides, Cu(II) compounds containing phenanthroline (phen) ligands have also been tested *in vitro* to know their potential as anticancer agents. However, there are some drawbacks related to their efficacy, their low selectivity to bind a DNA sequence, and the formation of complexes with two phen as ligands is unfavorable due to the second phen presents a small association constant[54].

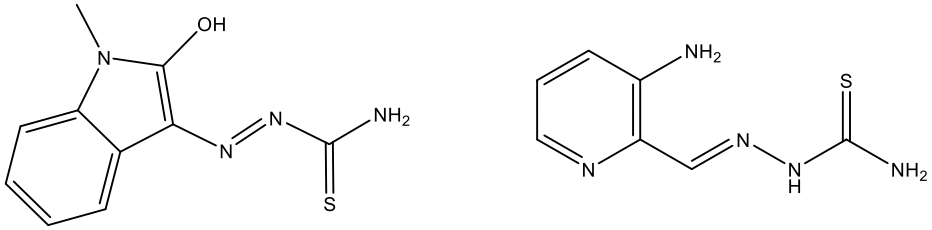

Figure 6. Structures of Marboran ™ and Triapine ™, noncoordinating to copper atoms ™

1.4.4. Nickel compounds

Nickel is known to have interactions with DNA and proteins related, and it is considered as a weak carcinogenic metal in the medicinal field. However, high levels of nickel concentration are related to lung and nasal cancer types[55]. The carcinogenic mechanism of this metal is still unknown, but it is proposed that involves genetics and epigenetic alterations (changes in DNA structure that do not change the coding sequence)[55,56]. Even when the capability of certain nickel species to bind DNA has been confirmed, this kind of compounds were mainly used only for research instead of the development of new nickel-based drugs against cancer[57]. Regarding relevant compounds, several studies have been made to a complex with more than 40 years of existence. The nickel compound possesses a ligand called CR (2,12-dimethyl-3,7,11,17-tetraazabicyclo-[11.3.1]-heptadeca-1(17),2,11,13,15-pentaene)[58].

The $[NiCR]^{2+}$ compound (represented ionically) marked the pathway to the development of several nickel complexes whose inhibitory evaluation has been tested[59]. The following relevant compound was an analog of the $[NiCR]^{2+}$ (Figure 7). In this case, the compound was functionalized by introducing an imine group; the imine presence represented a hint in the approach to reach anticancer properties[60]. The compound was presented as $[NiCR\text{-}2H]^{2+}$, and its activity was evaluated in murine erythroleukemia cancer cell line; the results showed that [NiCR-2H] may have cytotoxic effects in cancer cells, but not its precursor $[NiCR]^{2+}$ [61]. The complex $[NiCR\text{-}2H]^{2+}$ can damage DNA strands and cause cytotoxicity in the absence of oxidizing agents (as in the case of $[NiCR]^{2+}$). Parting from that, the design of novel nickel-based coordination compounds with improved selectivity for DNA cleavage becomes an interesting research field[62].

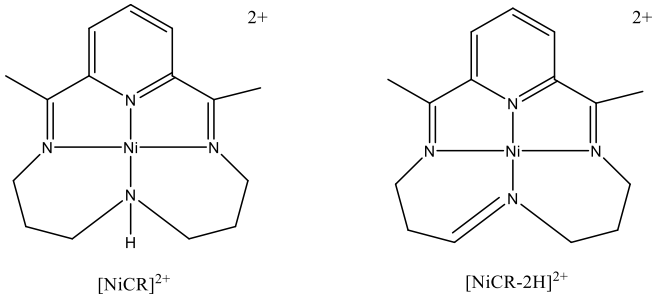

Figure 7.Structure of the Nickel compound $[NiCR]^{2+}$ and its analog $[NiCR-2H]^{+2}$

1.4.5. Ligands used in anticancer tests

In general, the properties of the coordination compounds, whether in classical inorganic coordination complexes, in bioinorganic model compounds, or organometallic compounds, will be determined by the nature of the ligands presented and the electron donor atoms around the metallic center[63]. The majority of the synthesized compounds which possessed a series of nitrogen or oxygen donor atoms exhibited anticancer activity, as seen previously. Nitrogen and oxygen donor atoms can bind specific structures called receptors that possess significant roles in cancer growth and, for instance, are relevant targets in cancer therapies[64]. Some receptors are Cathepsins B (Cat B)[65], carbonic anhydrase II (CA-II)[66], DNA-1 and DNA-2[67], BRAF kinase[68], ribonucleotide reductase (RNR)[69], thymidylate synthase (TS)[70], topoisomerase II (Top II)[71], and recombinant human albumin (RHA)[72]. The RHA is one of the most relevant receptors; it helps to deliver metal-based drugs to the specific target, but it is also capable of deactivating the compounds before arriving at the target[73]. In the case of Top II, it performs a crucial role related to the unrolling of coiled DNA to facilitate replications and transcription[74]. The TS helps to the maintenance of deoxynucleotides needed for DNA synthesis[75]. Also, the RNR is the one in charge of the synthesis of DNA from the blocks of RNA[69]. Following the previous considerations, the relevance of NO ligand types is taken into consideration in this work.

1.5. Lymphocytes as Study Targets

Lymphocytes are the cells responsible for the induction and expression of adaptive immunity of the body[76]. There are approximately $2x10^{12}$ lymphocytes in the human body, a quantity that can be compared with the brain in terms of the number of cells[77]. There are two major types of Lymphocytes, T cells, and B cells, which are called that way because of the organs they come from. In the case of T cells, they are developed in the thymus, and B cells are produced in the bone

marrow[77]. Lymphocytes are specialized cells that represent the principal mechanism of defense against extracellular pathogens like bacteria. The primary function of lymphocytes is to recognize antigens (strange molecules to the organism), the production of antibodies to neutralize them, regulation of the immune system, and the cell-mediated killing of the tumor and virus-infected cells[78].

Regarding the *in vitro* tested metals, in their ionic form or by forming coordination compounds, cobalt complexes used to study the effect on lymphocytes cell cultures have shown that as the concentrations of the complexes increase, the cell viability decreases[79]. The inhibition of lymphocyte proliferation at high concentrations ended with cells becoming apoptotic, and consequently, a reduction in cell activation and proliferation was experienced[79]. Copper (II) compounds with nitrogen donor ligands (ethylenediamine) have been studied in lymphocytes cell cultures; their apoptotic effect was explained by better penetration of the compound through the cell wall, which converts it into a potential anticancer drug[80]. Furthermore, *in vitro* studies involving nickel compounds revealed that normal human lymphocytes were sensitive to nickel, and processes such as depletion and reduction of the cytotoxic properties of Natural Killer cells (NK) were related to the enhancement of cell death mechanisms[81]. Mononuclear ruthenium complexes containing a series of pyridine and imidazole ligands have also demonstrated inhibitory proliferation activities against lymphocyte cell cultures[82]. Proposals suggest that the mechanism of action tends to differ for some of the complexes; then, the information obtained will serve to identify the specific targets of this compounds[82].

Taking into account the previous considerations, the studies of coordination compounds and its interactions with healthy and essential cell lines, such as lymphocytes, is a fundamental step if the approach of an efficient drug wants to be achieved.

1.6. Cell Viability Assays

In vitro assays are primordial due to their potential uses in drug discovery; their importance is established in the determination of tolerable and threshold levels of emerging drugs, but also in the determination of several points of DNA damage (genotoxicity), and cytotoxicity[83]. Cell-based assays are used to determine the effect of a series of compounds on cell proliferation, but also the direct cytotoxic responses that lead to cell death[84]. Despite the kind of cell-based assay used, the number of viable cells is going to be relevant at the end of the experiment. Then, there are several

methods used to determine the number of viable cells by considering several properties related to cells correct behavior. Examples of them are membrane leakage assays, mitochondrial activity, functional assays, genomic and proteomic assays, and flow cytometry assays.

In the case of membrane leakage assays, the use of dyes such as propidium iodide, trypan blue, and 7-Aminoactinomycin D serve as identifiers of the lactate dehydrogenase (LDH); an enzyme encountered in all types of cells, which can be detected when cell membranes are damaged, associating them with cell death[85]. Regarding mitochondrial activity, dyes like resazurin are irreversibly reduced to resofurin by aerobic respiration of metabolically active cells, which is an indication of cell viability[86]. Functional assays will depend on the type of cell investigated; for example, motility assays are used in the case of sperm cell function; characteristics like deformability, hemolysis, and hemoglobin content are assessed to red blood cells; and gamete survival can be an identifier of fertility[87]. Genomic and proteomic assays are made by activating stress pathways in the cells using DNA microarrays or protein chips, respectively[88,89]. The analysis of cell viability by flow cytometry represents an automized process used to determine and measure the number of viable cells, their characteristics, and functions[90].

Dose-Response curves emerge as a result of cell-based assays and are used to establish the relationship between the drug doses and the number of organisms that present a determined effect[91]. Generally, as the concentration of the dose increases, the number of affected individuals will increase as well. Several types of dose-response curves can be presented for a determined compound, depending on the type of effect. Usually, when toxic effects are studied in big populations, the curve possesses a sigmoidal form[92]. This kind of curves reveal the variations between the subjects of study which belong to the same population; the slope of the curve varies according to the chemical substance used and the type of response[92]. There are some cases in which compounds possess specific effects (carcinogenic, mutagenic, initiators) whose dose-response curves present linearity from the zero dose, which means there is no threshold, representing a potential risk[92].

In toxicology, there is a term called *dose descriptor*, which is used to identify the relationship that exists between a drug dose and the specific effect presented. Dose descriptors are generally expressed as LD_{50} (median lethal dose), LC_{50} (median concentration dose), EC_{50} (median effective concentration), NOAEL (No Observed Adverse Effect Level), etc. Each dose descriptor is used

depending on the conditions and effects to be evaluated; for example, LD_{50} is used to present the dose at which 50% of a species is expected to die; at lower values, the compounds are more cytotoxic[93]. LC_{50} is used to describe air concentration, i.e., inhalation toxicity[94]. EC_{50} is related to the concentration of the substance at which 50% immobilization reduction takes place, usually used in aquatic toxicity studies[95]. Finally, NOAEL is typically obtained in repeated dose studies that last 28 days, used to derive threshold safety dose for humans[96].

2. CHAPTER TWO: PROBLEM STATEMENT & HYPOTHESIS

The significant development and efficacy of antitumor drugs like Cisplatin, Carboplatin, and Oxaliplatin against ovarian, bladder, and testicular cancers have placed the starting pathway to the analysis and development of novel metallic – based drugs. There is the fact that the number of patients cured after Cisplatin cancer treatment is impressive; however, the potential activity displayed by Cisplatin got limited in the presence of most common types of cancer, such as colon and breast. Besides, a variety of adverse effects and acquired resistance are observed in patients receiving cisplatin chemotherapy. As a consequence, platinum-based drugs have provided a fertile ground for exciting bioinorganic and coordination chemistry research.

As mentioned in the previous chapter, a significant part of the coordination compounds that presented antitumoral activity contained nitrogen and oxygen donor atoms that were part of the ligands. Also, the different ways in which NO-based ligands can interact with biological receptors were presented. Moreover, the representative anticancer activities exposed by transition metals such as Co(II), Cu(II), and Ru(III) (in their ionic forms) can be used to potentiate the anticancer properties of the ligands.

As a hypothesis, it has been proposed that the synthesized coordination compounds will possess octahedral structures in which nitrogen and oxygen atoms will act as electron donors. Also, ligands such as chlorine atoms will favor the ionization of the compounds under physiological conditions, promoting an effect in the cell viability of lymphocytes cell cultures.

3. CHAPTER THREE: OBJECTIVES

3.1. General Objective

Design and develop novel types of coordination compounds with potential anticancer activities.

3.2. Specific Objectives

- Synthesis of a NO-based donor ligand using ethylenediamine and tartaric acid as starting reagents.
- Synthesis of the coordination compounds with the ligand obtained and the transition metals Co(II), Cu(II), Ni(II), and Ru (III).
- Characterization of the compounds by using Ultraviolet-Visible Spectroscopy (UV-Vis), Diffuse Reflectance Spectroscopy (DRS), Infrared Spectroscopy (IR), X-Ray Powder Diffraction (XRPD), X-ray Photoelectron Spectroscopy (XPS).
- Perform cell viability studies by using the obtained coordination compounds on lymphocytes cell cultures, and obtain the LD_{50} values (cytotoxicity) of the compounds.

4. CHAPTER FOUR: METHODOLOGY

4.1. Reagents and Equipment

Reactants

Biological system (Lymphocytes cell culture)	**Inorganic systems (Coordination compounds of Co, Ru, Cu, Ni)**
RPMI-1640 (Sigma Aldrich) Trypan Blue 0.4% (Sigma Aldrich) Formaldehyde 37% (Sigma Aldrich) Bovine Fetal Serum (Sigma Aldrich) Antibiotic (Sigma Aldrich) DMSO (≥99% Sigma Aldrich) NaCl Saline solution (Sigma Aldrich) Ficoll – Paque^{TM} reagent (Sigma Aldrich)	Tartaric acid (99% Sigma Aldrich) Ethylenediamine (99,5% Sigma Aldrich) HCl (37% Sigma Aldrich) $CoCl_2{*}6H_2O$ (98%Sigma Aldrich) $Cu(NO_3)_2$ hydrate (99.999% Sigma Aldrich) $NiCl_2$ anhydrous (99,99% Sigma Aldrich) $RuCl_3{*}3H_2O$ (99,98% Sigma Aldrich) Methanol (99.8% Sigma Aldrich) Acetone (≥99.5% Sigma Aldrich) KBr (Analytical reagent – Sigma Aldrich)

Laboratory Equipment

- Jenway 6705 UV/ Vis Spectrophotometer.
- FT-IR Bruker Tensor 27 Spectrophotometer
- Perkin Elmer LAMBDA 950 UV/Vis/NIR Spectrophotometer
- SPECS using a PHOIBOS 150 WAL analyzer.
- Rigaku Miniflex 600 X-Ray Diffractometer.
- Cell counting equipment-Hemocytometers (Bright-Line)
- Corning® 96 wells plates.
- Micropipettes (2,10, 100, 1000) µL

4.2. Synthesis of the ligand

A similar procedure proposed by Sheikh, Wani, Shreaz, and Hashmi (2016) was used[97]. Tartaric acid (0.05 mol) was dissolved in hot ethanol (25 mL). Then, a hot ethanolic solution (25mL) of ethylenediamine (3.34mL, 0.05 mol) was made. Both solutions were mixed and concentrated HCl (2mL) was added immediately. A white cream precipitate was formed. Then,

the reaction was kept with constant stirring at 70 ^{o}C for 30min. The precipitate was filtered at vacuum, washed with ethanol, and recrystallized from hot water. Yield: 78%; mp = 144 – 148 ^{o}C

4.3. Synthesis of the Cobalt (II) complex

A solution of NaOH (0.080 g) in 10 mL of methanol was added to a solution of the ligand (0.243 g) in 5 mL of hot water with continuous stirring. Then, $CoCl_2{*}6H_2O$ (0.124 g) was added to the resulting solution. A dark pink precipitate was formed immediately. After 1h under constant stirring and heating at 60 ^{o}C, the precipitate was filtered at vacuum, washed with ethanol, acetone, and pulverized in the Agate Mortar. Yield: 60%; mp = 120 – 130 ^{o}C.

4.4. Synthesis of the Ruthenium (III) complex

The synthesis was made following the methodology described above but using $RuCl_3{*}xH_2O$ (0.144 g) instead of $CoCl_2{*}6H_2O$. The mass of NaOH used was 0.077 g, and the quantity of the ligand 0.242 g. The volumes and temperature used were the same as in the Co (II) compound. A gray-black precipitate was formed, filtrated, washed with ethanol, and homogenized using the Agate mortar. Yield: 56%; mp >350 ^{o}C

4.5. Synthesis of the Nickel (II) complex

Considering that $NiCl_2$ was anhydrous, three solutions were prepared. The first solution consisted of anhydrous $NiCl_2$ (0.136 g) in 3 mL of water to hydrate it, followed by the ligand solution, which was prepared by using 0.52 g in 7 mL of hot water. The third solution was made by using NaOH (0.168 g) in 16 mL of methanol. The NaOH solution was added to the ligand solution with constant stirring, followed by the addition of the $NiCl_2$ solution to the resulting one. A light green precipitate was formed immediately. After 30 min at 60 ^{o}C, it was filtrated at vacuum, washed with ethanol, and pulverized in the Agate Mortar. Yield: 75%; mp = 140 – 145 ^{o}C

4.6. Synthesis of the Copper (II) complex

The compound was synthesized by a similar methodology described in the case of Cobalt (II) and Ruthenium (III) compounds. The solution of NaOH was prepared by using 0.14 g in10 mL of methanol. The ligand solution was prepared by using 0.44 g in 7 mL of hot water; then, 0.16 g of $Cu(NO_3)_2{*}H_2O$ was added to the resulting solution. A sky-blue precipitate was formed instantly. The reaction was kept for 1h under stirring, and the compound was filtrated at vacuum, washed with acetone, and pulverized in the Agate Mortar. Yield: 50%; mp = 150 – 160 ^{o}C

4.7. Characterization of the compounds

4.7.1. UV Vis Spectroscopy

UV-Vis Spectra were recorded at Centro de Nanociencias y Nanotecnología – UNAM, using a Jenway 6705 UV/ Vis Spectrophotometer in the range of 200–1100 nm.

4.7.1.1. Analysis of the Optimal Concentration and Wavelength to Apply Jobs Method

Different standard solutions were prepared for the metals used on the synthesis. Those standard solutions were diluted to study different concentrations and observe which one is optimal to work, as well as its corresponding wavelength. In the case of Cobalt (II), 0.0238 g of $CoCl_2{*}6H_2O$ were taken to make 5 mL a solution of concentration 0.1 M. Then, the volumes observed in Table 1 were taken and filled with distilled water to reach 1 mL, the UV – Vis spectra measurements were from a concentration range of 0.01 M - 0.1 M.

Table 1. Concentrations and required volumes to generate the solutions.

Required Concentrations (M)	The volume took from metals solution (mL)	The volume of water needed to aforate (mL)	Total Volume of the new solution (mL)
0.09	0.9	0.1	1
0.08	0.8	0.2	1
0.07	0.7	0.3	1
0.06	0.6	0.4	1
0.05	0.5	0.5	1
0.04	0.4	0.6	1
0.03	0.3	0.7	1
0.02	0.2	0.8	1
0.01	0.1	0.9	1

Regarding Nickel (II), 0.013 g of anhydrous $NiCl_2$ were taken to make 5 mL of a 0.1 M solution. Then, the dilution and measurement procedures were the same as for Cobalt (II). To make the solution of Copper (II), 0.0187 g of $Cu(NO_3)_2{*}H_2O$ were taken, and a 5 mL solution of concentration 0.1 M was made. The measurement process used for Cobalt (II) was followed. In the case of Ruthenium (III), a first solution of $RuCl_3{*}H_2O$ with a concentration of 0.01 M was made. Then, it was diluted to a concentration of 0.001 M. From the second solution, different volumes were taken to give the required concentrations, the UV – Vis measurements were made in the range of $1x10^{-4}$ M – $1x10^{-3}$ M.

4.7.1.2. Job´s Method

Once the concentrations and wavelengths were determined for each metallic solution, the Job´s method was performed. It was used to know the stoichiometric relationship at which the formation of a coordination compound can be produced. It consisted of the reaction of two equimolar solutions in different proportions (metal: ligand), always keeping constant the final volume (1 mL in this case). Values in Table 2 were followed to prepare the needed solutions:

Table 2. Different quantities of the metal and ligand solutions, corresponding to the concentrations selected.

Taken volume of metal solution (mL)	Taken volume of ligand solution (mL)	Total volume in Eppendorf (mL)	(Metal:Ligand) proportions
0.1	0.9	1	1:9
0.2	0.8	1	2:8
0.3	0.7	1	3:7
0.4	0.6	1	4:6
0.5	0.5	1	5:5
0.6	0.4	1	6:4
0.7	0.3	1	7:3
0.8	0.2	1	8:2
0.9	0.1	1	9:1

Solutions were made in 1 mL Eppendorf tubes. The solvent used was distilled water. Then, the corresponding proportions of the metal solutions were added to the volume of ligand solution in the Eppendorf, and the spectra were recorded (from 200–1100 nm). The solutions of the ligand had the same concentrations as the ones for the metals.

4.7.1.3. Study of the behavior of the metals when coordinated with tartaric acid and ethylenediamine by separate.

The study consisted of the preparation of different solutions of the metals at determined concentrations, followed by the addition of tartaric acid, and ethylenediamine, in proportions of one, two, and three molar equivalents. Then, the different absorbance spectra were measured in a range of 200 – 1100 nm. The concentration of Ruthenium (III) chloride was $1x10^{-4}$M. In the case of Cobalt (II) chloride, Copper (II) nitrate, and Nickel (II) chloride, the concentration used was $1x10^{-2}$M.

4.7.1.4. UV - Vis spectroscopy of compounds in solution

The coordination compounds of Co(II), Cu(II), Ni(II), and Ru(III) were dissolved in water to the same concentrations as used in the Jobs method; a quartz cuvette (1 cm optical path) was used,

and the range of measurement was from 200 nm to 1100 nm. The UV-Vis spectra were obtained with Origin 2017.

4.7.2. Diffuse Reflectance Spectroscopy (DRS)

The diffuse reflectance spectra of the coordination compounds were measured at Yachay Tech University, Ecuador. The spectra were used to confirm the electronic transitions observed in UV-Vis, but also to visualize the effect of the solvent, i.e., if it caused a particular change in the position of the bands related to the electronic transitions of the metals. The equipment used was a Perkin Elmer LAMBDA 950 UV/Vis/NIR Spectrophotometer; the range of measurements was from 200 nm to 900 nm, and a Praying Mantis accessory was used to place the samples. The Diffuse Reflectance Spectra was obtained by using Origin 2017.

4.7.3. Fourier Transform -Infrared Spectroscopy (FT – IR)

IR spectra were recorded in the Centro de Nanociencias y Nanotecnología – UNAM, Mexico, employing an FT-IR Bruker Tensor 27 Spectrophotometer in the range of 4000–350 cm^{-1}. A minimum quantity of each sample compound was pulverized in an Agate mortar with KBr salt; then, a pressure machine was used to generate the disks, and the samples were measured. The Infrared spectra were obtained using Origin 2017.

4.7.4. X-Ray Powder Diffraction (XRPD)

X-Ray Diffractograms were recorded using a Rigaku Miniflex 300/600 X-ray Diffractometer in the range of 3 to 70^{o}; the X-Ray generator was fixed at 40 kV, 15 mA. The scan mode was 1D; the scan speed/duration time was 30.00^{o}/min, and the step width was 0.01^{o}. Crystalline sample of the ligand was pulverized in the Agate Mortar; then, the powder was used to fill the sample plate, and it was compacted with a glass plate. Finally, the samples were measured. The X-Ray diffractogram was obtained by using Origin 2017.

4.7.5. X-Ray Photoelectron Spectroscopy (XPS)

All the compounds, including the ligand and the four coordination compounds, were analyzed by XPS. The survey and high-resolution spectra for each one of the elements were taken. The spectra were collected at the Centro de Nanociencias y Nanotecnología - UNAM, Mexico, by using a SPECS system with a PHOIBOS 150 WAL analyzer and a monochromatized Al Kα line (1486.6

eV) from µ-FOCUS 500 x-ray monochromator. The samples were measured at110W with a base pressure of1e-9 torr. The graphs were obtained using CasaXPS.

4.8. Biological Activity Assays

4.8.1. Extraction of blood

Regarding the selection of the people, the requirements were healthy persons, without consuming any drugs, and with plenty of sleep to assure the correct state of the cells without being affected by other factors different from the stimulus assessed by the compounds. To be reported, each experiment has to be repeated at least three times, preferably on different days. Blood (15 mL) was extracted from the subject by using three EDTA-Vacutainer^{TM} tubes (5 mL each). Then, the blood samples were placed in a Falcon (50 mL) sterile tube, followed by the same quantity of saline NaCl solution. The total volume in the tube was 30 mL The blood and saline solution were mixed by gently inverting the tube several times.

4.8.2. Separation of lymphocytes

The Ficoll-Paque product has to be prepared; for this, a temperature between 18 and 20 °C is needed, which can be achieved by introducing the reagent into the laminar airflow hood. Another Falcon tube (50 mL) was used to place 5.5 mL of the Ficoll reagent. The content of the tube containing blood was slowly added to the tube containing Ficoll. The content started to separate into layers. The process was followed by centrifugation at 400 *g* for 25 minutes. After the centrifugation, three layers appeared in the tube, the bottom one corresponding to red cells (erythrocytes), the medium layer contains lymphocytes, and the upper layer containing platelets. The top layer was saved. The lymphocytes were carefully collected by using a 1000 µL micropipette. The lymphocytes content (1.5 mL approximately) was placed in a (15 mL) Falcon tube, followed by the addition of RPMI-1640 (6 mL) and 0.6 mL from the upper layer of the previous tube. The cells were resuspended and placed under centrifugation at 400 *g* for 15 minutes. After the centrifugation, the supernatant was removed.

4.8.3. Incubation

Inside the laminar airflow hood, two Petri plates were prepared with 8 mL of RPMI-1640 medium. To each of these plates, half the content of the tube with lymphocytes was deposited. Antibiotic (3 µL) was added to avoid contamination of the sample. The cells were resuspended

using a micropipette, and 10 µL were taken in order to realize a cell counting before the incubation. This process was made to know what is the approximate number of cells that we could work with. The 10uL were placed in an Eppendorf tube and taken out of the hood. The Petri plate was closed and collocated to incubate for 2h at 37 ºC and 5% CO_2.

4.8.4. Cell counting

Once the cells have been placed to incubation, to the Eppendorf tube with 10 µL of medium with lymphocytes, 10 µL of a (9:1) solution of trypan blue was added. The content of the Eppendorf tube was removed with the help of a micropipette, and 10µL were placed in a hemocytometer camera, also called Neubauer camera. The Neubauer camera was collocated in the microscope, and the number of cells was counted at 40x. From this number, calculations were made according to the number compounds used, its concentrations, and the desired amount of repetitions.

4.8.5. Cell Viability Assays - Lymphocytes culture

A number of 4 x 10^4 Lymphocytes per well was used in a 96 – well microplate with RPMI-1640 supplemented with 10% fetal bovine serum (FBS). Samples without the addition of stimulus were used as control. The negative control was RPMI-1640, and the positive control was DMSO. Then, the addition of 10 µL of the test compounds at different concentrations was carried out; the ranges of concentrations were from millimolar to micromolar values. The plate was placed to incubate at 37 ºC and 5% CO_2 for 24 h.

4.8.6. Trypan Blue Exclusion Method

Once the incubation time was ended, the cells in the wells were subjected to staining and fixation using 2 µL of Trypan Blue solution and 20 µL of Formaldehyde (3.7%), respectively. Then, the plate was moved to the fridge, and after 30 min, each one of the wells was counted using a Neubauer camera and a microscope at 40x.

The experiments in this thesis project were performed in triplicate. Cell viability graphs and dose-response curves were obtained using the mean values of the three experiments. The program used was Prism GraphPad 8.

5. CHAPTER FIVE: EXPERIMENTAL RESULTS AND DISCUSSION

The content of this chapter will be divided into two sections. The first part will consist of the characterization of the synthesized ligand and the respective coordination compounds by several spectroscopic techniques. In addition, the second part will cover the analysis of the results corresponding to the cell viability studies performed in lymphocytes cell cultures.

5.1. X-Ray Powder Diffraction (XRPD)

5.1.1. Ligand

The X-Ray diffractogram (Figure 8) of the synthesized ligand (red) was compared with the diffractogram data stored in the Crystallography Open Database (COD)[98] giving the following diffractogram and the structures seen in :

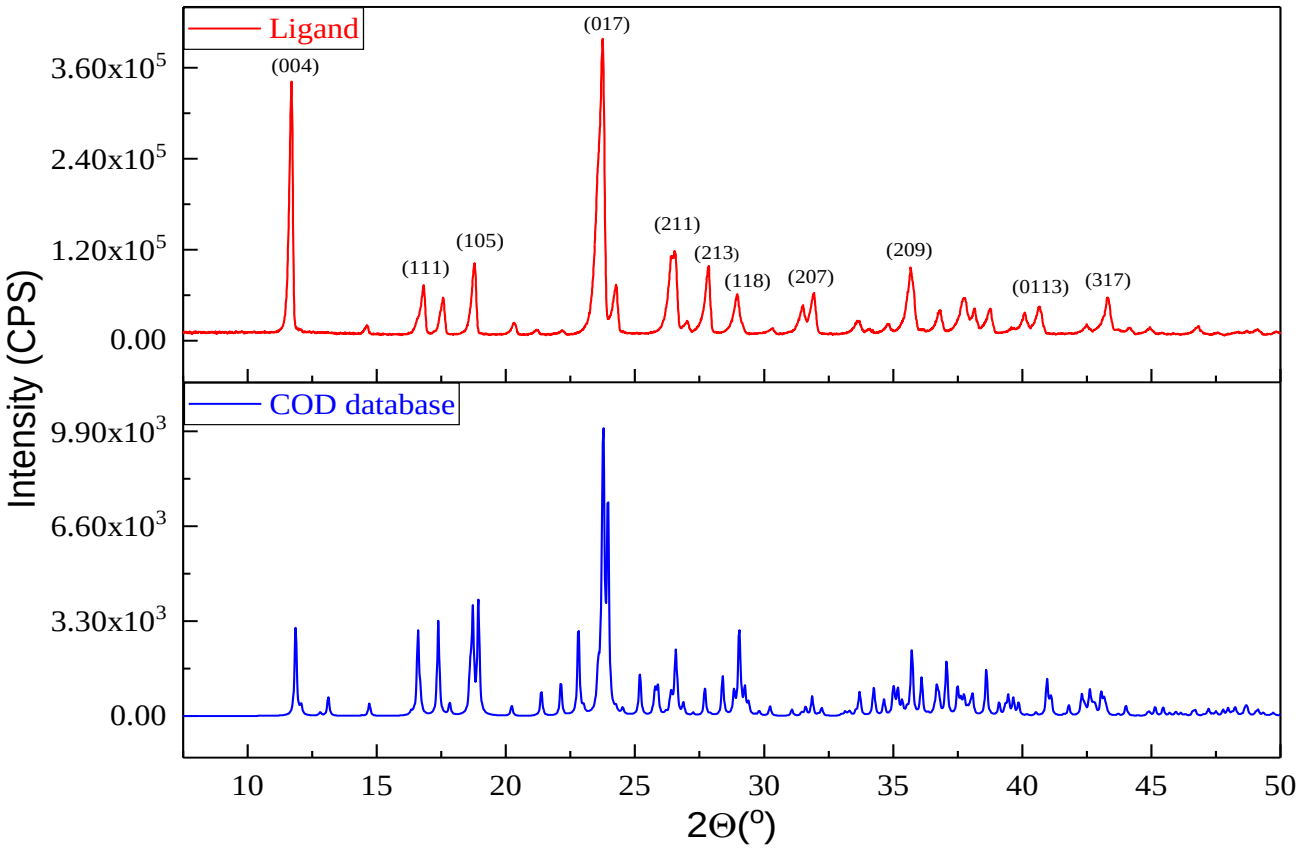

Figure 8. X-Ray Diffractogram corresponding to the synthesized ligand compared with the COD Database (Adapted from. Ref 98)

The diffractogram corresponding to the ligand presented the same signals as the compound in the COD database. As the XRPD is a deterministic technique, the structure of the synthesized

ligand is presented and will be evaluated by other spectroscopic techniques such as infrared spectroscopy and XPS.

Regarding the structural information, the formula is $C_5H_{14}N_2^{2+}$, $2(C_4H_5O_6)^-$, H_2O. It is an orthorhombic structure with the corresponding space group $P2_12_12_1$. The cell lengths a= 7.5571, b=7.7903, c=29.8324, and cell angles α=90 °, β=90 °, γ=90°. The cell volume is 1756.3 $Å^3$.

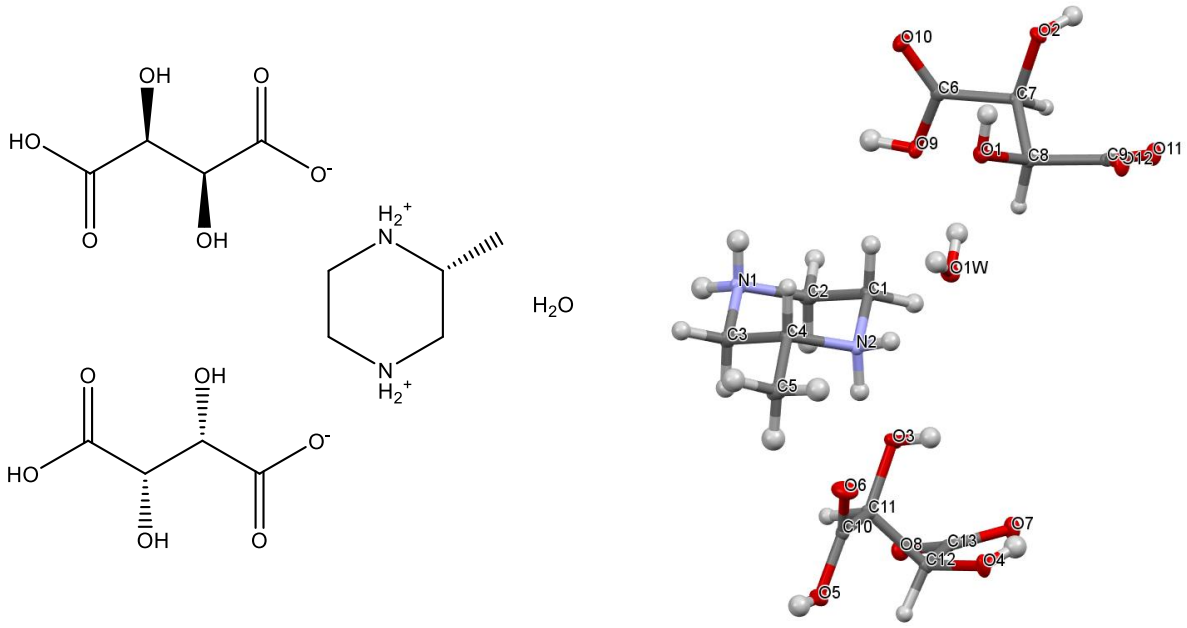

Figure 9. Structure of the ligand (R)-2-methylpiperazine-1,4-diium (2S,3S)-3-carboxy-2,3-dihydroxypropanoate hydrate and its 3D structure asymmetric unit (Adapted from Ref 98)

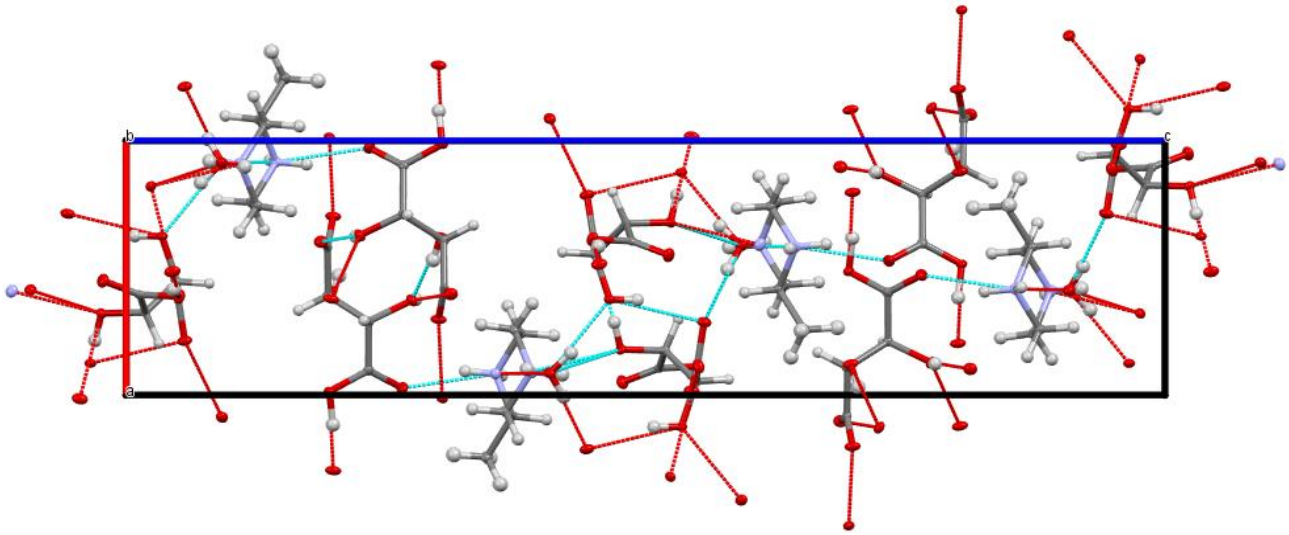

Figure 10.The 3D packing structure of the ligand along the b axis (Adapted from Ref 98).

The compound $C_{13}H_{26}N_2O_{13}$ possesses a molecular weight of 418.35 g/mol. Also, the 3D structure of the ligand was obtained in Mercury. As can be observed, 2-methylpiperazine has two nitrogen atoms; each of them possesses two hydrogen atoms, which converts them into quaternary ammonium ions.

The piperazine ring has a stable chair conformation which possesses a methyl group in an equatorial position. Also, it was found the presence of two tartrate units that regulate the cationic charge presented by the cycle. A high presence of hydrogen bonds can be assessed and related to the contribution of hydroxyl groups in the tartrate ions, but also in the piperazine ring. The Figure 9 shows the 3D structure of the asymmetric unit of the ligand with labeled atoms. The water molecules seem to be interacting with the tartrate units and the piperazine cycle. Moreover, the packing structure along the *b* axis was obtained and shown in Figure 10. From the packing structure, it can be visualized the formation of layers between the tartrate ions by the hydrogens corresponding to hydroxyl groups. Also, the tartrate groups belonging to different layers do not present hydrogen bonds. In addition, the piperazine ion is located between the tartrate layers and possesses four hydrogen bonds, two with water molecules, but also two with tartrate. The high presence of hydrogen bonds gives great stability to the ligand. Finally, the data used to plot the ligand diffractogram and error graph associated with the coincidence of structures will be shown in the appendixes section.

5.2. Fourier Transform Infrared (FT-IR)

5.2.1. Tartaric acid

The infrared spectra of tartaric acid is presented in Figure 11 (black signal). The presence of the bands at 3406 cm^{-1} and 3336 cm^{-1} are assigned to OH stretching modes of the alcoholic, and carboxyl groups in tartaric acid. The weak bands at 2968 cm^{-1} and 2935 cm^{-1} correspond to CH stretching modes. Also, the strong band presented at 1738 cm^{-1} is characteristic of the carboxyl groups stretching. In addition, the band presented at 1448 cm^{-1} correspond to the CO mode. The bands observed at lower frequencies are not described as the structure of tartaric acid has been confirmed.

5.2.2. Ligand

IR spectra of the ligand is shown in Figure 11 (red signal). The presence of a secondary amine can be suggested by the non-well-defined band presented at 3500 cm^{-1}, which not appeared in a sharped form due to the intensity corresponding to hydroxyl groups stretching of the tartrate unities that are shown at 3330 cm^{-1} and 3272 cm^{-1}. Also, there is the presence of a shoulder band at 3190

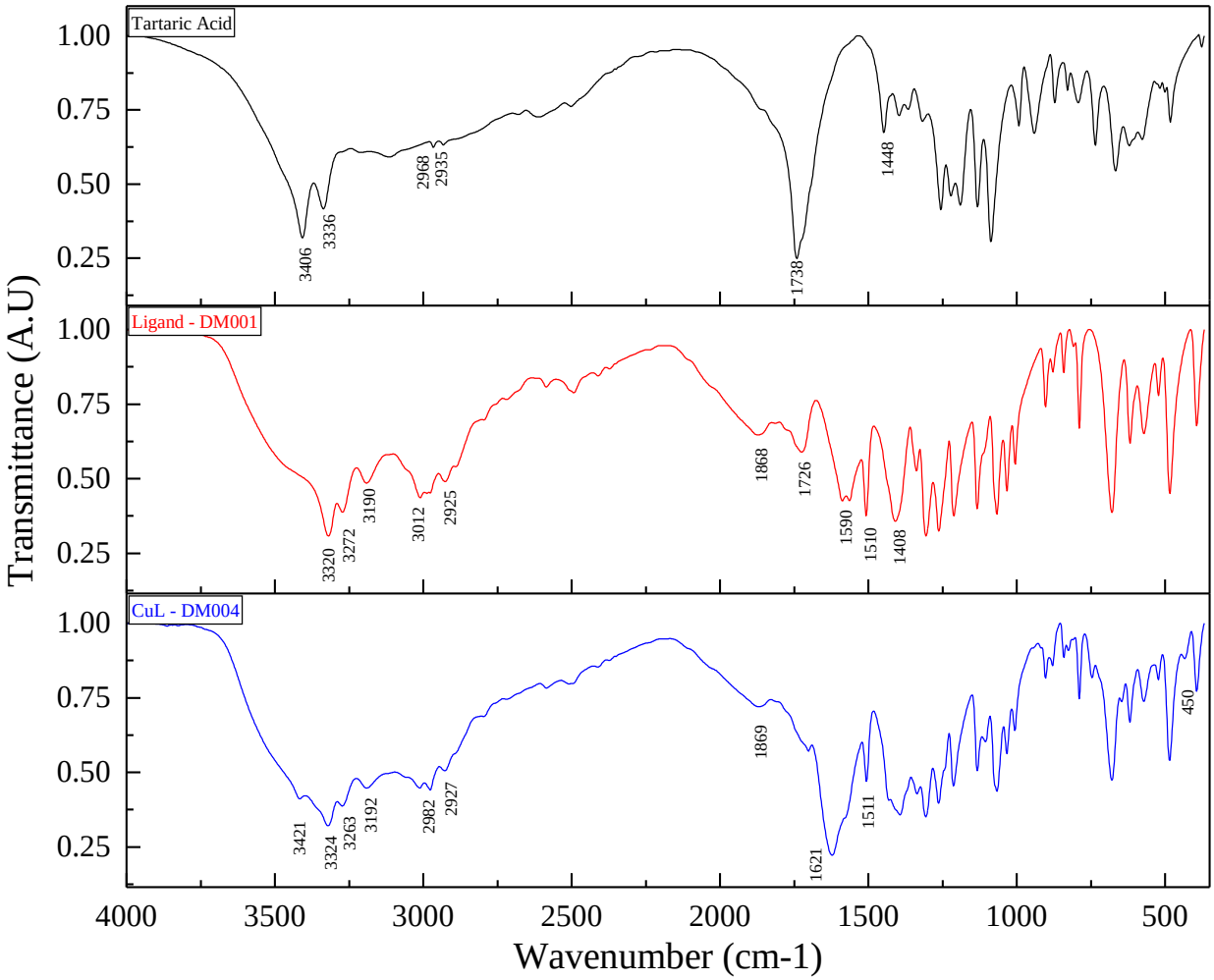

Figure 11. Infrared spectra corresponding to Tartaric acid, the ligand, and Copper coordinated.

cm^{-1}, which used to appear in the presence of primary amines or secondary amines. The bands at 3012 and 2925 cm^{-1} are from the CH stretching bonds. In addition, the bands present at 1868 cm^{-1} and 1726 cm^{-1} correspond to two different types of carbonyls; from the carboxylate (ionized) and carboxylic (non-ionized) groups of the tartrate, respectively. The double-humped band at 1590 cm^{-1} can be associated with the presence of the amine. Finally, the band at 1411 cm^{-1} is related to the carbon-nitrogen bond, which is visible and comparable in the structure.

5.2.3. Metallic Compounds (ML):

In the case of coordination compounds, Figure 11 (blue signal) corresponds to the Copper (II) compound, used as an example. The amine band (not clearly defined in the ligand spectra) is presented at 3421 cm^{-1}. The bands corresponding to hydroxyl (3324 and 3263 cm^{-1}) and CH (2982 and 2927 cm^{-1}) stretching groups are presented as well. Moreover, the bands corresponding to carbonyl groups (1800 cm^{-1}) almost disappeared from the spectra; instead, a high-intensity band appears at 1621 cm^{-1}, which is typically presented in the case of amines, and sometimes is confused with carbonyl signal. The presence of bands in the region around 550 – 330 cm^{-1} is related to metal – nitrogen (M-N) bonds, but also to metal-oxygen (M-O) bonds[99]. In the case of cobalt, copper, and nickel compounds, those bands were presented at 450 cm^{-1}, 435 cm^{-1}, and 560 cm^{-1}, respectively. Regarding the ruthenium compound, the resolution of the spectra does not allow us to identify peaks related to M-N bonds or M-O bonds.

In all cases, when the metal is coordinated to the ligand, the masked N-H band at 3500 cm^{-1} became visible; furthermore, the appearance of a broadband in the range of 1625 – 1614 cm^{-1} (characteristic of amines), and the disappearance of the carbonyl signals suggest that the coordination was made by oxygen atoms from carbonyls. If the metals were coordinated to nitrogen atoms from the amine, it would become a tertiary amine, giving no signals in the spectra.

5.3. UV-Vis

5.3.1. UV-Vis of the metallic salts

$CoCl_2$ hexahydrate dissolved in water: The electronic configuration of a Co^{2+} ion is [Ar] $3d^7$. Cobalt (II) chloride spectra (Figure 12) reveals two almost overlapped absorption bands at λ_1 = 477 nm (20964 cm^{-1}) and λ_2 = 512 (10Dq = 19550 cm^{-1}), which correspond to the high spin electronic transitions $^4T_{1g}$ (F) → $^4A_{2g}$ (F) and $^4T_{1g}$ (F) →$^4T_{1g}$ (P), respectively. Also, around 1100 nm, there is the presence of another band of lower energy. In this case, the associated transition is $^4T_{1g}$ (F) → $^4T_{2g}$ (F).

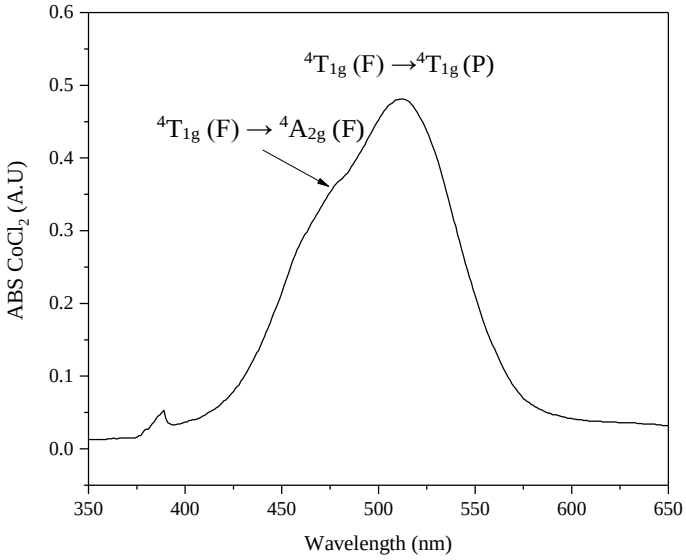

Figure 12. UV – Vis spectra of the metallic $CoCl_2$ in solution in the range of 350 – 650 nm.

$Cu(NO_3)_2$ hydrate dissolved in water: Cu^{2+} ion possesses the [Ar] $3d^9$ electronic configuration. Copper (II) nitrate shows one absorption band (Figure 13) at λ_1 = 800 (10Dq = 12500 cm^{-1}), which corresponds to the electronic transition $^2E_g \rightarrow {}^2T_{2g}$. Additionally, there is a band at 300 nm related to a charge transfer process.

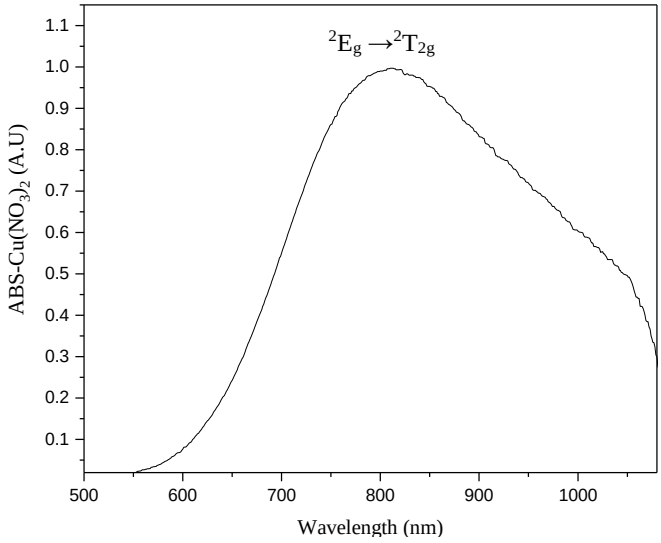

Figure 13. UV – Vis spectra of the $Co(NO_3)_2$ in solution in the range of 500 – 1060 nm

$NiCl_2$ anhydrous dissolved in water: The electronic configuration of the Ni^{2+} ion is [Ar] $3d^8$. For a d^8 octahedral species, three absorption bands are typically present. Those bands are at λ_1 = 398 nm (25125 cm^{-1}), λ_2 = 655 nm (15267 cm^{-1}), and λ_3 = 726 nm (10Dq = 13774 cm^{-1}) (Figure 14). The electronic transitions related to the bands are $^3A_{2g}$ (F) →$^3T_{1g}$ (P), $^3A_{2g}$ (F) →$^3T_{1g}$ (F), and $^3A_{2g}$ (F) →$^3T_{2g}$ (F), respectively.

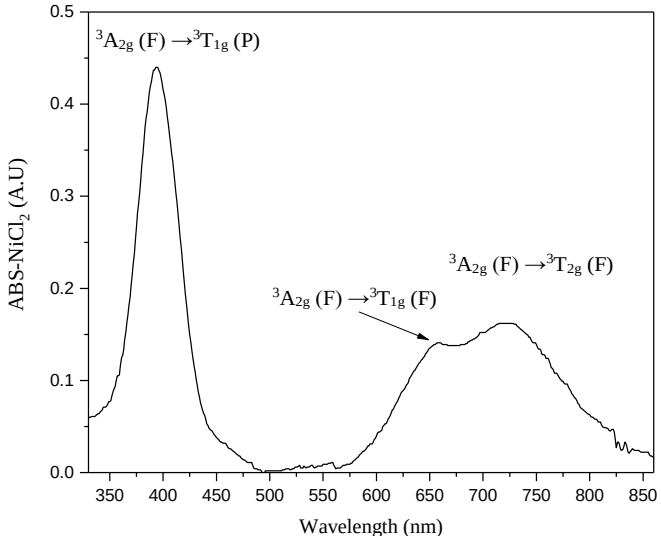

Figure 14. UV -Vis spectra of the Nickel compound in solution

$RuCl_3$ hydrate dissolved in water: The metallic ion Ru^{3+} presents an electronic configuration of [Kr] $4d^5$. Ruthenium (III) chloride revealed and absorption band (Figure 15) at λ = 508 nm (10Dq = 19685 cm^{-1}), corresponding to the spin forbidden electronic transition $^6A_{1g} \rightarrow ^4A_{1g}$ (D). The transition possessed lower intensity, this because is due to species like Ru (III) and Fe (III) present a d^5 configuration with high spin behavior of the ligands (in this case, water molecules), meaning that only forbidden transitions would be present according to Tanabe-Sugano diagram for a d^5 species; then, the transitions can be observed at low absorbance values or even not observed[100].

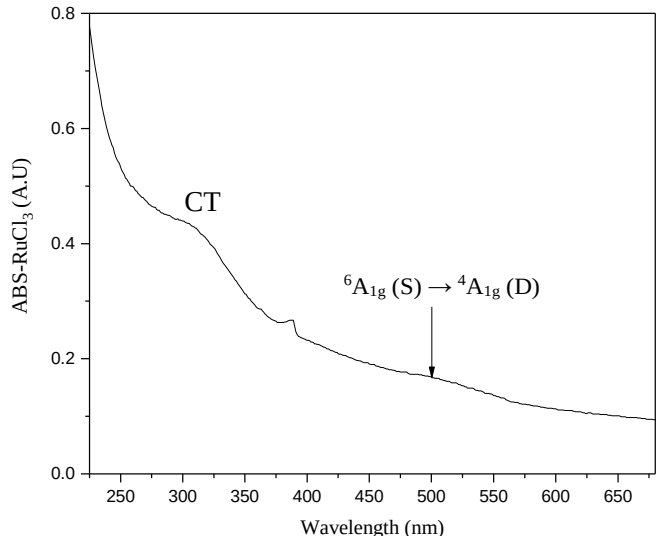

Figure 15. Ruthenium Chloride UV – Vis spectra in the range of 200 – 680 nm.

5.3.2. Analysis of the Optimal Concentration and Wavelength to Apply Jobs Method

In order to apply the Job´s method, the optimal concentrations and wavelengths corresponding to the metallic salts in solutions were determined. In the case of the Cobalt(II) solution, the selected concentration was 0.01 M and the wavelength 512 nm. The Copper (II) solution had a concentration of 0.01 M, and the selected wavelength was 810 nm. The preferred concentration was 0.01 M, with a wavelength of 394 nm for the Nickel (II) compound. Finally, in the case of Ruthenium (III), the selected concentration was $1x10^{-4}$ M; the concentration chosen is due to Ruthenium presented absorbance values much higher as the concentration increased. The chosen wavelength was 508 nm.

5.3.3. Study of the Behavior of the Metals When Coordinated to Tartaric Acid and Ethylenediamine by Separate.

In the case of the addition of tartaric acid, it was observed that for each metal, the absorbance peaks moved towards higher values of energy, i.e., lower wavelengths. The contrary behavior was observed with the addition of ethylenediamine to the solution of the metals. Then, oxygen-containing ligands induce hypsochromic shits, while nitrogen-based ligands induced a bathochromic shift in the absorbance spectra. Therefore, as both compounds possess electron donor atoms sharing contrary energy shifting properties, it is useful to determine if the metallic ions coordinate to form the respective coordination compounds with the ligand.

5.3.4. Job´s Method

Job´s method was used to determine the possible coordination compounds that should be produced, depending on the concentrations of metal:ligand used. The figures present in the Y-axis, the absorbance of the compounds, and in the X-axis, the increasing molar fraction of the metal respect the ligand.

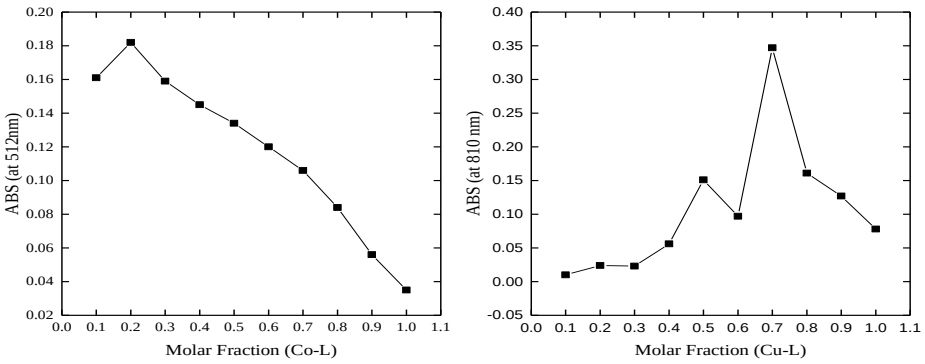

Figure 16. Job's method applied to the coordination compounds of Cobalt (II) and Copper (II).

Regarding the Cobalt (II) and Copper (II) compounds, Figure 16 shows the absorbance values at the chosen wavelength (512 nm) for each one of the metallic salts plotted against the molar fraction of the metallic ion. In the case of Cobalt (II), only one compound is probable to be produced between the ligand and the Co^{2+} ion, resulting in a stoichiometric relationship (metal: ligand) of (1:4). In the case of Copper (II), the absorbance values were taken at 810 nm. There are two possibilities of compounds that can be obtained using the ligand and the Cu (II) compound, with stoichiometric relationships (1:1) and (4:1).

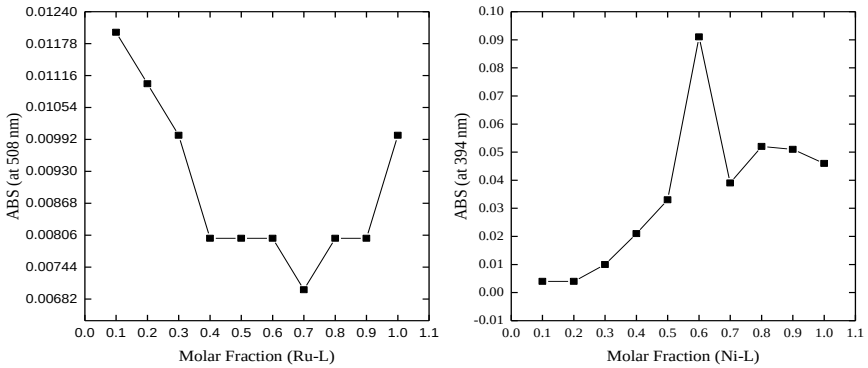

Figure 17. Job´s method applied to the Ruthenium (III) and Nickel (II) compound.

Besides, Figure 17 shows the different absorbance values taken at 508 and 394 nm in the case of Ruthenium(III) and Nickel(II) solutions, respectively. In the case of Ruthenium, it can be proposed that there are two possibilities of compounds formed. The possible stoichiometric relationships (metal: ligand) were (2:3) and (2:1). In the case of Nickel, the Jobs plot suggest that the stoichiometric relationship is (3:2). The changes of one type of compound to another by varying the quantity of reagents can be observed in the appendixes section.

5.3.5. UV-Vis of the coordination compounds

Ligand dissolved in water: The electronic spectra of the synthesized ligand did not present absorption bands in the visible region.

Cobalt Complex (DM002) dissolved in water: The electronic spectra of the compound (Figure 18) revealed two absorption bands at λ_1 = 371 nm (26954 cm^{-1}) and λ_2 = 520 nm (10Dq = 19230 cm^{-1}). The bands correspond to the electronic transitions $^4T_{1g}$ (F) → $^4A_{2g}$ (F) and $^4T_{1g}$ (F) →$^4T_{1g}$ (P), respectively. Moreover, the electronic transition $^4T_{1g}$ (F) → $^4T_{2g}$ (F) is not observed due to it is beyond the reach of the UV-Vis spectrophotometer.

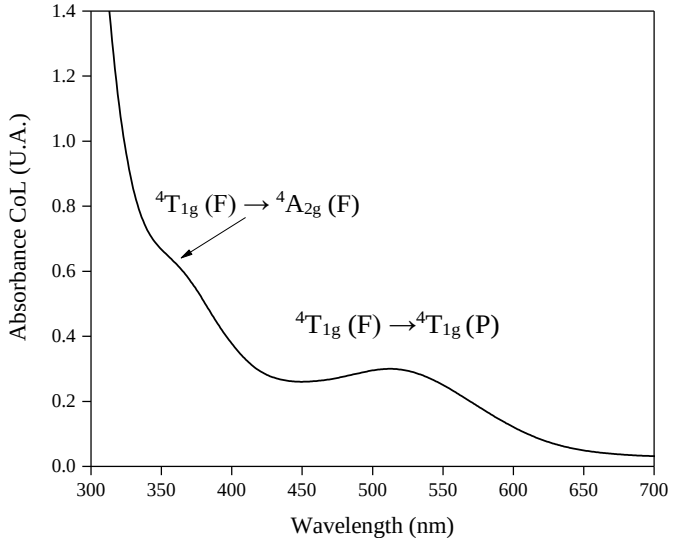

Figure 18. UV- Vis spectra of the CoL (DM002) Compound in solution (range of 300 – 700 nm).

Copper Complex (DM003) dissolved in water: The spectra of the compound (Figure 19) had one absorption band at λ_1 = 760 nm (10Dq = 13157 cm^{-1}) corresponding to the electronic transition ^2E_g →$^2T_{2g}$, which suggested a distorted octahedral structure [101].

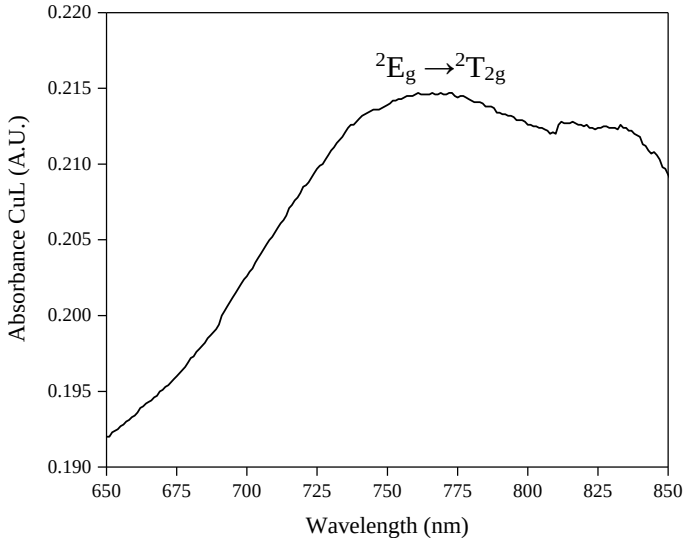

Figure 19 UV -Vis of the CuL (DM003) compound in solution (range 650 – 850 nm)

Nickel Complex (DM004) dissolved in water: Three absorption bands are present in the spectra (Figure 20) at λ_1 = 364 nm (27472 cm^{-1}), λ_2 = 575 nm (17391 cm^{-1}), and λ_3 = 593 nm (10Dq = 16863 cm^{-1}), which correspond to the following electronic transitions $^3A_{2g}$ (F) $\rightarrow {}^3T_{1g}$ (P), $^3A_{2g}$ (F) $\rightarrow {}^3T_{1g}$ (F), and $^3A_{2g}$ (F) $\rightarrow {}^3T_{2g}$ (F), respectively. Besides, there is a band at 221 nm, which was assigned as a charge transfer band.

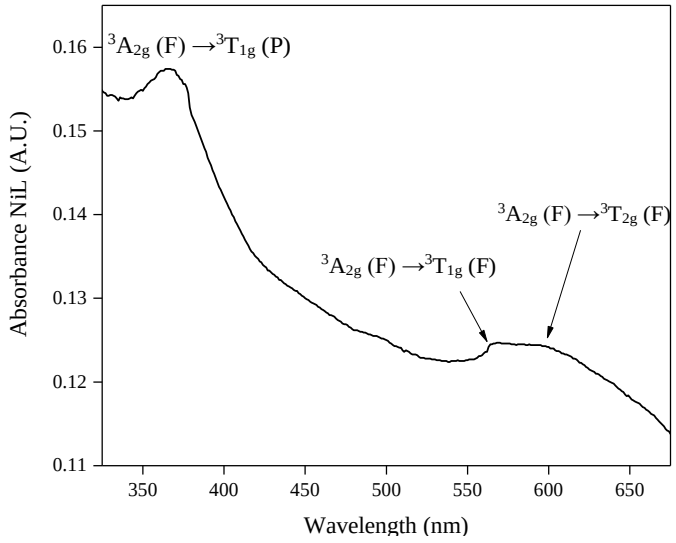

Figure 20. UV – Vis spectra of the NiL (DM004) compound (range 300 – 675 nm).

Ruthenium complex (DM005) dissolved in water: The absorption spectra of the Ruthenium (III) compound (Figure 21) presents one weak band at λ_1 = 342nm (10Dq = 29239 cm^{-1}). The band corresponds to a spin forbidden electronic transition $^6A_{1g}$ (S) $\rightarrow {}^4T_{1g}$ (D). Regarding to the Racah parameter $B_{(complex)}$ = 737 cm^{-1}.

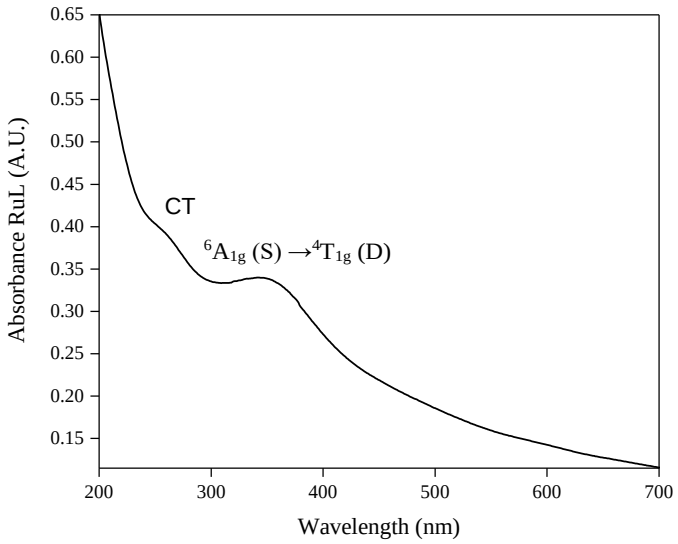

Figure 21. UV-Vis spectra of the RuL (DM005) in aqueous solution (range 200 – 700 nm)

5.4. Diffuse Reflectance

The diffuse reflectance spectroscopy was performed to observe the energy shift difference in the bands corresponding to electronic transitions caused by the effect of the solvent in the measurements of UV – Vis spectroscopy of the coordination compounds.

5.4.1. Cobalt (II) compound

The spectra corresponding to the Cobalt (II) compound in its solid-state (Figure 22), presented two absorption bands at λ_1 = 458 nm (21834 cm^{-1}) and λ_2 = 506 nm (10Dq = 19762 cm^{-1}). If the values are compared with the ones obtained in UV – Vis spectroscopy, the compound in water solution presents displacements of both bands to lower wavelength values, which suggests an increase in the bonding energy. Regarding to Racah parameters, $B_{(complex)}$ = 1091 cm^{-1}. Also, the Racah parameter of the free ion is 1120 cm^{-1}. Then, the nephelauxetic parameter (calculated as the ratio of the Racah parameter of the compound to the free ion) will be β = 0.97. This value reveals the facilities that the cobalt (II) compound possesses to be in a free ion form. Then, it can be suggested that the ligands are mainly labile atoms, in this case, chlorine.

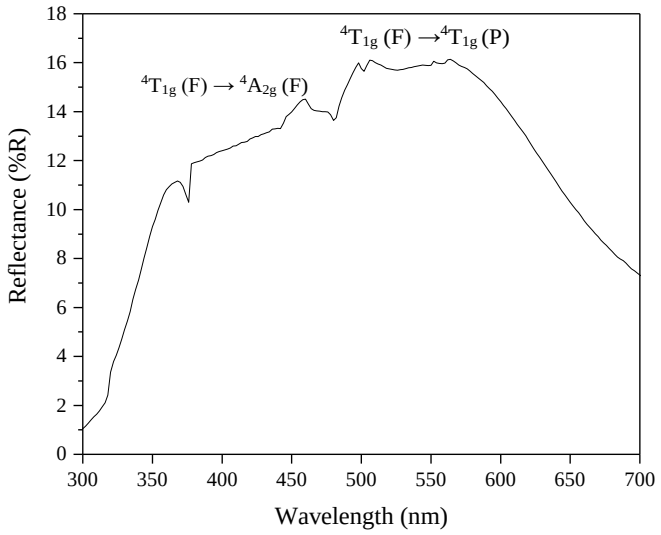

Figure 22. Diffuse Reflectance spectra of the Cobalt (II) compound.

5.4.2. Copper (II) compound

Regarding Copper (II) compound, the spectra (Figure 23), presents two one band at λ_1 = 822 nm (10 Dq = 12165 cm^{-1}). The band of the solid compound is located in a higher wavelength value compared with the compound in aqueous solution, which suggests the same behavior as in the case of the Cobalt (II) compound.

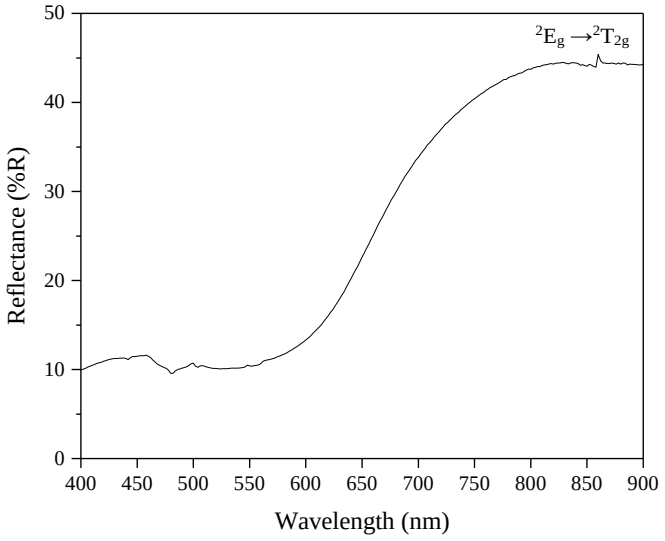

Figure 23. Diffuse reflectance spectra of the Copper (II) compound.

5.4.3. Nickel (II) compound

The diffuse reflectance spectra corresponding to solid Nickel (II) compound (Figure 24) presented three characteristic bands in the visible region, which were located at λ_1 = 497 nm (20120

cm^{-1}), λ_2 = 744 nm (13440 cm^{-1}), and λ_3 = 798 nm (10Dq = 12531 cm^{-1}). The effect of the solvent is more notorious in this case when water molecules are coordinated to the central metallic atom; there exists a decrease in the appearance wavelength of the electronic transition signals.

The Racah parameter B can be calculated using the Tanabe -Sugano diagram for a d8 species[102]. $B_{(complex)}$ = 670 cm^{-1}. As the Nickel (II) in the gaseous state has a B value of 1030 cm^{-1} [103], the nephelauxetic value is $\beta = 0.65$, which is indicative of few interelectronic repulsions in the metal ion. These phenomena can be explained by taking into account that there exists an overlap of the metal ion orbitals with the ligand orbitals, which promotes electron delocalization, giving the compound a higher covalent behavior.

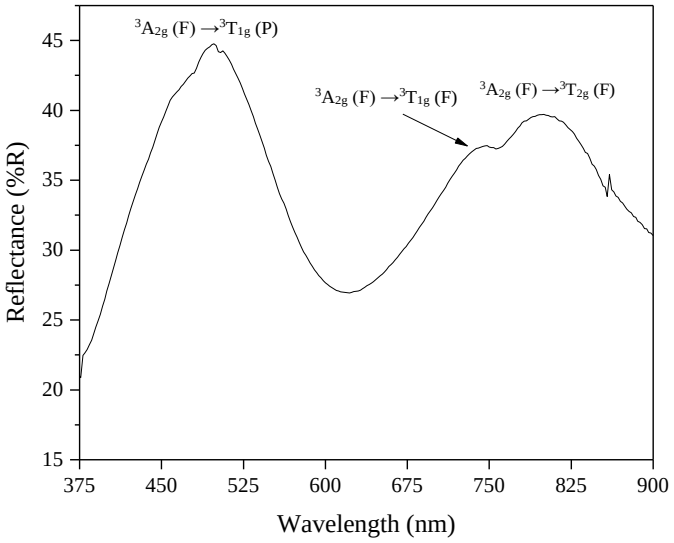

Figure 24. Diffuse reflectance spectra of the Nickel (II) compound

5.4.4. Ruthenium (III) compound

In the case of the ruthenium compound, the diffuse reflectance spectra not presented bands associated with electronic transitions. Eventually, the effects of the solvent could not be assessed.

5.5. XPS

XPS analysis will be focused on the coordination of the metallic ions to the ligand, primarily to determine the electron donor group coordinated to the metallic ion. Each compound possesses the high-resolution windows for the atoms involved in the structure. To analyze the spectra, the main source used is an XPS reference handbook from Perkin – Elmer Corporation (Ref. 105).

5.5.1. Ligand

The characteristic 1s nitrogen band (located at 398.1 eV) was displaced to higher values of binding energy (401 eV), The zone from 400 eV to 403 eV is related to ammonium salts, which is consistent with the cationic structure obtained by using XRPD. Also, Figure 25 shows the deconvolution of the nitrogen band into two signals, which correspond to two types of nitrogen bonds, in concordance with the ones revealed in the methylpiperazine structure. Regarding the 1s band of carbon (characteristic at 285 nm), it was deconvoluted into five types of carbon bonds presented in their specific ranges (Figure 25). For example, the CO binding energy corresponding to carbonate is in 289 eV; the CO related to hydroxyl groups located in 286.5 eV, and the carboxyl signal is in 288 eV.

In the case of the high-resolution oxygen window (Figure 26), its characteristic 1s band (usually located at 531 eV) was displaced to lower binding energy values (530.6 eV), the band is in agreement with the hydroxyl and carbonate groups presented in the ligand structure. Additionally, Figure 26 shows the deconvolution of different types of oxygen bonds were presented in concordance with the tartrate and water structures.

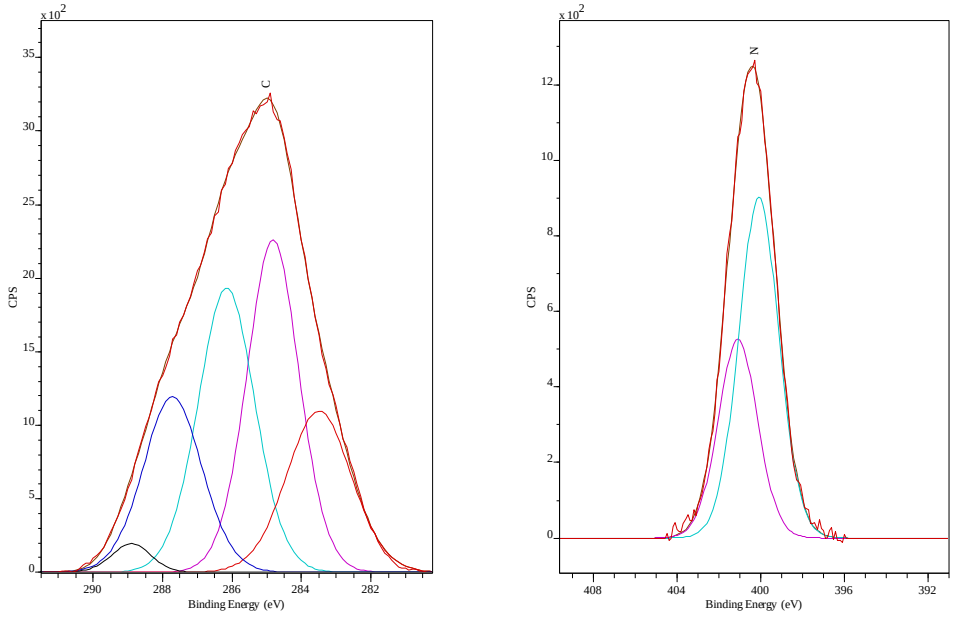

Figure 25. XPS high resolution windows for carbon and nitrogen atoms corresponding to the synthesized ligand.

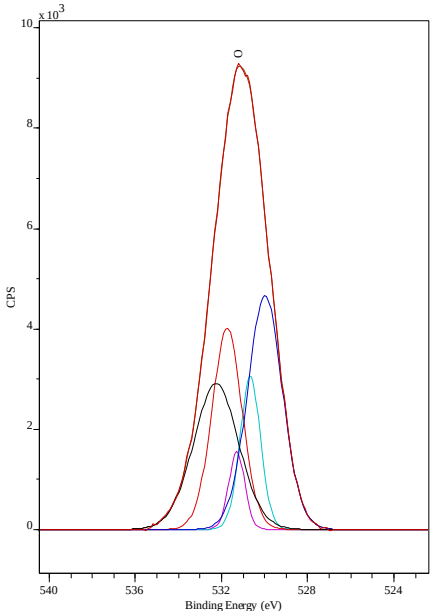

Figure 26. XPS high resolution windows for oxygen atoms corresponding to the synthesized ligand.

5.5.2. Cobalt (II) Compound

Metallic cobalt presents two characteristic bands at 778 and 793 eV, which corresponds to the $2p_{3/2}$ and $2p_{1/2}$ spin-orbit species, respectively. In the case of $CoCl_2$, the bands corresponding to the mentioned species are located at 784.0 and 798.2 eV[104]. Moreover, the $CoCl_2$ shake-up satellite lines are showed at 785.8 and 788.2 eV[104]. Regarding the synthesized cobalt (II) compound, the high-resolution window (Figure 27) presents the displacement of the $2p_{3/2}$ and $2p_{1/2}$ spin-orbit signals to lower binding energy values (780 and 795 eV). The displacement can be explained from the increase of the electronic density around the cobalt (II) atom due to the receiving of electrons from the oxygen atoms of the ligand.

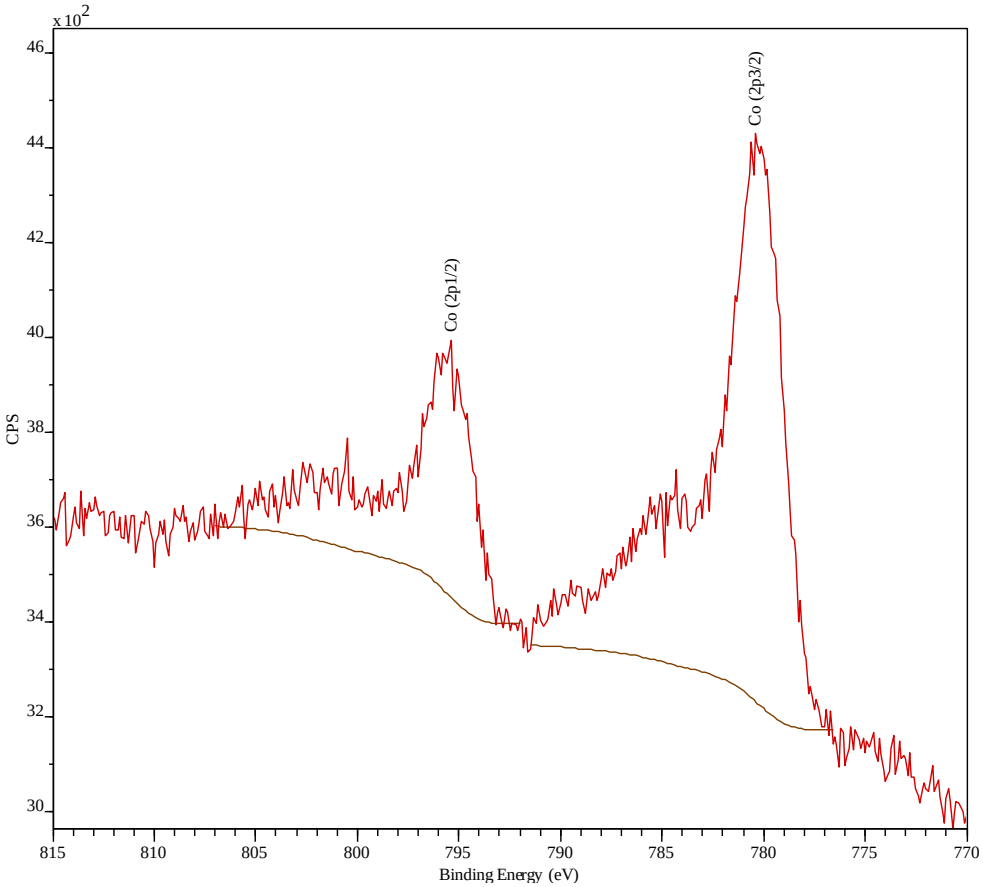

Figure 27.XPS spectra of the synthesized cobalt (II) compound in the cobalt region

To study coordination, only the band corresponding to $2p_{3/2}$ spin-orbit was analyzed (Figure 28). The band is presented in the range of CoOOH bonding type (approximately at 779.8 - 780.2 eV[105]), indicating the coordination of the cobalt ion with the oxygen atoms presented in the ligand structure. Furthermore, the deconvolution of the $2p_{3/2}$ band is presented in Figure 28; in this case, the bands corresponding to Co-O and Co-Cl bonds are presented at 780.5 and 779.6, respectively. The presence of Cobalt (II) hydroxide is confirmed as the corresponding signal appeared at 781.5 eV. In addition, two prominent shake-up satellite lines (located at 789.3 and 784.5 eV) provide information about the magnetic state of the metallic center[105]. It has been reported that in the case of transition metals, the appearance of strong satellite lines corresponds to elements with paramagnetic behavior[105]. In the case of non-appearance of satellite signals, the compound tends to be diamagnetic[105]. The binding energies for the shake-up signals are consistent when compared with the signals of $CoCl_2$, which suggests that the coordination compound is a high spin species and possess a coordination number of six, promoting the idea of an octahedral coordination

geometry. Furthermore, none of the signals presented was in agreement with a binding energy corresponding to the bond between a Co (II) atom and nitrogen species, usually located in the range of 781-782 eV.

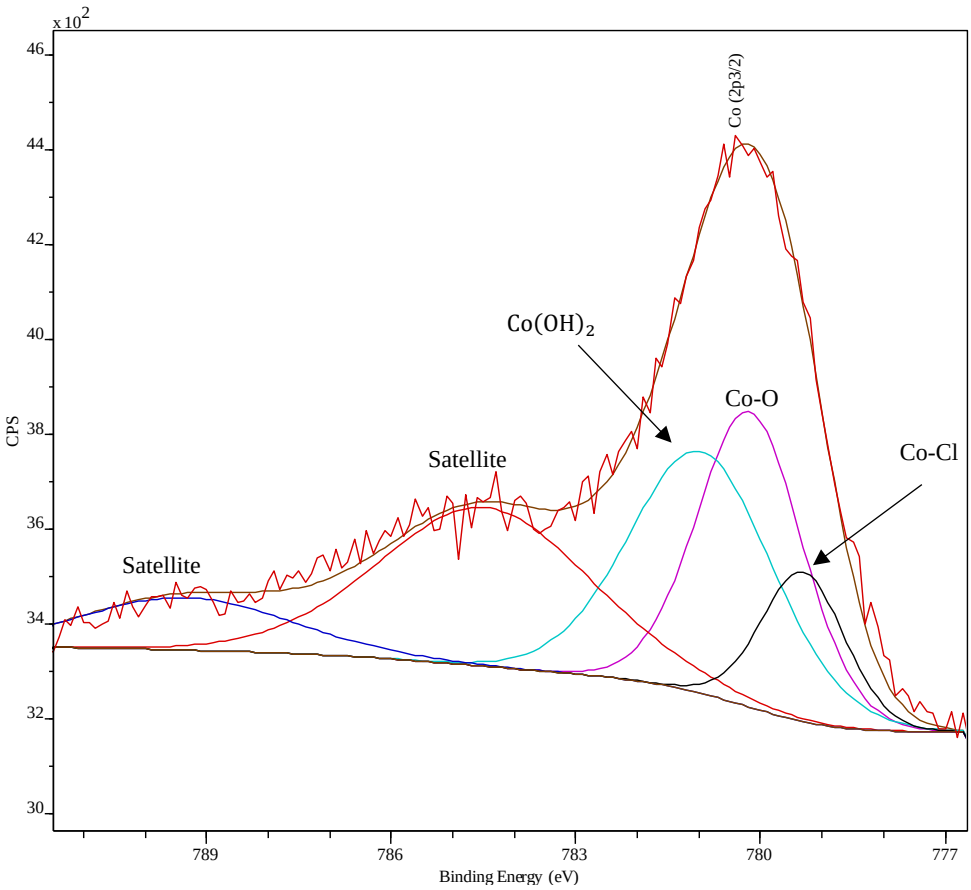

Figure 28. Deconvolution of the signal corresponding to the $2p_{3/2}$ spin-orbit species of cobalt (II) compound.

5.5.3. Copper (II) Compound

Copper possesses two characteristic bands at 933 and 953 eV, which belong to the $2p_{3/2}$ and $2p_{1/2}$ spin-orbit species, respectively. Regarding to $Cu(NO_3)_2$, the bands corresponding to those species are located at 938.6 and 958.4 eV. Also, the satellite bands of the $2p_{3/2}$ species is placed at 945.2 eV. In the case of the synthesized copper (II) compound, Figure 29 shows the XPS high resolution spectra, The bands corresponding to the $2p_{3/2}$ and $2p_{1/2}$ species are displaced to higher binding energy values (934.5 and 954.4 eV).

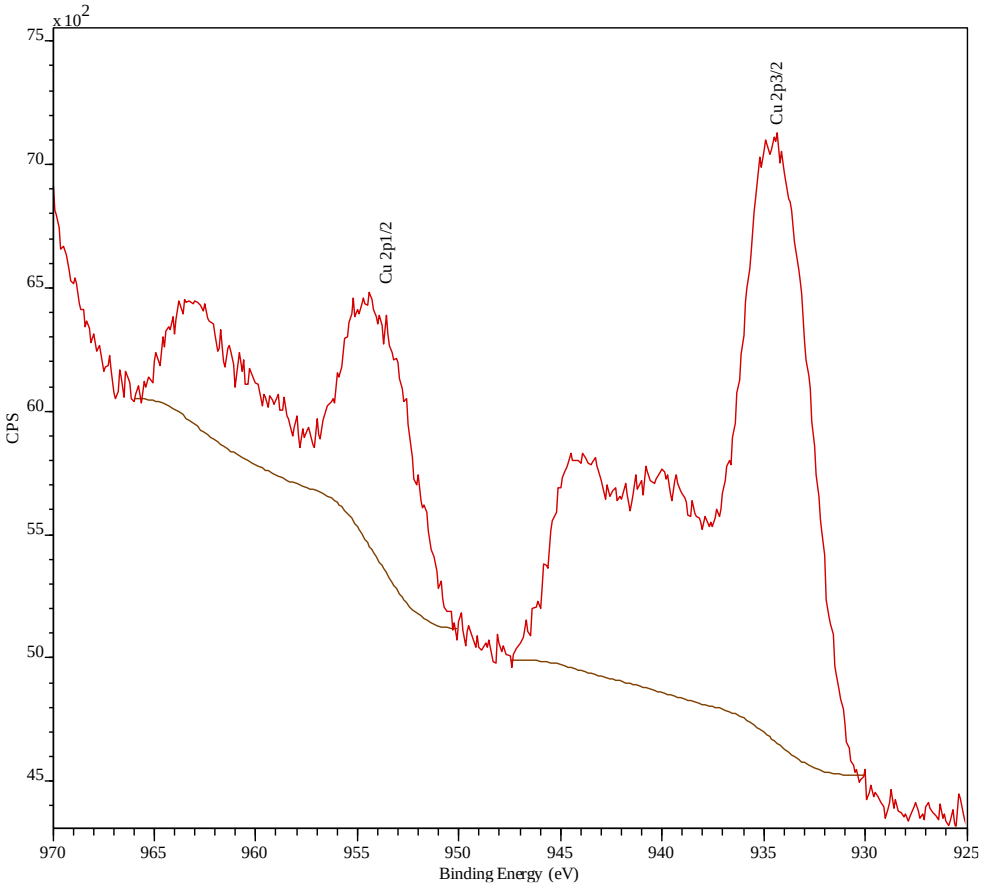

Figure 29. XPS spectra of the synthesized copper (II) compound in the cobalt region

As in the previous case, the band corresponding to $2p_{3/2}$ spin-orbit (Figure 30) was used to analyze the chemical environment of the copper atom. The band was deconvoluted and three signals were presented at 932.3, 933.9 and 935.3 eV; the signals were assigned to metallic copper, Cu-O (ligand), and copper (II) hydroxide, respectively. Moreover, two prominent shake-up satellite lines are presented in this case (located at 939.7 and 943.9 eV) which denote a paramagnetic state of the metallic center[106]. Also, the satellite lines are in agreement with the ones presented for $Cu(NO_3)_2$, which suggests that the coordination number of the compound is four, suggesting the idea of an square planar or tetrahedral coordination geometries. Taking into account the bulkiness of the ligand and repulsion interactions, a tetrahedral coordination geometry might be favored.

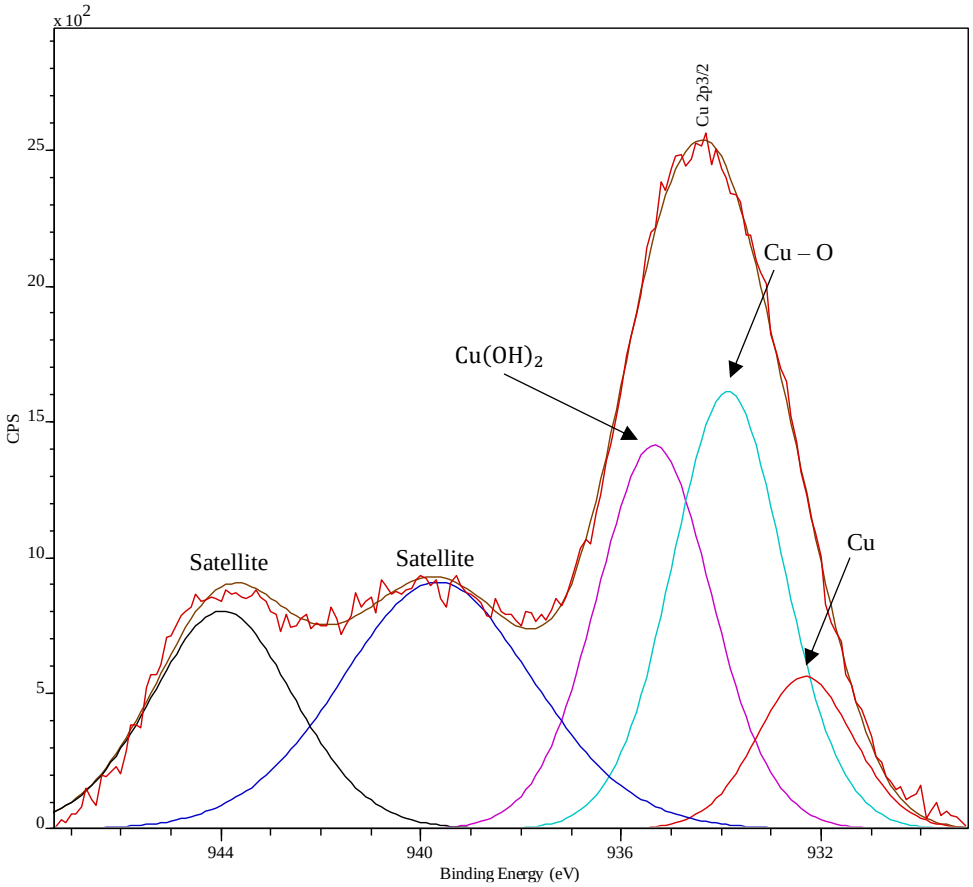

Figure 30. Deconvolution of the signal corresponding to the $2p_{3/2}$ spin-orbit species of copper (II) compound.

5.5.4. Nickel (II) Compound

Metallic nickel presents two characteristic bands at 853 and 870 eV; they correspond to the $2p_{3/2}$ and $2p_{1/2}$ spin-orbit species, respectively. In the case of the $NiCl_2$, the bands corresponding to the mentioned species are located at 856.8 and 874.2 eV[107]. The Nickel (II) compound presented the bands at 854.7 and 872.2 eV (Figure 31); then, the displacement to lower bonding energies is related to the coordination of the metals with the ligand.

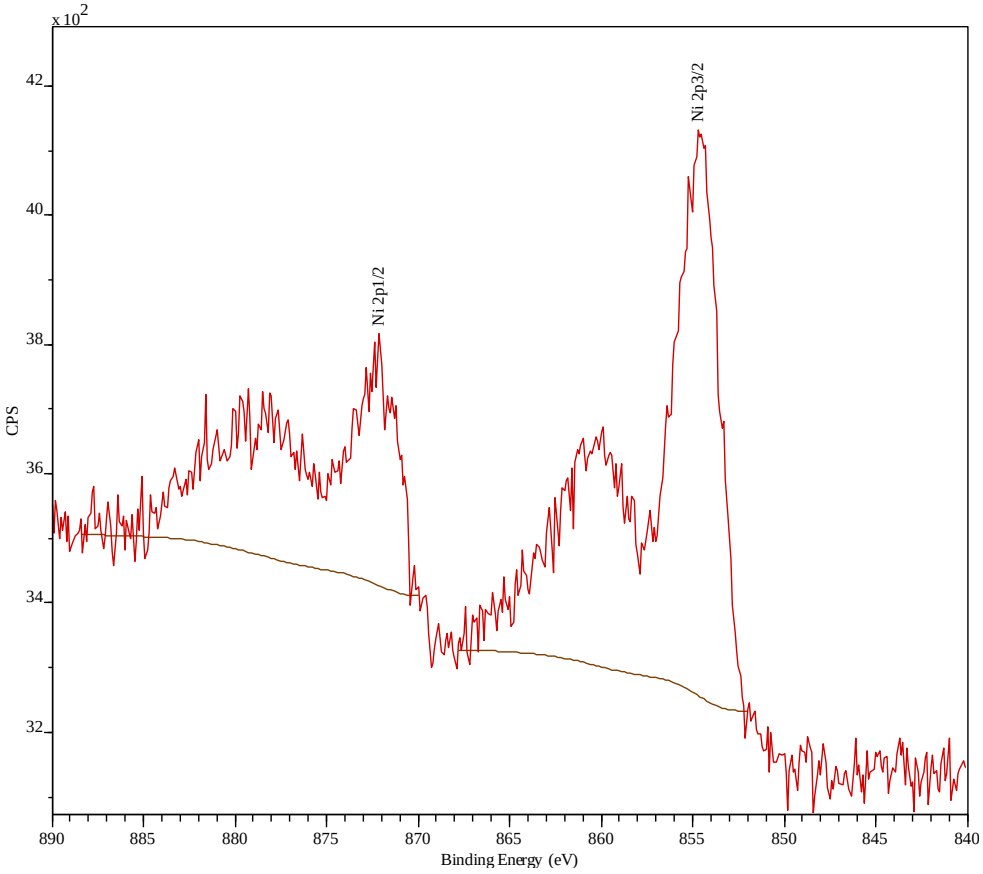

Figure 31. XPS spectra of the synthesized Nickel (II) compound in the Ni high resolution region.

The deconvolution of $2p_{3/2}$ spin-orbit band (Figure 32) was used to propose a structure for the coordination compound. In this case, three signals were observed at 853.7, 854.5, and 855.8 eV and assigned as Ni – O (ligand), nickel (II) hydroxide and Ni – Cl, respectively. Moreover, no signal corresponding to nickel with nitrogen atoms are presented.

The shake-up satellite line is presented at 860.6 eV, which denotes a paramagnetic state of the metallic center. Comparing the satellite line of the compound with the one for $NiCl_2$ (located at 859.8 eV[107]), the consistency of binding energy presented suggests that the coordination number of the compound is six (due to $NiCl_2$ possesses an octahedral geometry).

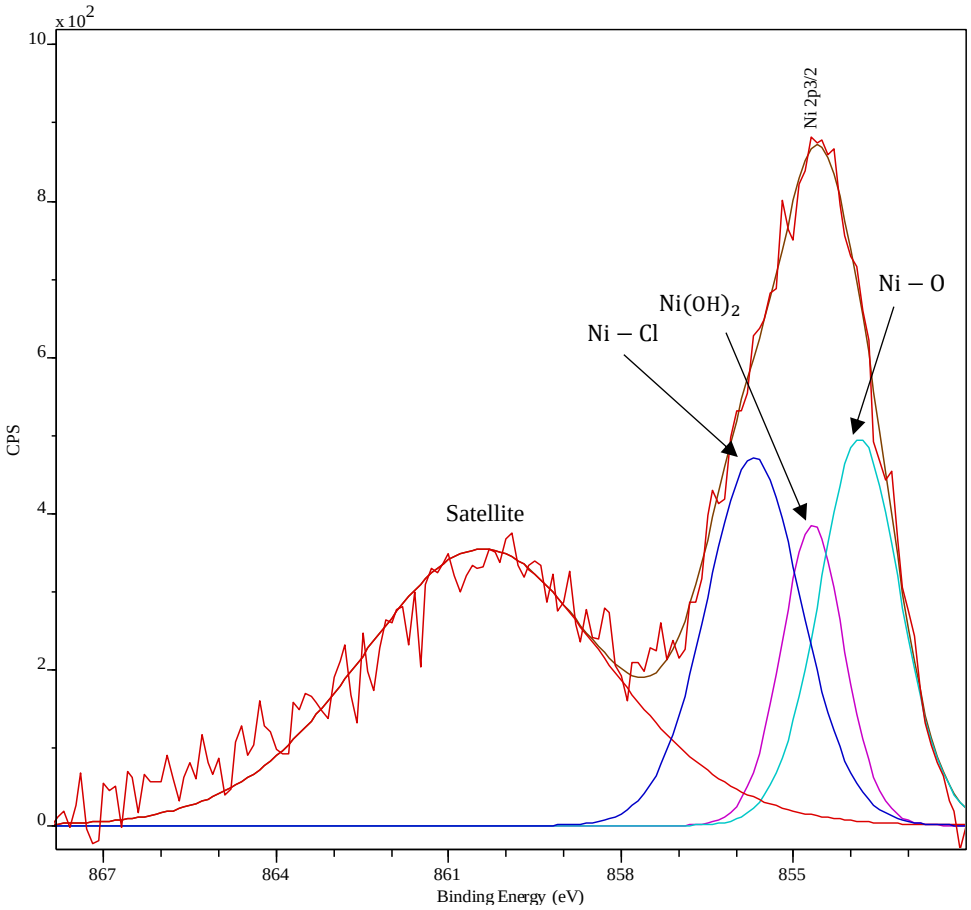

Figure 32. Deconvolution of the signal corresponding to the $2p_{3/2}$ spin-orbit species of Nickel (II) compound.

5.5.5. Ruthenium (III) Compound

Ruthenium presents two prominent bands in the spectra, which are located at 280 and 284 eV for the $3d_{5/2}$ and $3d_{3/2}$, respectively. The precursor $RuCl_3$ presents the $3d_{5/2}$band at 281.7eV[105] and octahedral structure. The synthesized Ruthenium (III) compound presented only one band at 280.6 eV ($3d_{5/2}$), and the next one was masked by the signal corresponding to carbon (located at 281.2 eV). Then, the $3d_{5/2}$ species was used for the analysis; its band (Figure 33) was deconvoluted and three different types of bond appeared at 279.8, 280.5 and 281.4 eV, which correspond to the metallic ruthenium, Ru – O (ligand) and Ru – Cl, respectively. All of the compounds presented bands that assured the coordination between metallic ions and oxygen atoms of the ligand. Furthermore, the band corresponding to $Ru(OH)_3$ is found at higher binding energies, but it is masked from carbon 1s signal. The fact that the nitrogen atoms presented in the

piperazine structure do not possess free electron pairs in the structure makes them unavailable to act as a Lewis base and form coordination compounds.

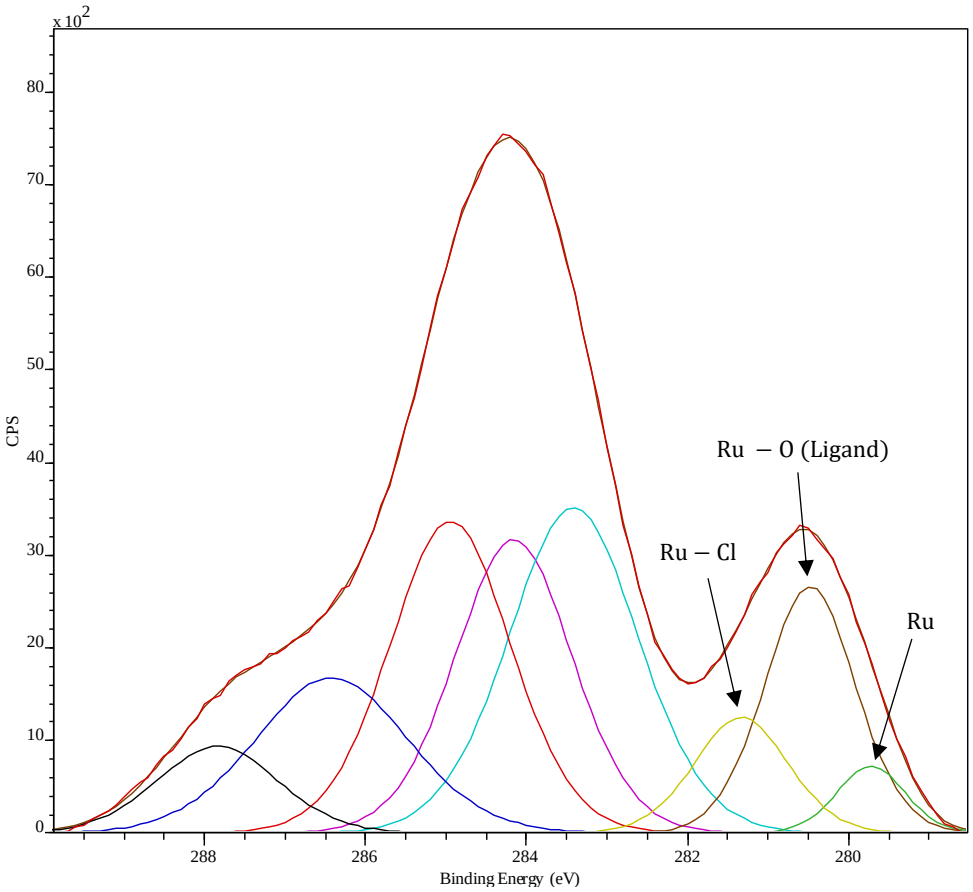

Figure 33. Deconvolution of the signal corresponding to the $3d_{5/2}$ spin-orbit species of Ruthenium (III) compound

5.5.6. Structure of the synthesized coordination compounds

Based on the results obtained with the Jobs experiment, the ligand structure determined with XRPD, the XPS, and with previous reactivity observed for the interactions between several metal ions with tartrate in solution[108]; we propose a general structure for the complexes including one metal and two coordinated tartrates forming anions which could be ionically stabilized with 2-methylpiperazinediium as the cation in the compound. In Figure 34, we show the general structure of the complexes explained before. Moreover, Figure 35 shows the 3D structure for each one

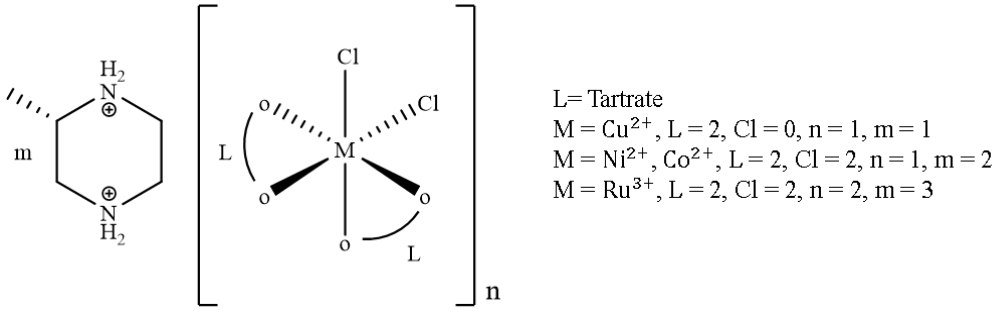

Figure 34. The general structure of the synthesized complexes

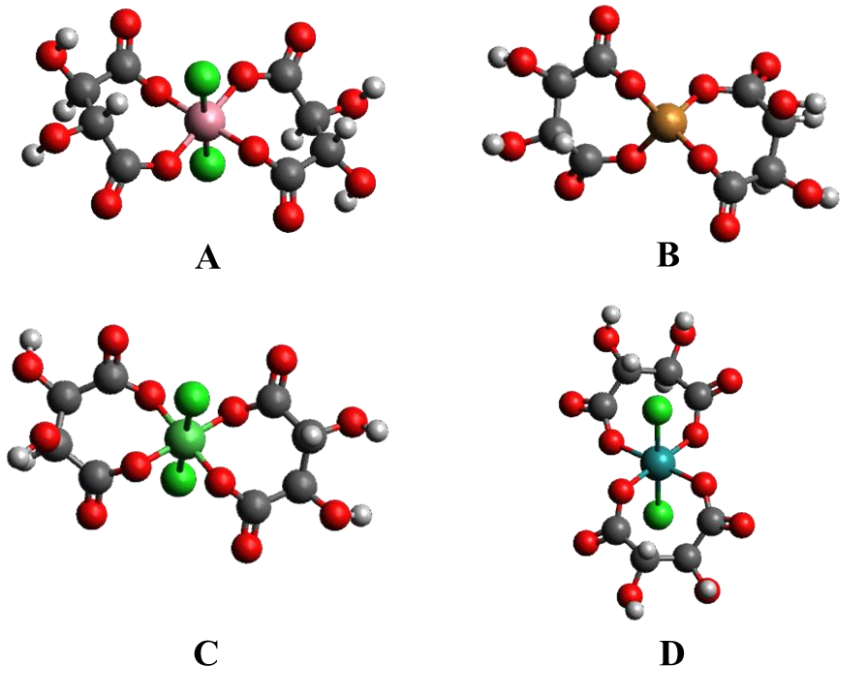

Figure 35. 3D structures of the anionic complexes, A) Cobalt (II) complex; B) Copper (II) complex; C) Nickel (II) complex; D) Ruthenium (III) complex.

5.6. Cell Viability Assays

The cell viability assays in lymphocytes cell cultures were performed in triplicate. Trypan blue dye exclusion method was used to count the number of viable cells (using a Neubauer chamber), which means that the criteria used to evaluate the viability of the cells was the integrity of the cell membrane. Lymphocytes with intact cell membranes excluded the trypan blue dye, counting as living viable cells; if an intracellular blue tonality appeared, it suggests the nonviability of the cells, i.e., cellular death[92].

5.6.1. Ligands used as a stimulus

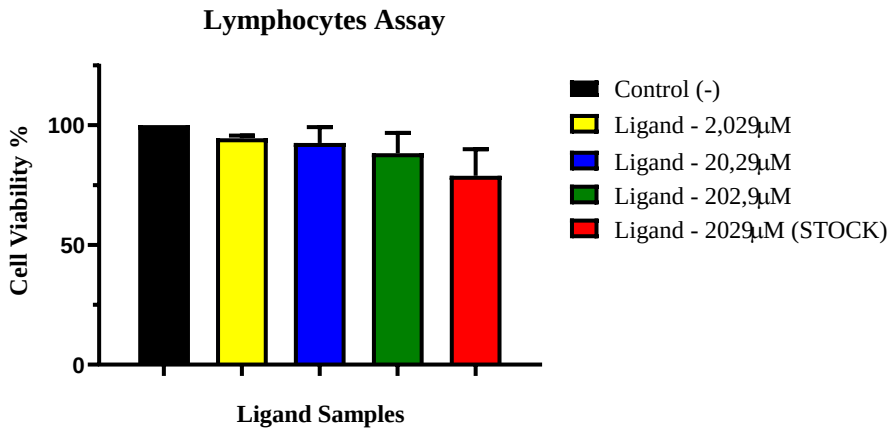

Figure 36. Lymphocytes assay one using the synthesized Ligand as a stimulus.

In the case of the synthesized ligand, Figure 36 shows the different concentrations used as a stimulus and the effect of the compound in the number of viable cells. The three concentrations made from the stock solution did not significantly affect the number of living cells. Moreover, it is observed that as the concentration of the compound increased, the number of viable cells diminished. LD_{50} values were not calculated due to any of the concentrations used affected the cell viability percentage in a 50%

5.6.2. Cobalt (II) Compound

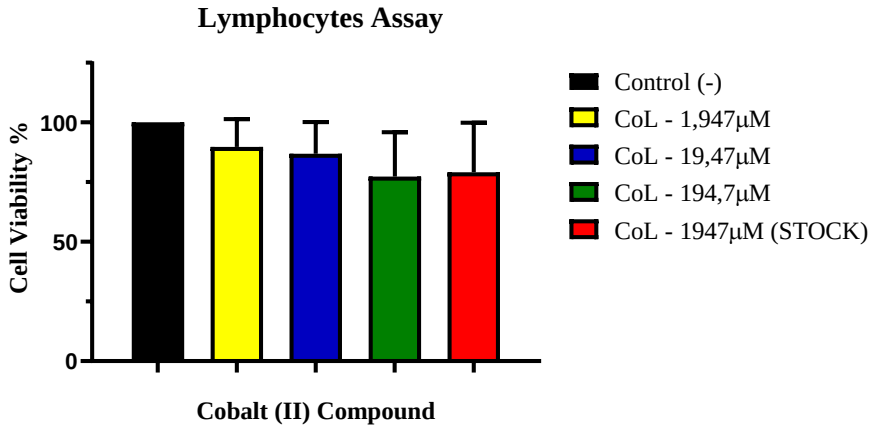

Figure 37. Lymphocytes assay one using the Cobalt (II) compound as a stimulus.

Regarding the synthesized Cobalt (II) compound, Figure 37 reveals a similar behavior as observed in the case of the ligand; the concentration of the compounds did not affect the cell viability percentage in a meaningful manner. In this case, LD_{50} values were not calculated for the

same reason mentioned previously. Even when the percentages are lower compared to the ligand case, there are not values that affect half of the total percentage.

5.6.3. Copper (II) Compound

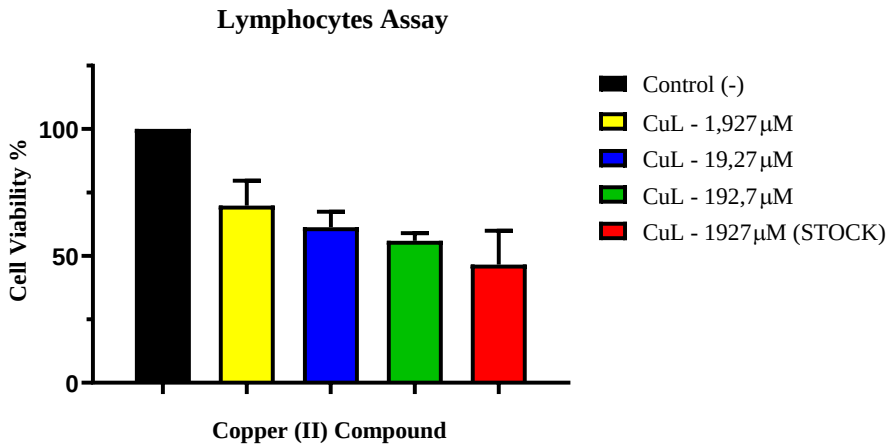

Figure 38. Lymphocytes assay with Copper (II) compound as a stimulus.

The synthesized Cooper (II) compound differs from the behavior presented by the ligand compound, and the Co (II) complex, the decrease in cell viability percentage is notorious even at the minor concentration used. Figure 38 shows a high reduction in the number of viable cells as the concentration of the compound increases, which is generally observed. In this case, there is a concentration which affects more than 50% of the initially viable cells; then, the LD_{50} (Figure 39) could be calculated by using Prism8 Graphpad. The LD_{50} = 817 uM suggests us that the copper compound presents high cytotoxicity; even at the most diluted concentration, the cell viability values are lower than 75%.

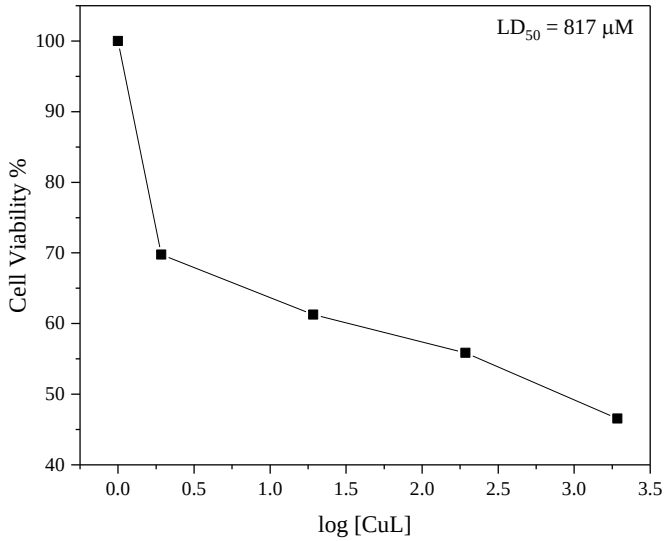

Figure 39. The dose-response curve obtained for the Copper compound

5.6.4. Nickel (II) Compound

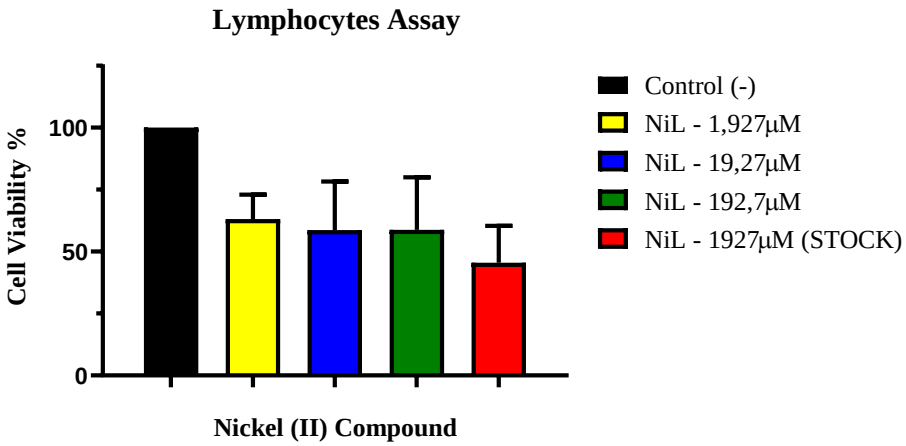

Figure 40. Lymphocytes assay using the Nickel (II) compound as a stimulus.

In the case of the synthesized Nickel (II) compound, Figure 40 reveals that this compound has a similar behavior than the copper (II) compound. The cell viability has decreased to percentages between 60 and 40%, which suggests high cytotoxicity. The second (blue) and third (green) concentrations presented similar viability percentage values; this difference can be assessed to the blockage of cell membranes at higher concentrations of the drug, making processes like endosmosis not favored; however, more studies should be developed to explain this behavior. Moreover, the decrease in the cell viability corresponding to the Stock solution suggests that the interval of concentrations is correct. The corresponding graph of the dose-response effect and the medium lethal dose value is presented in Figure 41.The LD_{50} is equal to 882.01 µM, meaning that

it possesses a similar behavior to kill half of the lymphocytes in the cell culture as the Copper (II) compound.

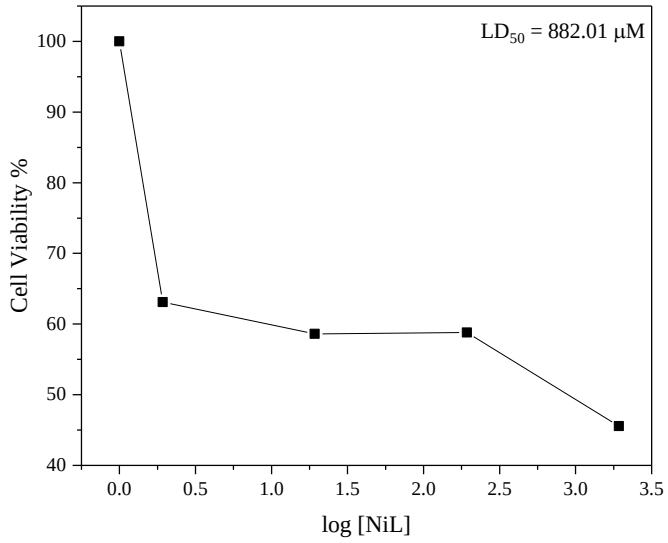

Figure 41. The dose-response curve corresponding to the stimulus presented by the Nickel compound.

5.6.5. Ruthenium (III) Compound

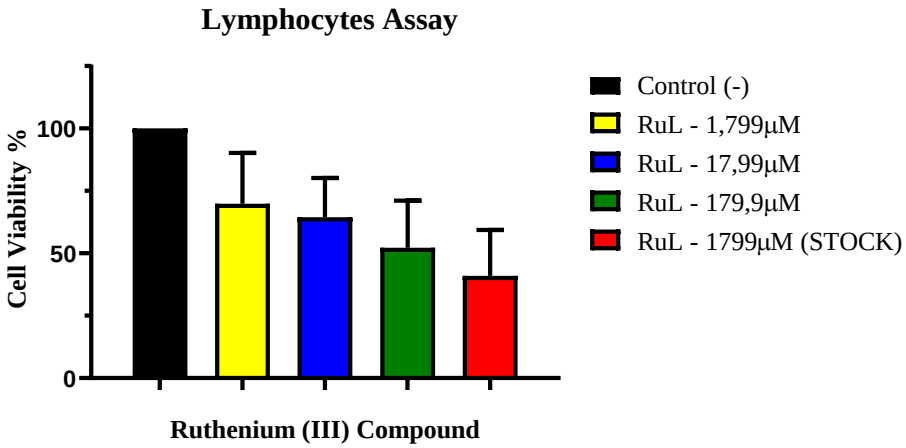

Figure 42. Lymphocytes assay one, Ruthenium (III) as a stimulus.

Regarding the synthesized Ruthenium (III) compound, the cell viability percentage is affected in almost a linear trend (Figure 42); as the concentration increased, the number of living cells diminished. The interval of concentrations and the decrease in cell viability is coherent about what is mostly expected to happen. Furthermore, the stock solution presented the highest cytotoxic behavior of the compounds studied. An explanation suggested to this fact is that cells are not used to deal with this type of transition metals (same case as Cisplatin), which is not the case for the

essential metals used in the previous compounds. The graph corresponding to LD_{50} = 279.10 µM is presented in Figure 43. This value is the lowest from the compounds tested in lymphocytes cell cultures, which accounts for a high cytotoxicity as lower concentrations are needed to achieve a similar effect compared with Ni(II) and Cu(II).

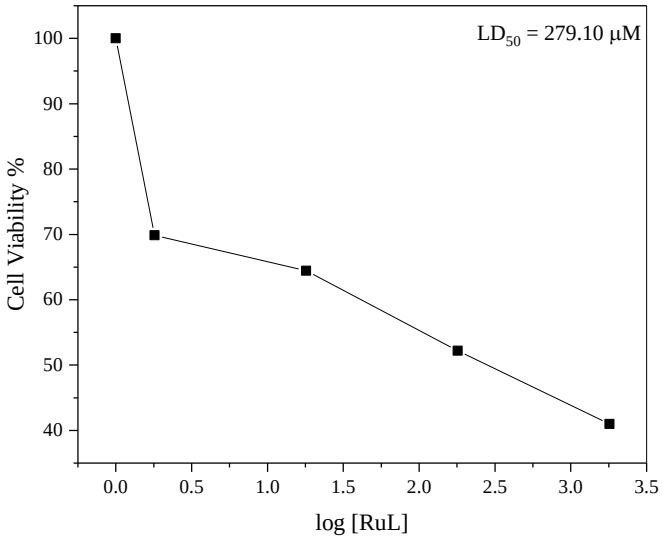

Figure 43. Dose-Response Curve obtained from the Ruthenium Compound Stimulus.

6. CHAPTER SIX: SUMMARY & CONCLUSIONS

An oxygen donor ligand based on a reaction between tartaric acid and ethylenediamine was synthesized and characterized; XRPD was used to obtain the structure of the synthesized ligand with molecular formula $C_{13}H_{26}N_2O_{13}$ and name (R)-2-methylpiperazinediium bis[hydrogen (2S,3S)-tartrate] monohydrate. The process was followed by the successful synthesis of coordination compounds with Co(II), Cu(II), Ni(II) and Ru(III).

Infrared Spectroscopy was used to confirm the presence of the functional groups in the molecule, such as hydroxyl, secondary amines, and carbonyls. In addition, the signals corresponding to metal-oxygen appeared in the far-infrared part of the spectra, suggesting the formation of coordination compounds.

Electronic spectroscopy studies indicated the formation of coordination compounds by changes in the position of the bands corresponding to the electronic transitions of the metallic atoms, the Job's curves demonstrate the presence of (M:L) relationships for the complexes CuL, CoL, NiL, and RuL as follows: (1:1), (1:4), (3:2), and (2:3).

Furthermore, XPS spectra were used to determine the coordination of each metal with the ligand by taking into account the displacement in the bonding energy of the bands and the appearance of the corresponding signals for each type of bond. Then, it was concluded that metallic atoms coordinate with the oxygen species presented in the ligand. Also, it was proposed that the cause of non-nitrogen bonding is the lack of electron pairs (nitrogen in ammonium form) that interact with metallic ions.

The results obtained with the Jobs curves, the XRPD of the ligand, IR, UV-Vis, DRS, and XPS of the compounds allow to propose a general structure for the complexes; in which two tartrates are coordinated to one metallic center, resulting in the formation of anions that are stabilized by the presence of a cationic 2-methylpiperazinediium in the ionic compound.

Regarding cell viability studies, the effect of the compounds was analyzed by means of the cell membrane damage, and the concentration used. The ligand and cobalt (II) compounds did not significantly affect the cell viability even at millimolar concentrations; eventually, LD_{50} could not be calculated. In the case of copper (II), nickel (II), and ruthenium (III) compound, dose-response curves were obtained, and the value of LD_{50} was calculated. The cytotoxicity of the compounds suggested that Ru > Cu > Ni >Co ≥ Ligand.

Undoubtedly, further studies must be done in order to determine the structures of the obtained compounds unambiguously; however, the obtained results are encouraging towards the search for novel compounds with possible activity as anticancer drugs.

Future Prospects

Regarding the characterization of compounds, studies like NMR, EPR, Cyclic Voltammetry, and magnetic susceptibility are necessary. Also, analysis of the compound obtained and the steps of the synthesis will serve to improve the obtained yields. Further analysis needs to be made related to cell viability and mechanisms of action of the compounds within the lymphocytes. In the case of the Cobalt and Ligand compound, the concentration used can be increased and observe the effect. In addition, cell viability studies of the compounds in other types of healthy cell lines and cancer cell lines will be performed.

7. APPENDIXES

Selection of the concentration and required wavelengths

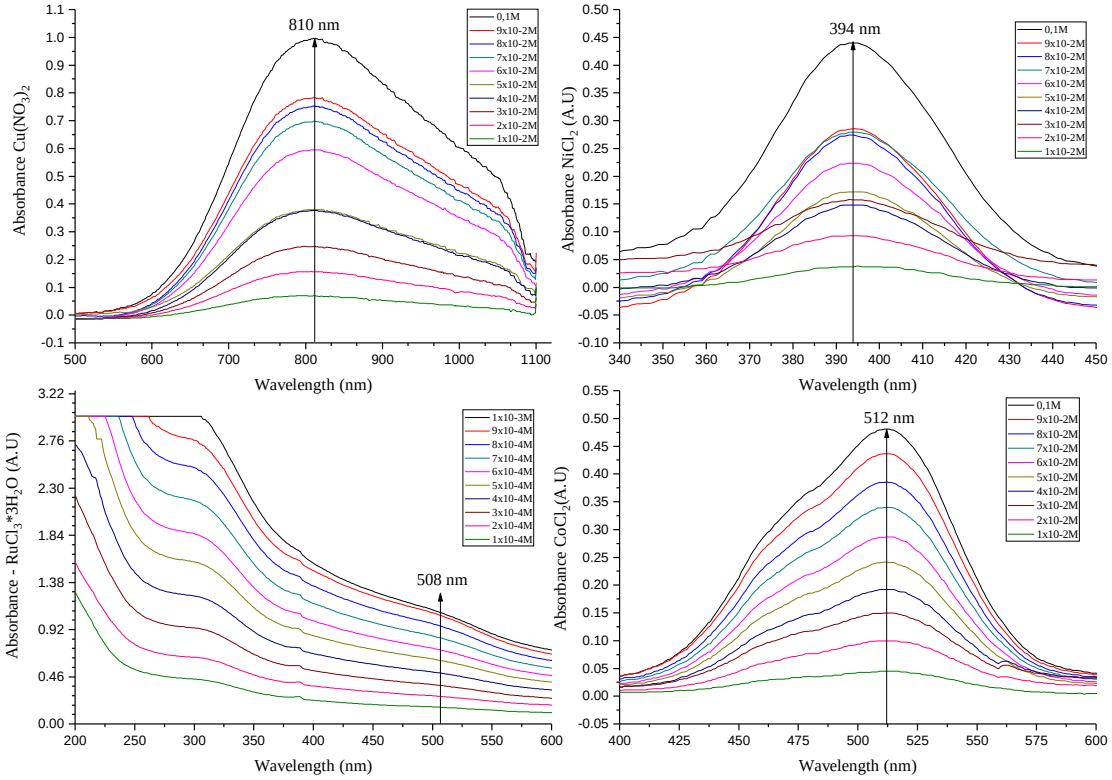

Figure 44. Selection of the wavelength and Concentrations for each compound to apply Jobs method.

Jobs Method - Ruthenium (III) + Ligand

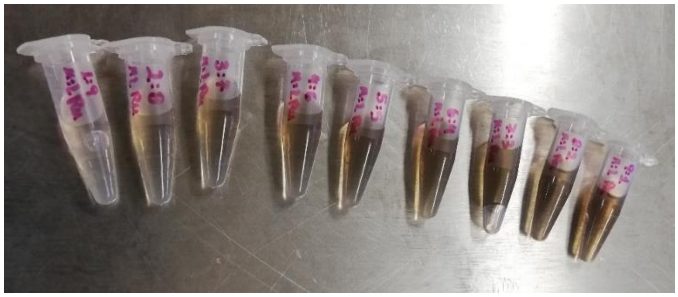

Figure 45. Metal: Ligand solutions in different proportions (Ruthenium case)

Jobs Method - Cobalt (II) + Ligand

Figure 46. Metal: Ligand solutions in different proportions (Cobalt case)

Jobs Method - Copper (II) + Ligand

Figure 47. Metal: Ligand solutions in different proportions (Copper case).

XRD information and tables

No.	2θ, °	d, Å	Height, cps	FWHM, °	Int. I., cps°	Int. W., °	Asymmetry	Decay(ηL/mL)	Decay(ηH/mH)	Size, Å
1	11.7029(15)	7.5557(9)	220433(2620)	0.1603(11)	42952(214)	0.195(3)	2.92(13)	0.337(14)	0.52(3)	520(4)
2	14.628(7)	6.051(3)	7231(364)	0.159(6)	1278(51)	0.177(16)	2.9(7)	0.18(15)	0.0(3)	527(20)
3	16.783(3)	5.2784(11)	47473(1317)	0.152(4)	11665(202)	0.246(11)	1.06(7)	1.55(8)	0.02(9)	551(15)
4	17.573(6)	5.0429(16)	32130(949)	0.202(5)	7896(148)	0.246(12)	2.8(4)	0.46(7)	0.18(13)	416(10)
5	18.793(2)	4.7181(6)	65348(1440)	0.1981(19)	16693(92)	0.255(7)	3.3(2)	0.52(2)	0.61(6)	424(4)
6	20.336(9)	4.363(2)	11761(544)	0.202(10)	3812(66)	0.32(2)	2.7(6)	1.12(10)	0.8(2)	418(20)
7	21.199(15)	4.188(3)	4924(293)	0.216(17)	1722(47)	0.35(3)	2.1(9)	1.11(16)	1.0(4)	391(31)
8	22.165(8)	4.0073(14)	3112(193)	0.18(3)	880(69)	0.28(4)	1.6(12)	1.3(2)	0.0(6)	459(77)
9	23.7569(6)	3.74228(9)	241665(2707)	0.3127(15)	87122(379)	0.361(6)	4.8(2)	0.211(8)	0.36(3)	271.2(13)
10	24.2832(14)	3.6623(2)	41605(1119)	0.237(6)	11388(190)	0.274(12)	4.8(2)	0.211(8)	0.36(3)	358(9)
11	26.538(3)	3.3560(4)	75698(1558)	0.346(2)	28324(180)	0.374(10)	3.68(16)	0.057(18)	0.01(10)	246.4(16)
12	27.019(4)	3.2975(4)	9054(394)	0.242(12)	2369(80)	0.26(2)	3.68(16)	0.057(18)	0.01(10)	353(17)
13	27.860(3)	3.1998(3)	61326(1381)	0.213(4)	17466(154)	0.285(9)	4.9(5)	0.67(3)	0.43(10)	401(7)
14	28.967(3)	3.0799(3)	31198(898)	0.242(3)	9404(258)	0.301(17)	3.8(3)	0.49(3)	0.27(9)	354(5)
15	29.152(5)	3.0609(5)	8926(406)	0.22(2)	2495(253)	0.28(4)	3.8(3)	0.49(3)	0.27(9)	382(39)
16	30.288(9)	2.9486(9)	5501(313)	0.163(15)	1486(52)	0.27(2)	1.3(3)	1.55(14)	0.0(3)	529(47)
17	31.506(2)	2.8373(2)	23067(758)	0.240(4)	7257(75)	0.315(14)	3.8(2)	0.56(2)	0.66(6)	359(6)
18	31.931(2)	2.80044(18)	38256(1087)	0.231(3)	11575(95)	0.303(11)	3.8(2)	0.56(2)	0.66(6)	374(4)
19	33.37(19)	2.683(15)	2001(122)	0.29(19)	632(1064)	0.3(6)	1.3(5)	0.05(16)	0.00(18)	295(191)
20	33.625(14)	2.6632(11)	11285(497)	0.24(6)	2913(1065)	0.26(11)	1.3(5)	0.05(16)	0.00(18)	361(88)
21	34.040(19)	2.6317(14)	3345(195)	0.17(2)	623(50)	0.19(3)	1.3(5)	0.05(16)	0.00(18)	500(57)
22	34.788(17)	2.5767(12)	6386(310)	0.180(14)	1226(88)	0.19(2)	1.9(8)	0.0(3)	0.0(5)	482(38)
23	35.697(4)	2.5132(3)	53926(1248)	0.299(3)	18833(148)	0.349(11)	2.13(12)	0.33(3)	0.14(5)	292(3)
24	36.823(3)	2.43886(17)	19686(704)	0.210(5)	4631(69)	0.235(12)	4.4(3)	0.16(3)	0.12(10)	416(9)
25	37.781(3)	2.37924(19)	30447(903)	0.310(4)	10560(150)	0.347(15)	4.4(3)	0.16(3)	0.12(10)	283(4)
26	38.166(3)	2.35608(17)	20326(695)	0.251(9)	5705(134)	0.281(16)	4.4(3)	0.16(3)	0.12(10)	350(13)
27	38.765(3)	2.32106(18)	20703(712)	0.280(5)	6490(88)	0.313(15)	4.4(3)	0.16(3)	0.12(10)	314(6)
28	39.585(6)	2.2748(3)	3995(212)	0.134(15)	803(55)	0.20(2)	1.72(16)	1.18(6)	0.17(6)	657(72)
29	40.075(4)	2.2482(2)	17828(683)	0.194(8)	5177(99)	0.290(17)	1.72(16)	1.18(6)	0.17(6)	456(20)
30	40.650(5)	2.2177(3)	26610(890)	0.247(7)	9851(114)	0.370(17)	1.72(16)	1.18(6)	0.17(6)	358(10)
31	42.497(4)	2.12548(17)	8792(421)	0.129(5)	1971(48)	0.224(16)	1.66(17)	1.55(10)	0.1(2)	691(27)
32	43.302(2)	2.08779(11)	36313(1082)	0.205(5)	11828(205)	0.326(15)	1.63(9)	1.38(3)	0.00(10)	436(10)
33	43.657(11)	2.0716(5)	3879(229)	0.31(4)	1935(199)	0.50(8)	1.63(9)	1.38(3)	0.00(10)	285(32)
34	44.139(3)	2.05013(15)	6786(380)	0.177(11)	1907(68)	0.28(3)	1.63(9)	1.38(3)	0.00(10)	506(33)
35	44.948(8)	2.0151(3)	6394(339)	0.211(13)	2011(51)	0.31(2)	2.9(6)	0.96(11)	0.7(3)	426(27)
36	45.414(9)	1.9955(4)	1286(87)	0.12(3)	234(35)	0.18(4)	2.9(6)	0.96(11)	0.7(3)	740(181)
37	46.827(2)	1.93851(9)	7101(368)	0.254(7)	2041(53)	0.29(2)	4.9(10)	0.08(9)	0.61(15)	356(10)
38	48.336(17)	1.8814(6)	1838(121)	0.25(3)	491(44)	0.27(4)	2.1(5)	0.0(3)	0.0(3)	362(48)
39	48.700(10)	1.8683(4)	3112(196)	0.17(2)	551(42)	0.18(2)	2.1(5)	0.0(3)	0.0(3)	548(67)
40	49.088(14)	1.8544(5)	4403(262)	0.231(19)	1081(44)	0.25(2)	2.1(5)	0.0(3)	0.0(3)	395(32)
41	49.836(9)	1.8283(3)	2574(165)	0.19(2)	539(32)	0.21(3)	1.6(2)	0.00(12)	0.29(15)	483(51)
42	50.194(8)	1.8161(3)	2025(140)	0.111(15)	249(24)	0.12(2)	1.6(2)	0.00(12)	0.29(15)	825(111)
43	50.682(8)	1.7997(3)	2572(171)	0.167(18)	475(29)	0.18(2)	1.6(2)	0.00(12)	0.29(15)	550(60)
44	51.455(12)	1.7745(4)	2677(174)	0.35(2)	1032(40)	0.39(4)	1.6(2)	0.00(12)	0.29(15)	264(15)
45	52.172(7)	1.7518(2)	2895(188)	0.161(16)	515(28)	0.18(2)	1.6(2)	0.00(12)	0.29(15)	575(56)
46	53.106(14)	1.7232(4)	3968(234)	0.472(15)	2072(48)	0.52(4)	1.6(2)	0.00(12)	0.29(15)	197(6)
47	54.434(12)	1.6842(3)	5750(315)	0.41(2)	2584(121)	0.45(5)	1.6(2)	0.00(12)	0.29(15)	230(13)
48	54.780(7)	1.67438(19)	5361(314)	0.19(2)	1114(121)	0.21(3)	1.6(2)	0.00(12)	0.29(15)	497(54)
49	55.228(18)	1.6619(5)	1398(105)	0.28(5)	441(54)	0.32(6)	1.6(2)	0.00(12)	0.29(15)	329(62)
50	55.807(11)	1.6460(3)	3741(230)	0.352(18)	1458(55)	0.39(4)	1.6(2)	0.00(12)	0.29(15)	266(14)
51	57.645(5)	1.59780(13)	4199(260)	0.488(15)	2185(76)	0.52(5)	5.0(11)	0.00(12)	0.0(3)	194(6)
52	58.416(10)	1.5785(3)	825(67)	0.09(3)	76(30)	0.09(4)	2.7(7)	0.0(3)	0.0(4)	1101(364)
53	58.778(14)	1.5697(3)	3355(227)	0.254(17)	906(65)	0.27(4)	2.7(7)	0.0(3)	0.0(4)	375(25)
54	62.879(9)	1.47679(18)	3325(230)	0.25(3)	1306(71)	0.39(5)	3.0(14)	1.19(19)	0.0(5)	386(53)
55	64.14(2)	1.4509(4)	784(64)	0.20(5)	167(44)	0.21(7)	0.5(5)	0.0(16)	0.0(11)	489(130)
56	66.348(12)	1.4078(2)	850(70)	0.10(3)	86(28)	0.10(4)	2.0(7)	0.0(4)	0.0(5)	1041(325)
57	66.82(2)	1.3990(4)	2477(169)	0.30(3)	779(68)	0.31(5)	2.0(7)	0.0(4)	0.0(5)	337(29)

Figure 48 Data obtained from the XRPD software to plot the diffractogram

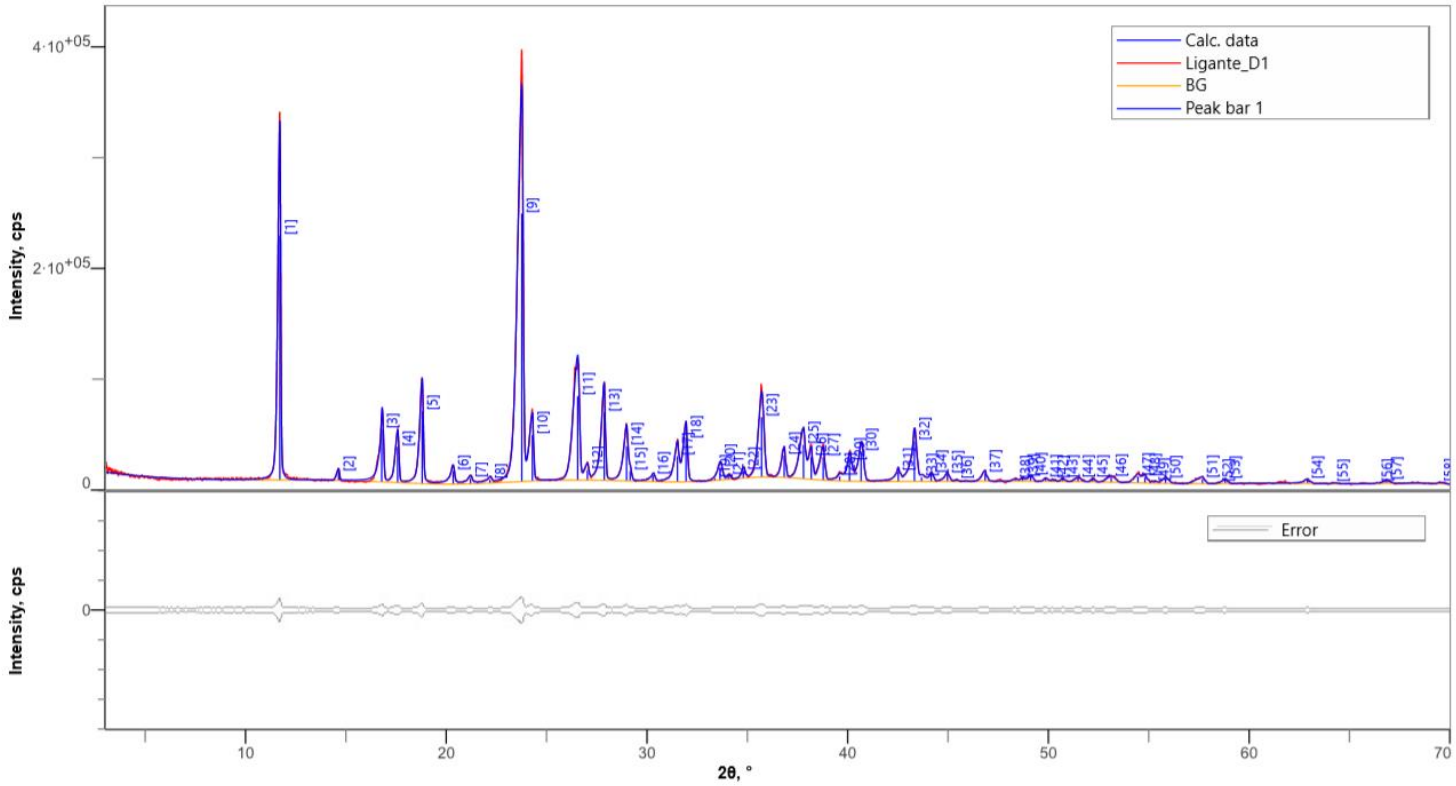

Figure 49. Comparison of the data in the COD database and the synthesized ligand. The error associated is also shown.

XPS Cobalt (II) compound - High resolution window for oxygen, nitrogen, carbon and chlorine atoms

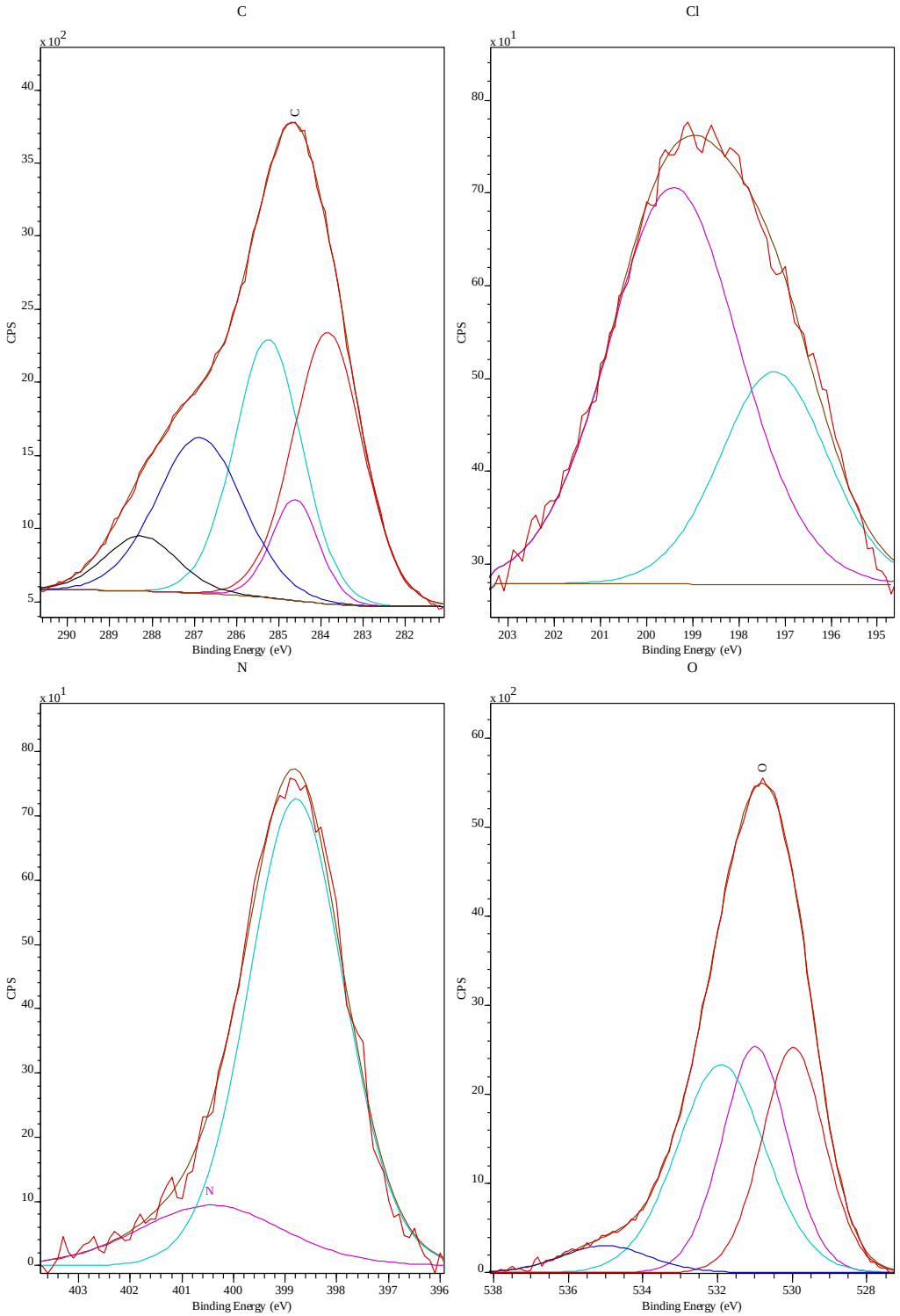

Figure 50.High resolution XPS of the atoms present in the cobalt (II) compound

XPS Copper (II) compound - High resolution window for oxygen, nitrogen, and carbon atoms

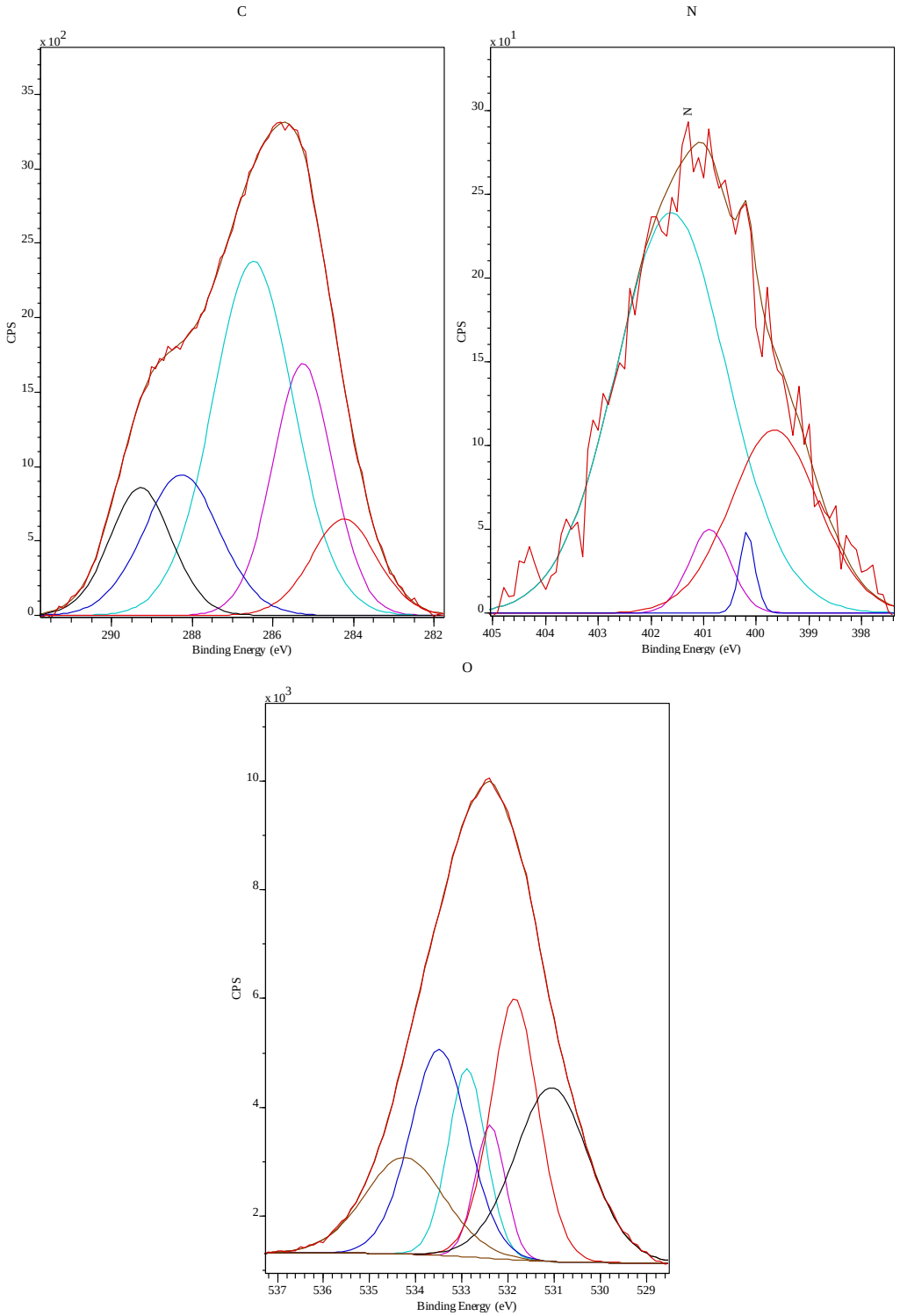

Figure 51. High resolution XPS of the atoms present in the copper (II) compound

XPS Nickel (II) compound - High resolution window for oxygen, nitrogen, carbon and chlorine atoms

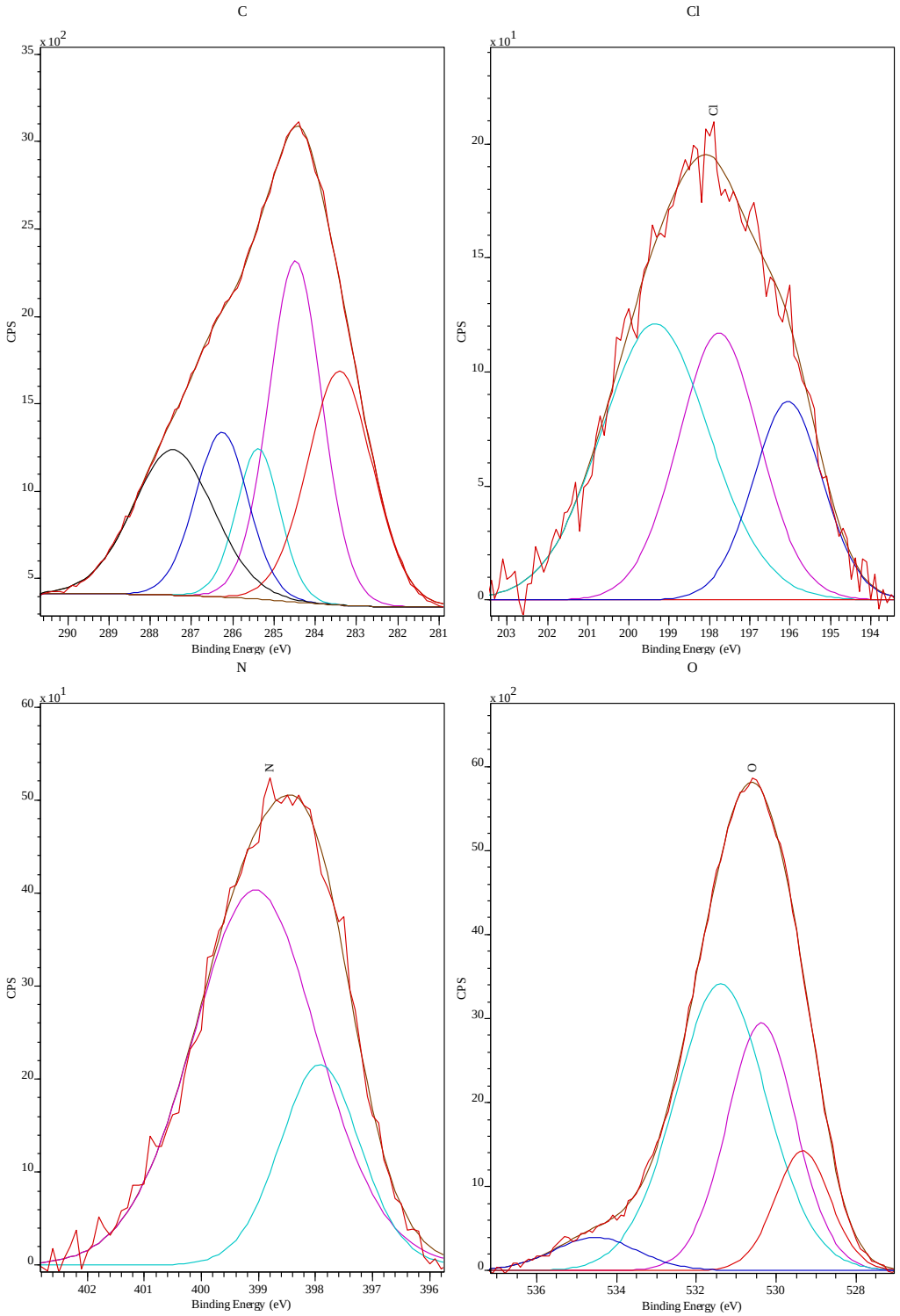

Figure 52. High resolution XPS of the atoms present in the nickel (II) compound

XPS Ruthenium (III) compound -High resolution window for oxygen, nitrogen, carbon and chlorine atoms

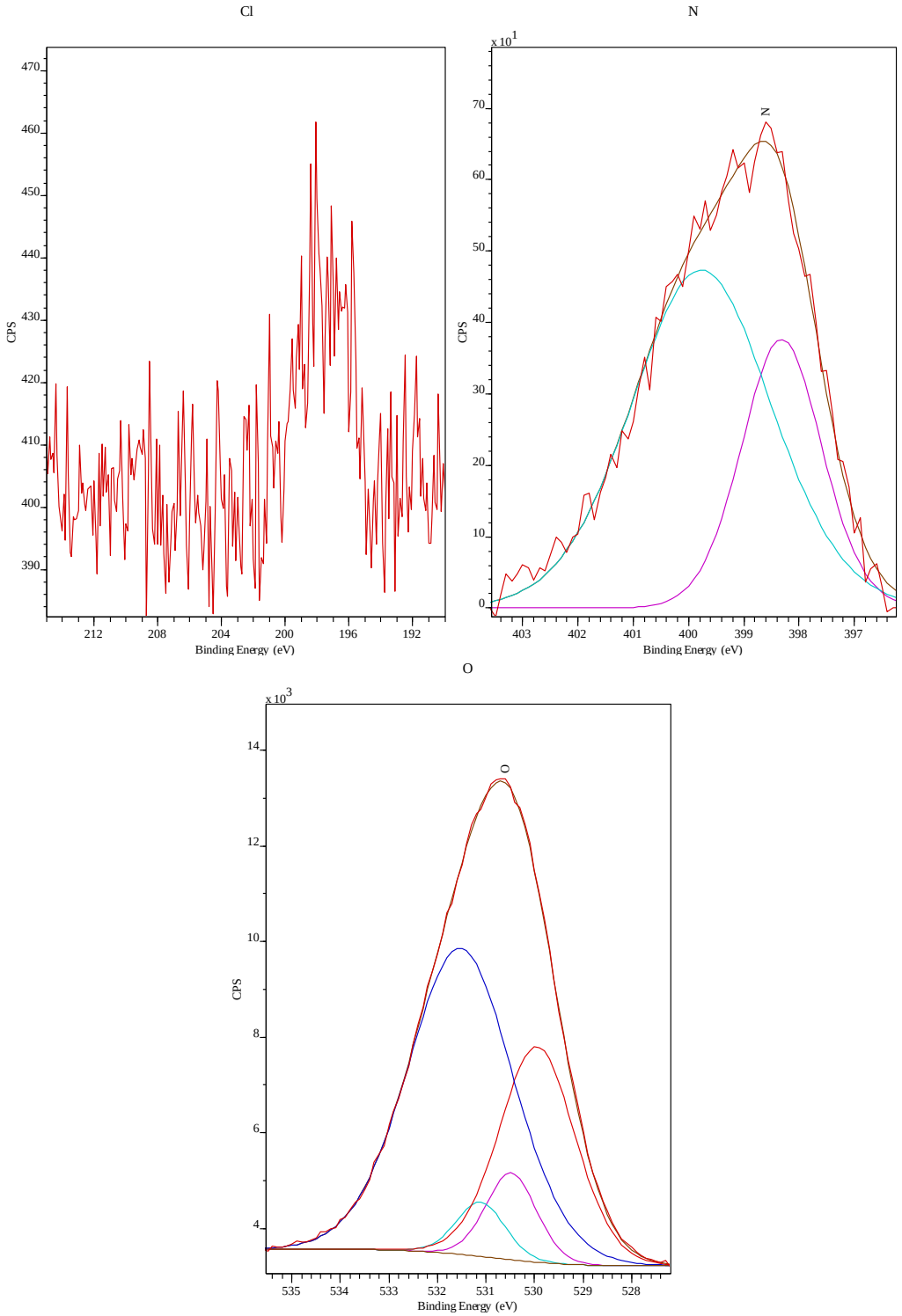

Figure 53. High resolution XPS of the atoms present in the ruthenium (III) compound.

8. REFERENCES

(1) Lawrance, G. A. *Introduction to Coordination Chemistry*; John Wiley & Sons, Ltd: Chichester, UK, 2010. https://doi.org/10.1002/9780470687123.

(2) Constable, E. C.; Housecroft, C. E. Coordination Chemistry: The Scientific Legacy of Alfred Werner. *Chem. Soc. Rev.* **2013**, *42* (4), 1429–1439. https://doi.org/10.1039/c2cs35428d.

(3) Jurca, T.; Marian, E.; Vicaş, L. G.; Mureşan, M. E.; Fritea, L. Metal Complexes of Pharmaceutical Substances. *Spectrosc. Anal. - Dev. Appl.* **2017**. https://doi.org/10.5772/65390.

(4) Farrell, N. Metal Complexes as Drugs and Chemotherapeutic Agents. *Compr. Coord. Chem. II* **2004**, *9*, 809–840. https://doi.org/10.1016/B0-08-043748-6/09021-6.

(5) Haas, K. L.; Franz, K. J. Application of Metal Coordination Chemistry To Explore and Manipulate Cell Biology. *Chem. Rev.* **2009**, *109* (10), 4921–4960. https://doi.org/10.1021/cr900134a.

(6) Fricker, S. P. Metal Based Drugs: From Serendipity to Design. *Dalt. Trans.* **2007**, No. 43, 4903–4917. https://doi.org/10.1039/b705551j.

(7) Fricker, S. P. Medical Uses of Gold Compounds: Past, Present and Future. *Gold Bull.* **1996**, *29* (2), 53–60. https://doi.org/10.1007/bf03215464.

(8) Srivastava, A. K. Anti-Diabetic and Toxic Effects of Vanadium Compounds. *Mol. Cell. Biochem.* **2000**, *206* (1–2), 177–182. https://doi.org/10.1023/A:1007075204494.

(9) Kostova, I. Platinum Complexes as Anticancer Agents. *Recent Pat. Anticancer. Drug Discov.* **2006**, *1* (1), 1–22. https://doi.org/10.2174/157489206775246458.

(10) Kostova, I. Ruthenium Complexes as Anticancer Agents. *Curr. Med. Chem.* **2006**, *13* (9), 1085–1107. https://doi.org/10.2174/092986706776360941.

(11) Askari, A.; Long, C. L.; Blakemore, W. S. Zinc, Copper, and Parenteral Nutrition in Cancer. A Review. *J. Parenter. Enter. Nutr.* **1980**, *4* (6), 561–571. https://doi.org/10.1177/014860718000400656l.

(12) Lin, K.; Zhao, Z. Z.; Bo, H. Ben; Hao, X. J.; Wang, J. Q. Applications of Ruthenium Complex in Tumor Diagnosis and Therapy. *Front. Pharmacol.* **2018**, *9* (NOV), 1–10. https://doi.org/10.3389/fphar.2018.01323.

(13) Bergamo, A.; Messori, L.; Piccioli, F.; Cocchietto, M.; Sava, G. Biological Role of Adduct Formation of the Ruthenium(III) Complex NAMI-A with Serum Albumin and Serum Transferrin. *Invest. New Drugs* **2003**, *21* (4), 401–411. https://doi.org/10.1023/A:1026243000320.

(14) Hartinger, C. G.; Zorbas-Seifried, S.; Jakupec, M. A.; Kynast, B.; Zorbas, H.; Keppler, B. K. From Bench to Bedside - Preclinical and Early Clinical Development of the Anticancer Agent Indazolium Trans-[Tetrachlorobis(1H-Indazole)Ruthenate(III)] (KP1019 or FFC14A). *J. Inorg. Biochem.* **2006**, *100* (5–6), 891–904.

https://doi.org/10.1016/j.jinorgbio.2006.02.013.

(15) Heffeter, P.; Atil, B.; Kryeziu, K.; Groza, D.; Koellensperger, G.; Körner, W.; Jungwirth, U.; Mohr, T.; Keppler, B. K.; Berger, W. The Ruthenium Compound KP1339 Potentiates the Anticancer Activity of Sorafenib in Vitro and in Vivo. *Eur. J. Cancer* **2013**, *49* (15), 3366–3375. https://doi.org/10.1016/j.ejca.2013.05.018.

(16) Smithen, D. A.; Yin, H.; Beh, M. H. R.; Hetu, M.; Cameron, T. S.; McFarland, S. A.; Thompson, A. Synthesis and Photobiological Activity of Ru(II) Dyads Derived from Pyrrole-2-Carboxylate Thionoesters. *Inorg. Chem.* **2017**, *56* (7), 4121–4132. https://doi.org/10.1021/acs.inorgchem.7b00072.

(17) Kurzwernhart, A.; Kandioller, W.; Bartel, C.; Bächler, S.; Trondl, R.; Mühlgassner, G.; Jakupec, M. A.; Arion, V. B.; Marko, D.; Keppler, B. K.; et al. Targeting the DNA-Topoisomerase Complex in a Double-Strike Approach with a Topoisomerase Inhibiting Moiety and Covalent DNA Binder. *Chem. Commun.* **2012**, *48* (40), 4839–4841. https://doi.org/10.1039/c2cc31040f.

(18) Le Gac, S.; Rickling, S.; Gerbaux, P.; Defrancq, E.; Moucheron, C.; Kirsch-De Mesmaeker, A. A Photoreactive Ruthenium(II) Complex Tethered to a Guanine-Containing Oligonucleotide: A Biomolecular Tool That Behaves as a Seppuku Molecule. *Angew. Chemie - Int. Ed.* **2009**, *48* (6), 1122–1125. https://doi.org/10.1002/anie.200804503.

(19) Wang, J. Q.; Zhang, P. Y.; Qian, C.; Hou, X. J.; Ji, L. N.; Chao, H. Mitochondria Are the Primary Target in the Induction of Apoptosis by Chiral Ruthenium(II) Polypyridyl Complexes in Cancer Cells. *J. Biol. Inorg. Chem.* **2014**, *19* (3), 335–348. https://doi.org/10.1007/s00775-013-1069-2.

(20) Sano, R.; Hou, Y. C. C.; Hedvat, M.; Correa, R. G.; Shu, C. W.; Krajewska, M.; Diaz, P. W.; Tamble, C. M.; Quarato, G.; Gottlieb, R. A.; et al. Endoplasmic Reticulum Protein BI-1 Regulates Ca2+-Mediated Bioenergetics to Promote Autophagy. *Genes Dev.* **2012**, *26* (10), 1041–1054. https://doi.org/10.1101/gad.184325.111.

(21) Tan, C.; Lai, S.; Wu, S.; Hu, S.; Zhou, L.; Chen, Y.; Wang, M.; Zhu, Y.; Lian, W.; Peng, W.; et al. Nuclear Permeable Ruthenium(II) β-Carboline Complexes Induce Autophagy to Antagonize Mitochondrial-Mediated Apoptosis. *J. Med. Chem.* **2010**, *53* (21), 7613–7624. https://doi.org/10.1021/jm1009296.

(22) Deng, Z.; Gao, P.; Yu, L.; Ma, B.; You, Y.; Chan, L.; Mei, C.; Chen, T. Ruthenium Complexes with Phenylterpyridine Derivatives Target Cell Membrane and Trigger Death Receptors-Mediated Apoptosis in Cancer Cells. *Biomaterials* **2017**, *129*, 111–126. https://doi.org/10.1016/j.biomaterials.2017.03.017.

(23) Sigel, A.; Sigel, H.; Sigel, R. K. O. *Interrelations between Essential Metal Ions and Human Diseases*; Sigel, A., Sigel, H., Sigel, R. K. O., Eds.; Metal Ions in Life Sciences; Springer Netherlands: Dordrecht, 2013; Vol. 13. https://doi.org/10.1007/978-94-007-7500-8.

(24) Jogl, G.; Wang, X.; Mason, S. A.; Kovalevsky, A.; Mustyakimov, M.; Fisher, Z.; Hoffman, C.; Kratky, C.; Langan, P. High-Resolution Neutron Crystallographic Studies of

the Hydration of the Coenzyme Cob(II)Alamin. *Acta Crystallogr. Sect. D Biol. Crystallogr.* **2011**, *67* (6), 584–591. https://doi.org/10.1107/S090744491101496X.

(25) Munteanu, C. R.; Suntharalingam, K. Advances in Cobalt Complexes as Anticancer Agents. *Dalt. Trans.* **2015**, *44* (31), 13796–13808. https://doi.org/10.1039/c5dt02101d.

(26) Dai, Q.; Kelly, J. C.; Elgowainy, A. Cobalt Life Cycle Analysis Update for the GREET Mode. **2018**, No. September.

(27) Adewuyi, S.; Kareem, K. T.; Atayese, A. O.; Amolegbe, S. A.; Akinremi, C. A. Chitosan-Cobalt(II) and Nickel(II) Chelates as Antibacterial Agents. *Int. J. Biol. Macromol.* **2011**, *48* (2), 301–303. https://doi.org/10.1016/j.ijbiomac.2010.12.004.

(28) Ajibade, P. A.; Kolawole, G. A. Cobalt(III) Complexes of Some Antimalarial Drugs: Synthesis, Characterization, and in Vitro Antiprotozoal Studies. *Synth. React. Inorganic, Met. Nano-Metal Chem.* **2010**, *40* (4), 273–278. https://doi.org/10.1080/15533171003766691.

(29) Patel, M.; Chhasatia, M.; Bhatt, B. In Vitro Bacteriostatic and DNA Interaction Studies of Drug-Based Mixed-Ligand Complexes of Cobalt(II). *Med. Chem. Res.* **2011**, *20* (2), 220–230. https://doi.org/10.1007/s00044-010-9310-9.

(30) Sathyadevi, P.; Krishnamoorthy, P.; Alagesan, M.; Thanigaimani, K.; Thomas Muthiah, P.; Dharmaraj, N. Synthesis, Crystal Structure, Electrochemistry and Studies on Protein Binding, Antioxidant and Biocidal Activities of Ni(II) and Co(II) Hydrazone Complexes. *Polyhedron* **2012**, *31* (1), 294–306. https://doi.org/10.1016/j.poly.2011.09.021.

(31) Shreaz, S.; Sheikh, R. A.; Bhatia, R.; Neelofar, K.; Imran, S.; Hashmi, A. A.; Manzoor, N.; Basir, S. F.; Khan, L. A. Antifungal Activity of α-Methyl Trans Cinnamaldehyde, Its Ligand and Metal Complexes: Promising Growth and Ergosterol Inhibitors. *BioMetals* **2011**, *24* (5), 923–933. https://doi.org/10.1007/s10534-011-9447-0.

(32) Dhahagani, K.; Mathan Kumar, S.; Chakkaravarthi, G.; Anitha, K.; Rajesh, J.; Ramu, A.; Rajagopal, G. Synthesis and Spectral Characterization of Schiff Base Complexes of Cu(II), Co(II), Zn(II) and VO(IV) Containing 4-(4-Aminophenyl)Morpholine Derivatives: Antimicrobial Evaluation and Anticancer Studies. *Spectrochim. Acta - Part A Mol. Biomol. Spectrosc.* **2014**, *117*, 87–94. https://doi.org/10.1016/j.saa.2013.07.101.

(33) Martinez-Bulit, P.; Garza-Ortíz, A.; Mijangos, E.; Barrón-Sosa, L.; Sánchez-Bartéz, F.; Gracia-Mora, I.; Flores-Parra, A.; Contreras, R.; Reedijk, J.; Barba-Behrens, N. 2,6-Bis(2,6-Diethylphenyliminomethyl)Pyridine Coordination Compounds with Cobalt(II), Nickel(II), Copper(II), and Zinc(II): Synthesis, Spectroscopic Characterization, X-Ray Study and in Vitro Cytotoxicity. *J. Inorg. Biochem.* **2015**, *142* (Ii), 1–7. https://doi.org/10.1016/j.jinorgbio.2014.09.007.

(34) Stewart, M.; Watson, I. Standard Units for Expressing Drug Concentrations in Biological Fluids. *Br. J. Clin. Pharmacol.* **1983**. https://doi.org/10.1111/j.1365-2125.1983.tb02136.x.

(35) Kirubavathy, S. J.; Velmurugan, R.; Karvembu, R.; Bhuvanesh, N. S. P.; Parameswari, K.; Chitra, S. Synthesis, Structure, and Pharmacological Evaluation of Co(III) Complex Containing Tridentate Schiff Base Ligand. *Russ. J. Coord. Chem. Khimiya* **2015**, *41* (5),

345–352. https://doi.org/10.1134/S1070328415050048.

(36) Ghosh, P.; Chowdhury, A. R.; Saha, S. K.; Ghosh, M.; Pal, M.; Murmu, N. C.; Banerjee, P. Synthesis and Characterization of Redox Non-Innocent Cobalt(III) Complexes of a O,N,O Donor Ligand: Radical Generation, Semi-Conductivity, Antibacterial and Anticancer Activities. *Inorganica Chim. Acta* **2015**, *429* (Iii), 99–108. https://doi.org/10.1016/j.ica.2015.01.029.

(37) Raja, D. S.; Bhuvanesh, N. S. P.; Natarajan, K. A Novel Water Soluble Ligand Bridged Cobalt(Ii) Coordination Polymer of 2-Oxo-1,2-Dihydroquinoline-3-Carbaldehyde (Isonicotinic) Hydrazone: Evaluation of the DNA Binding, Protein Interaction, Radical Scavenging and Anticancer Activity. *Dalt. Trans.* **2012**, *41* (15), 4365–4377. https://doi.org/10.1039/c2dt12274j.

(38) Kumar, R. S.; Riyasdeen, A.; Dinesh, M.; Paul, C. P.; Srinag, S.; Krishnamurthy, H.; Arunachalam, S.; Akbarsha, M. A. Cytotoxic Property of Surfactant-Cobalt(III) Complexes on a Human Breast Cancer Cell Line. *Arch. Pharm. (Weinheim).* **2011**, *344* (7), 422–430. https://doi.org/10.1002/ardp.201000144.

(39) Kumar, R. S.; Arunachalam, S. Synthesis, Micellar Properties, DNA Binding and Antimicrobial Studies of Some Surfactant-Cobalt(III) Complexes. *Biophys. Chem.* **2008**, *136* (2–3), 136–144. https://doi.org/10.1016/j.bpc.2008.05.007.

(40) Kumar, R. S.; Arunachalam, S.; Periasamy, V. S.; Preethy, C. P.; Riyasdeen, A.; Akbarsha, M. A. Surfactant-Cobalt(III) Complexes: Synthesis, Critical Micelle Concentration (CMC) Determination, DNA Binding, Antimicrobial and Cytotoxicity Studies. *J. Inorg. Biochem.* **2009**, *103* (1), 117–127. https://doi.org/10.1016/j.jinorgbio.2008.09.010.

(41) Marzano, C.; Pellei, M.; Tisato, F.; Santini, C. Copper Complexes as Anticancer Agents. *Anticancer. Agents Med. Chem.* **2012**, *9* (2), 185–211. https://doi.org/10.2174/187152009787313837.

(42) Halliwell, B.; Gutteridge, J. M. C. Role of Free Radicals and Catalytic Metal Ions in Human Disease: An Overview. *Methods Enzymol.* **1990**, *186* (C), 1–85. https://doi.org/10.1016/0076-6879(90)86093-B.

(43) Turnlund, J. R.; Keyes, W. R.; Anderson, H. L.; Acord, L. L. Copper Absorption and Retention in Young Men at Three Levels of Dietary Copper by Use of the Stable Isotope65Cu. *Am. J. Clin. Nutr.* **1989**, *49* (5), 870–878. https://doi.org/10.1093/ajcn/49.5.870.

(44) Wang, T.; Guo, Z. Copper in Medicine: Homeostasis, Chelation Therapy and Antitumor Drug Design. *Curr. Med. Chem.* **2006**, *13* (5), 525–537. https://doi.org/10.2174/092986706776055742.

(45) Daniel, Kenyon, G. Copper Storage Diseases: Menkes, Wilson's, and Cancer. *Front. Biosci.* **2004**, *9* (1–3), 2652. https://doi.org/10.2741/1424.

(46) Koppenol, W. H. The Haber-Weiss Cycle - 70 Years Later. *Redox Rep.* **2001**, *6* (4), 229–234. https://doi.org/10.1179/135100001101536373.

(47) Galaris, D.; Evangelou, A. The Role of Oxidative Stress in Mechanisms of Metal-Induced Carcinogenesis. *Crit. Rev. Oncol. Hematol.* **2002**, *42* (1), 93–103. https://doi.org/10.1016/S1040-8428(01)00212-8.

(48) Crim, J. A.; Petering, H. G. The Antitumor Activity of Cu(II)KTS, the Copper (II) Chelate of 3-Ethoxy-2-Oxobutyraldehyde Bis(Thiosemicarbazone). *Cancer Res.* **1967**, *27* (7), 1278–1285.

(49) BROCKMAN, R. W.; THOMSON, J. R.; BELL, M. J.; SKIPPER, H. E. Observations on the Antileukemic Activity of Pyridine-2-Carboxaldehyde Thiosemicarbazone and Thiocarbohydrazone. *Cancer Res.* **1956**, *16* (2), 167–170.

(50) Tamura, H.; Imai, H.; Kuwahara, J.; Sugiura, Y. A New Antitumor Complex: Bis(Acetato)Bis(Imidazole)Copper(II). *J. Am. Chem. Soc.* **1987**, *109* (22), 6870–6871. https://doi.org/10.1021/ja00256a062.

(51) Habib, N.; Rida, S.; Badawey, E.; Fahmy, H.; Ghozlan, H. Synthesis and Biological Investigations of Some Novel Thiazolylbenzimidazoles, and Benzimidazolyl-Thiazolo[4,5-d]Pyrimidines. *Pharmazie* **1997**, *52*, 346–350.

(52) Zhang, H.; Liu, C. Sen; Bu, X. H.; Yang, M. Synthesis, Crystal Structure, Cytotoxic Activity and DNA-Binding Properties of the Copper (II) and Zinc (II) Complexes with 1-[3-(2-Pyridyl)Pyrazol-1- Ylmethyl]Naphthalene. *J. Inorg. Biochem.* **2005**, *99* (5), 1119–1125. https://doi.org/10.1016/j.jinorgbio.2005.02.005.

(53) Tardito, S.; Bussolati, O.; Maffini, M.; Tegoni, M.; Giannetto, M.; Dall'Asta, V.; Franchi-Gazzola, R.; Lanfranchi, M.; Pellinghelli, M. A.; Mucchino, C.; et al. Thioamido Coordination in a Thioxo-1,2,4-Triazole Copper(II) Complex Enhances Nonapoptotic Programmed Cell Death Associated with Copper Accumulation and Oxidative Stress in Human Cancer Cells. *J. Med. Chem.* **2007**, *50* (8), 1916–1924. https://doi.org/10.1021/jm061174f.

(54) Pitié, M.; Donnadieu, B.; Meunier, B. Preparation of the New Bis(Phenanthroline) Ligand "Clip-Phen" and Evaluation of the Nuclease Activity of the Corresponding Copper Complex. *Inorg. Chem.* **1998**, *37* (14), 3486–3489. https://doi.org/10.1021/ic980044x.

(55) Kasprzak, K. S.; Sunderman, F. W.; Salnikow, K. Nickel Carcinogenesis. *Mutat. Res. - Fundam. Mol. Mech. Mutagen.* **2003**, *533* (1–2), 67–97. https://doi.org/10.1016/j.mrfmmm.2003.08.021.

(56) Lu, H.; Shi, X.; Costa, M.; Huang, C. Carcinogenic Effect of Nickel Compounds. *Mol. Cell. Biochem.* **2005**, *279* (1–2), 45–67. https://doi.org/10.1007/s11010-005-8215-2.

(57) Matkar, S. S.; Wrischnik, L. A.; Jones, P. R.; Hellmann-Blumberg, U. Two Closely Related Nickel Complexes Have Different Effects on DNA Damage and Cell Viability. *Biochem. Biophys. Res. Commun.* **2006**, *343* (3), 754–761. https://doi.org/10.1016/j.bbrc.2006.03.019.

(58) KARN, J. L.; BUSCH, D. H. Nickel (II) Complexes of the Tetradentate Macrocycle 2,12-Dimethyl-3,7,11,17-Tetraazabicyclo (11.3.1) Heptadeca-1 (17),2,11,13,15-Pentaene. *Nature* **1966**, *211* (5045), 160–162. https://doi.org/10.1038/211160a0.

(59) Rodrìguez-Argüelles, M. C.; Ferrari, M. B.; Bisceglie, F.; Pelizzi, C.; Pelosi, G.; Pinelli, S.; Sassi, M. Synthesis, Characterization and Biological Activity of Ni, Cu and Zn Complexes of Isatin Hydrazones. *J. Inorg. Biochem.* **2004**, *98* (2), 313–321. https://doi.org/10.1016/j.jinorgbio.2003.10.006.

(60) Barefield, E. K.; Lovecchio, F. V.; Tokel, N. E.; Ochiai, E.; Busch, D. Y. H. Synthesis, Properties, and Electrochemical Studies of a Series of Nickèl(II) Complexes with Related Macrocyclic Ligands of Varied Unsaturation. *Inorg. Chem.* **1972**, *11* (2), 283–288. https://doi.org/10.1021/ic50108a018.

(61) Singh, N. P.; McCoy, M. T.; Tice, R. R.; Schneider, E. L. A Simple Technique for Quantitation of Low Levels of DNA Damage in Individual Cells. *Exp. Cell Res.* **1988**, *175* (1), 184–191. https://doi.org/10.1016/0014-4827(88)90265-0.

(62) Liang, Q.; Ananias, D. C.; Long, E. C. Ni(II)·Xaa-Xaa-His Induced DNA Cleavage: Deoxyribose Modification by a Common "activated" Intermediate Derived from KHSO5, MMPP, or H2O2. *J. Am. Chem. Soc.* **1998**, *120* (2), 248–257. https://doi.org/10.1021/ja9720218.

(63) Leigh, G. J. Comprehensive Coordination Chemistry II From Biology to Nanotechnology. *J. Organomet. Chem.* **2004**, *689* (16), 2733–2742. https://doi.org/10.1016/j.jorganchem.2004.05.003.

(64) Adeniyi, A. A.; Ajibade, P. A. The Anticancer Activities of Some Nitrogen Donor Ligands Containing Bis-Pyrazole, Bipyridine, and Phenanthroline Moiety Using Docking Methods. *Bioinorg. Chem. Appl.* **2018**, *2018* (Top II). https://doi.org/10.1155/2018/5796287.

(65) Planta, R. J.; Gruber, M. Specificity of Cathepsin C. *BBA - Biochim. Biophys. Acta* **1961**, *53* (2), 443–444. https://doi.org/10.1016/0006-3002(61)90469-3.

(66) Mavrić, Ž.; Zaputović, L.; Vitezić, D. Diuretics. *Medicus* **2010**, *19* (2), 117–122. https://doi.org/10.5694/j.1326-5377.1963.tb23353.x.

(67) Zhao, Y.; Biertümpfel, C.; Gregory, M. T.; Hua, Y. J.; Hanaoka, F.; Yang, W. Structural Basis of Human DNA Polymerase η-Mediated Chemoresistance to Cisplatin. *Proc. Natl. Acad. Sci. U. S. A.* **2012**, *109* (19), 7269–7274. https://doi.org/10.1073/pnas.1202681109.

(68) Xie, P.; Streu, C.; Qin, J.; Bregman, H.; Pagano, N.; Meggers, E.; Marmorstein, R. The Crystal Structure of BRAF in Complex with an Organoruthenium Inhibitor Reveals a Mechanism for Inhibition of an Active Form of BRAF Kinase. *Biochemistry* **2009**, *48* (23), 5187–5198. https://doi.org/10.1021/bi802067u.

(69) Eriksson, M.; Uhlin, U.; Ramaswamy, S.; Ekberg, M.; Regnström, K.; Sjöberg, B. M.; Eklund, H. Binding of Allosteric Effectors to Ribonucleotide Reductase Protein R1: Reduction of Active-Site Cysteines Promotes Substrate Binding. *Structure* **1997**, *5* (8), 1077–1092. https://doi.org/10.1016/S0969-2126(97)00259-1.

(70) Newby, Z.; Lee, T. T.; Morse, R. J.; Liu, Y.; Liu, L.; Venkatraman, P.; Santi, D. V.; Finer-Moore, J. S.; Stroud, R. M. The Role of Protein Dynamics in Thymidylate Synthase Catalysis: Variants of Conserved 2′-Deoxyuridine 5′-Monophosphate (DUMP)-Binding

Tyr-261. *Biochemistry* **2006**, *45* (24), 7415–7428. https://doi.org/10.1021/bi060152s.

(71) Overholtzer, M.; Rao, P. H.; Gorlick, R.; Levine, A. J.; Linkiewicz, A. M.; Dubcovsky, J.; Hummel, D.; Lazo, G. R.; Chao, S.; Anderson, O. D.; et al. Topoisomerase II ATPase Region and Its Mechanism of Inhibition by the Chemotherapeutic Agent ICRF-187,'' by Scott Classen, Stephane Olland, and James M. Berger, Which Appeared in Issue 19, September 16, 2003, Of. *Proc. Natl. Acad. Sci. U. S. A.* **2003**, *100* (20), 11547–11552.

(72) Sugio, S.; Kashima, A.; Mochizuki, S.; Noda, M.; Kobayashi, K. Crystal Structure of Human Serum Albumin at 2.5 Å Resolution. *Protein Eng.* **1999**, *12* (6), 439–446. https://doi.org/10.1093/protein/12.6.439.

(73) Hanif, M.; Henke, H.; Meier, S. M.; Martic, S.; Labib, M.; Kandioller, W.; Jakupec, M. A.; Arion, V. B.; Kraatz, H. B.; Keppler, B. K.; et al. Is the Reactivity of M(II)-Arene Complexes of 3-Hydroxy-2(1 H)-Pyridones to Biomolecules the Anticancer Activity Determining Parameteŕ. *Inorg. Chem.* **2010**, *49* (17), 7953–7963. https://doi.org/10.1021/ic1009785.

(74) Kettmann, V.; Košt'álová, D.; Höltje, H. D. Human Topoisomerase I Poisoning: Docking Protoberberines into a Structure-Based Binding Site Model. *J. Comput. Aided. Mol. Des.* **2004**, *18* (12), 785–796. https://doi.org/10.1007/s10822-004-7878-1.

(75) Zhuang, W.; Wu, X. T.; Zhou, Y.; Liu, G. J.; Wu, T. X.; Yao, X.; Du, L.; Wei, M. L. Polymorphisms of Thymidylate Synthase in the 5'- and 3'-Untranslated Regions and Gastric Cancer. *Dig. Dis. Sci.* **2009**, *54* (7), 1379–1385. https://doi.org/10.1007/s10620-008-0511-8.

(76) Vanguri, V. K. The Adaptive Immune System. In *Pathobiology of Human Disease: A Dynamic Encyclopedia of Disease Mechanisms*; 2014. https://doi.org/10.1016/B978-0-12-386456-7.01101-1.

(77) Alberts, B.; Johnson, a; Lewis, J. Lymphocytes and the Cellular Basis of Adaptive Immunity. *Mol. Biol. Cell* **2002**.

(78) LaRosa, D. F.; Orange, J. S. 1. Lymphocytes. *J. Allergy Clin. Immunol.* **2008**, *121* (2 SUPPL. 2), 364–369. https://doi.org/10.1016/j.jaci.2007.06.016.

(79) Akbar, M.; Brewer, J. M.; Grant, M. H. Effect of Chromium and Cobalt Ions on Primary Human Lymphocytes in Vitro. **2011**, *8* (August 2010), 140–149. https://doi.org/10.3109/1547691X.2011.553845.

(80) Gloria, Æ.; Joaquı, A. Æ.; Æ, Æ. L. C.; Gonza, M.; Manuel, J.; Gutie, M. Æ. A. Evaluation of Antiproliferative Activities and Apoptosis Induction Caused by Copper (II)– Benzothiazolesulfonamide Complexes in Jurkat T Lymphocytes and Caco-2 Cells. **2008**, 1249–1265. https://doi.org/10.1007/s00775-008-0409-0.

(81) Je, E.; Sikora, J.; Kasprzak, K. S. The Effect of Nickel Compounds on Immunophenotype and Natural Killer Cell Function of Normal Human Lymphocytes.

(82) Newcomb, J. R.; Rivnay, B.; Bastos, C. M.; Ocain, T. D.; Gordon, K.; Gregory, P.; Turci, S. M.; Sterne, K. A.; Jesson, M.; Krieger, J.; et al. In Vitro Immunomodulatory Activity of Ruthenium Complexes. **2003**, *52*, 263–271. https://doi.org/10.1007/s00011-003-1169-5.

(83) G., S.; Jamil, K. Application of Human Lymphocytes for Evaluating Toxicity of Anti-Cancer Drugs. *Int. J. Pharmacol.* **2006**, *2* (4), 374–381. https://doi.org/10.3923/ijp.2006.374.381.

(84) Riss, T. L.; Moravec, R. A.; Niles, A. L.; Duellman, S.; Benink, H. A.; Worzella, T. J.; Minor, L. *Cell Viability Assays*; 2004.

(85) Pegg, D. E. Viability Assays for Preserved Cells, Tissues, and Organs. *Cryobiology* **1989**, *26* (3), 212–231. https://doi.org/10.1016/0011-2240(89)90016-3.

(86) Reisch, A. S.; Elpeleg, O. Biochemical Assays for Mitochondrial Activity: Assays of TCA Cycle Enzymes and PDHc. *Methods Cell Biol.* **2007**, *80* (06), 199–222. https://doi.org/10.1016/S0091-679X(06)80010-5.

(87) Southard, J. H. Viability Assays in Organ Preservation. *Cryobiology* **1989**, *26* (3), 232–238. https://doi.org/10.1016/0011-2240(89)90017-5.

(88) Ding, W.; Higgins, D. P.; Yadav, D. K.; Godbole, A. A.; Pukkila-Worley, R.; Walker, A. K. Stress-Responsive and Metabolic Gene Regulation Are Altered in Low S-Adenosylmethionine. *PLoS Genet.* **2018**, *14* (11), 1–26. https://doi.org/10.1371/journal.pgen.1007812.

(89) Shulaev, V.; Oliver, D. J. Metabolic and Proteomic Markers for Oxidative Stress. New Tools for Reactive Oxygen Species Research: Figure 1. *Plant Physiol.* **2006**, *141* (2), 367–372. https://doi.org/10.1104/pp.106.077925.

(90) Picot, J.; Guerin, C. L.; Le Van Kim, C.; Boulanger, C. M. Flow Cytometry: Retrospective, Fundamentals and Recent Instrumentation. *Cytotechnology* **2012**, *64* (2), 109–130. https://doi.org/10.1007/s10616-011-9415-0.

(91) Barros, S. B. de M. Toxicologia. *Rev. Bras. Ciências Farm.* **2002**, *38* (4), 500–500. https://doi.org/10.1590/s1516-93322002000400015.

(92) Aslantürk, Ö. S. In Vitro Cytotoxicity and Cell Viability Assays: Principles, Advantages, and Disadvantages. *Genotoxicity - A Predict. Risk to Our Actual World* **2018**, 1–18. https://doi.org/10.5772/intechopen.71923.

(93) Zbinden, G.; Flury-Roversi, M. Significance of the LD50-Test for the Toxicological Evaluation of Chemical Substances. *Archives of Toxicology*. 1981. https://doi.org/10.1007/BF00332351.

(94) Zhang, M.; Aguilera, D.; Das, C.; Vasquez, H.; Zage, P.; Gopalakrishnan, V.; Wolff, J. Measuring Cytotoxicity: A New Perspective on LC50. *Anticancer Res.* **2007**.

(95) Sebaugh, J. L. Guidelines for Accurate EC50/IC50 Estimation. *Pharm. Stat.* **2011**. https://doi.org/10.1002/pst.426.

(96) Brown, K. G.; Erdreich, L. S. Statistical Uncertainty in the No-Observed-Adverse-Effect Level. *Toxicol. Sci.* **1989**. https://doi.org/10.1093/toxsci/13.2.235.

(97) Sheikh, R. A.; Wani, M. Y.; Shreaz, S.; Hashmi, A. A. Synthesis, Characterization and Biological Screening of Some Schiff Base Macrocyclic Ligand Based Transition Metal

Complexes as Antifungal Agents. *Arab. J. Chem.* **2016**, *9*, S743–S751. https://doi.org/10.1016/j.arabjc.2011.08.003.

(98) Katagiri, H.; Morimoto, M.; Sakai, K. A Pair of Diastereomeric 1:2 Salts of (R)- and (S)-2-Methyl-Piperazine with (2S,3S)-Tartaric Acid. *Acta Crystallogr. Sect. C Cryst. Struct. Commun.* **2010**, *66* (1), 20–24. https://doi.org/10.1107/S0108270109046460.

(99) Nakamoto, K. *Infrared and Raman Spectra of Inorganic and Coordination Compounds*; 2008. https://doi.org/10.1002/9780470405888.

(100) Tanabe, Y.; Sugano, S. On the Absorption Spectra of Complex Ions II. *J. Phys. Soc. Japan* **1954**, *9* (5), 766–779. https://doi.org/10.1143/JPSJ.9.766.

(101) Al-Hazmi, G. A. A.; El-Shahawi, M. S.; Gabr, I. M.; El-Asmy, A. A. Spectral, Magnetic, Thermal and Electrochemical Studies on New Copper(II) Thiosemicarbazone Complexes. *J. Coord. Chem.* **2005**, *58* (8), 713–733. https://doi.org/10.1080/00958970500092834.

(102) Tanabe, Y.; Sugano, S. On the Absorption Spectra of Complex Ions. *J. Phys. Soc. Japan* **1954**. https://doi.org/10.1143/JPSJ.9.753.

(103) Ramírez-Delgado, V.; Hernández-Ayala, L. F.; García-Ramos, J. C.; Flores-Alamo, M.; Galindo-Murillo, R.; Ruiz-Azuara, L.; Ortiz-Frade, L. A Range of Nitrato Coordination Modes in NiII Complexes with the Versatile Ligand 1,8-Bis(2-Pyridyl)-3,6-Dithiaoctane: Structural, Spectroscopic, Electrochemical, and Theoretical Studies. *Eur. J. Inorg. Chem.* **2015**, *2015* (20), 3307–3316. https://doi.org/10.1002/ejic.201500335.

(104) Huai-min, G.; Xian-su, C. Study of Cobalt (II) -Chitosan Coordination Polymer and Its Catalytic Activity and Selectivity for Vinyl Monomer Polymerization. **2004**, No. Ii, 89–92. https://doi.org/10.1002/pat.437.

(105) Briggs, D.Wanger, C. D., Riggs, W. M., Davis, L. E., Moulder, J. F., Muilenberg, G. E. Handbook of X-Ray Photoelectron Spectroscopy: A Reference Book of Standard Data for Use in x-Ray Photoelectron Spectroscopy. *Perkin-Elmer Corporation*. 1979.

(106) Ariponnammal, S.; Velvizhi, R. Structural , Spectroscopic , and Magnetic Studies on Copper Tartrate Crystals. **2019**, *74* (9), 813–819.

(107) Biesinger, M. C.; Lau, L. W. M.; Gerson, A. R.; St, R.; Smart, C. The Role of the Auger Parameter in XPS Studies of Nickel Metal , Halides and Oxides. **2012**, 2434–2442. https://doi.org/10.1039/c2cp22419d.

(108) Blomqvist, K.; Still, E. R. Solution Studies of Systems with Polynuclear Complex Formation. 5. Copper (II) and Cadmium(II) d-(+)-Tartrate Systems. *Inorg. Chem.* **1984**. https://doi.org/10.1021/ic00191a013.